iScience

CellPress

Article

Relative Strength of Common Directing Groups in Palladium-Catalyzed Aromatic C—H Activation

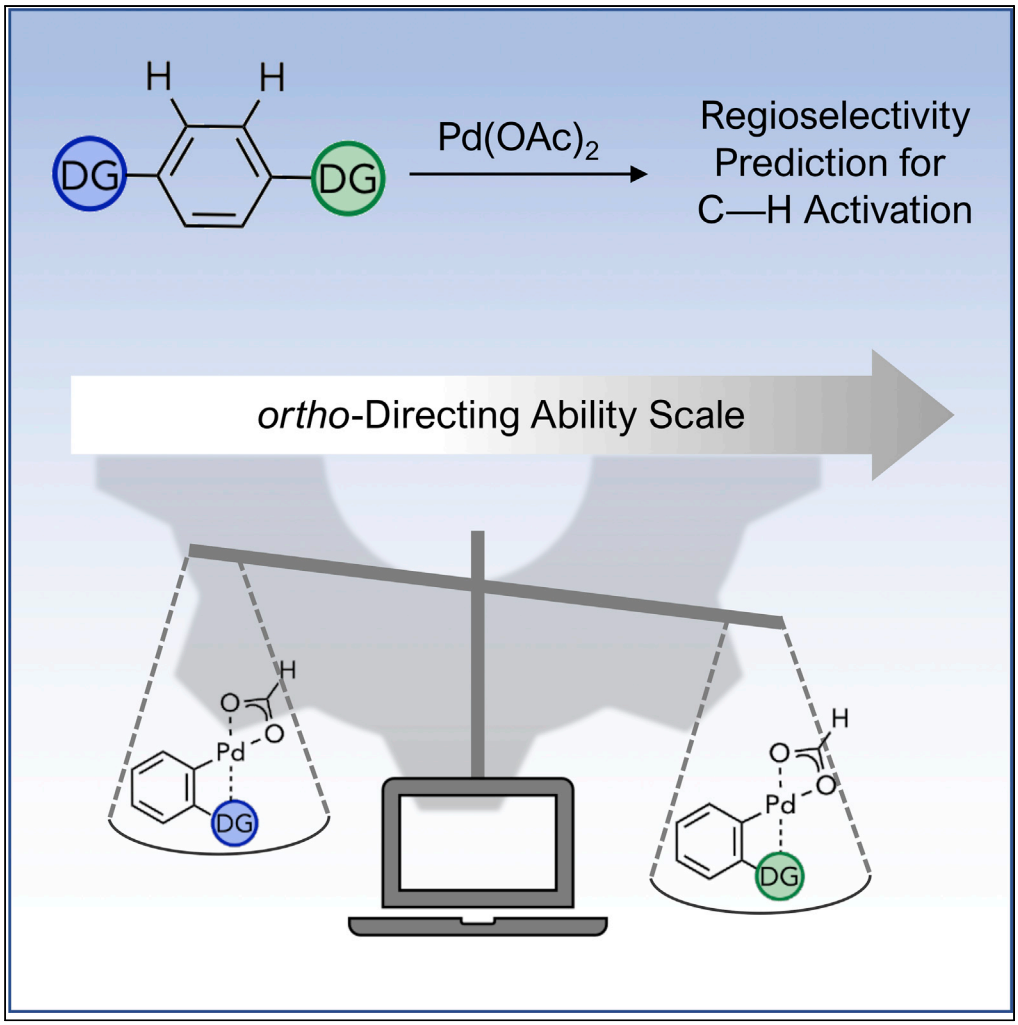

Anna Tomberg, Michael Éric Muratore, Magnus Jan Johansson, Ina Terstiege, Christian Sköld, Per-Ola Norrby

per-ola.norrby@astrazeneca.com

HIGHLIGHTS

Directing group strength for *ortho*-palladation can be predicted quantum chemically

Correlation with fragments allow regioselectivity predictions in complex molecules

Directing strength is enhanced by deprotonation under the reaction conditions

Palladation in between two directing groups is disfavored sterically; no synergy

Tomberg et al., iScience *20*, 373–391
October 25, 2019
https://doi.org/10.1016/j.isci.2019.09.035

iScience

CellPress

Article

Relative Strength of Common Directing Groups in Palladium-Catalyzed Aromatic C−H Activation

Anna Tomberg,[1] Michael Éric Muratore,[2] Magnus Jan Johansson,[2] Ina Terstiege,[3] Christian Sköld,[4] and Per-Ola Norrby[5,6,*]

SUMMARY

Efficient functionalization of C−H bonds can be achieved using transition metal catalysts, such as $Pd(OAc)_2$. To better control the regioselectivity in these reactions, some functional groups on the substrate may be used as directing groups, guiding the reactivity to an *ortho* position. Herein, we describe a methodology to score the relative strength of such directing groups in palladium-catalyzed aromatic C−H activation. The results have been collected into a scale that serves to predict the regioselectivity on molecules with multiple competing directing groups. We demonstrate that this scale yields accurate predictions on over a hundred examples, taken from the literature. In addition to the regioselectivity prediction on complex molecules, the knowledge of the relative strengths of directing groups can also be used to work with new combinations of functionalities, exploring uncharted chemical space.

INTRODUCTION

Synthetic protocols that allow direct activation/functionalization of inert C−H bonds have for a long time remained a Holy Grail in organic synthesis (Gensch et al., 2016). Potential applications would lead to atom economical processes with unmatched step-economy. However, the unreactive nature and high stability of C−H bonds (typical bond energy of $C(sp^2)$−H is 110 kcal/mol) have made them elusive targets for diverse functionalizations under mild conditions (Xue et al., 2017). Nonetheless, the mindset that these bonds are out of reach has changed. Nowadays, C−H bonds are considered functional groups and are utilized to introduce a plethora of functionalities, often with the help of organometallic catalysts (Cernak et al., 2016; Abrams et al., 2018).

The presence of multiple unsubstituted carbons in a given molecule makes controlling regioselectivity in these reactions a challenging task. In catalytic C−H functionalization, two main approaches are used to address this problem: (1) add special ligands on the metal catalyst (Lyons and Sanford, 2010; Wang et al., 2017); (2) use directing groups (DGs) on the substrate able to bind to the metal center and force the reactivity to specific positions (Figure 1) (Sambiagio et al., 2018). In addition to directed C−H activation, there are several elegant ways of overcoming the positional selectivity induced by pre-coordination of the metal to the substrate, including seminal contributions from the Yu and Hartwig labs (Liu et al., 2014; Hartwig and Larsen, 2016; Kiser et al., 2012).

One of the most developed C−H activation approaches takes advantage of palladium as catalyst, leading to $C(sp^2)$−$C(sp^2)$ bond formation or functionalization with N, O, P, and halogens (Lyons and Sanford, 2010). Using $Pd(OAc)_2$, a variety of couplings can be introduced regioselectively by employing DGs (McMurray et al., 2011; Chen et al., 2015). These need not be specially designed moieties: common motifs of organic molecules such as pyridines and carboxylic acids serve as effective DGs. Most DGs in palladium-catalyzed C−H activations are *ortho*-directing. In the case of functionalization of more complex molecules, the presence of multiple DGs can lead to activation on several sites. Therefore, the prediction of the regiochemical outcome plays an important role (Davies and Morton, 2017). Although general reactivity trends of common functional groups, steric hindrance, and acidity of the leaving proton can hint to the preferred regioselectivity, accurately predicting the site of reaction in compounds with several DGs of similar reactivity remains difficult.

To put things in perspective, several mechanistically diverse methods are available for activating $C(sp^2)$−H bonds (Scheme 1). At one end of the spectrum, a strong enough base (frequently directed by a

[1]Hit Discovery, Discovery Sciences, R&D, AstraZeneca Gothenburg, Mölndal 431 83, Sweden

[2]Medicinal Chemistry, Research and Early Development Cardiovascular, Renal and Metabolism, BioPharmaceuticals R&D, AstraZeneca Gothenburg, Mölndal 431 83, Sweden

[3]Respiratory, BioPharmaceuticals R&D, AstraZeneca Gothenburg, Mölndal 431 83, Sweden

[4]Department of Medicinal Chemistry, Drug Design and Development, Uppsala University, Box 574, Uppsala 751 23, Sweden

[5]Data Science & Modelling, Pharmaceutical Sciences, R&D, AstraZeneca Gothenburg, Mölndal 431 83, Sweden

[6]Lead Contact

*Correspondence: per-ola.norrby@astrazeneca.com

https://doi.org/10.1016/j.isci.2019.09.035

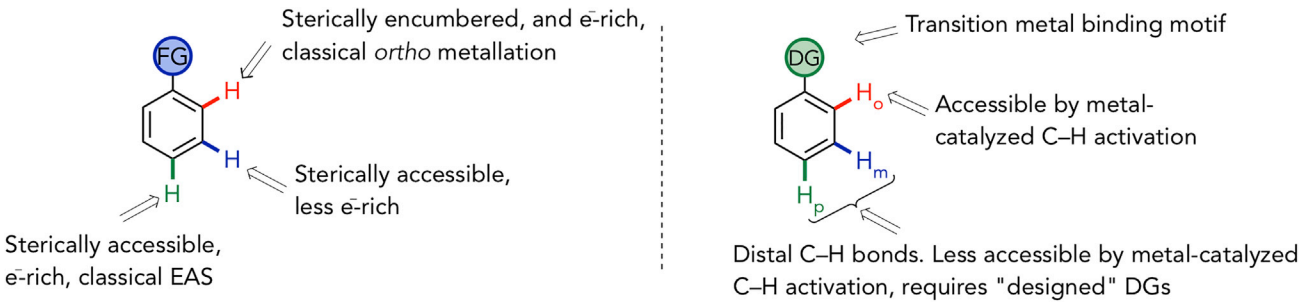

Figure 1. Achieving Regioselectivity in C–H Activation Reactions Is a Challenging Task

The electron-donating/withdrawing character of functional groups (FG = EDG or EWG) leads to the activation of different positions. Increased regioselectivity in metal-catalyzed reactions can be achieved with directing groups (DGs).

coordinating group) is able to abstract a proton directly from an aromatic ring. The immediate reaction product can be an organometallic reagent, e.g., an organolithium (Snieckus, 1990), used as a nucleophile in further reactions. At the other end of the reactivity scale, strong electrophiles can react with the π-system in a reaction in which bond formation to carbon is commonly the rate-limiting step, followed by a facile deprotonation. This is the classical Electrophilic Aromatic Substitution reaction (EAS), whereby selectivity is generally determined by the intrinsic reactivity of the aromatic system (Tomberg et al., 2019). Although the reagent can be an electrophile, a radical also reacts by a similar pathway, but with a different selectivity profile. The principle remains the same: the reagent selects the most reactive carbon and forms an addition product, whereupon the proton at that position is eliminated.

In between these two extremes, we find reagents that combine a weak electrophile with a weak bidentate base. Reactivity is enabled by the cooperativity between the two moieties of the catalyst, where an initial weak electrophilic attack will activate the hydrogen for deprotonation by the weak base in a concerted metallation deprotonation (CMD). With only a weak base and a weak electrophile, the reagent is compatible with a wide range of functionality. The mechanism of action for the prototypical CMD catalysts, palladium carboxylates (e.g., $Pd(OAc)_2$), was elucidated in pioneering studies by the groups of Fagnou

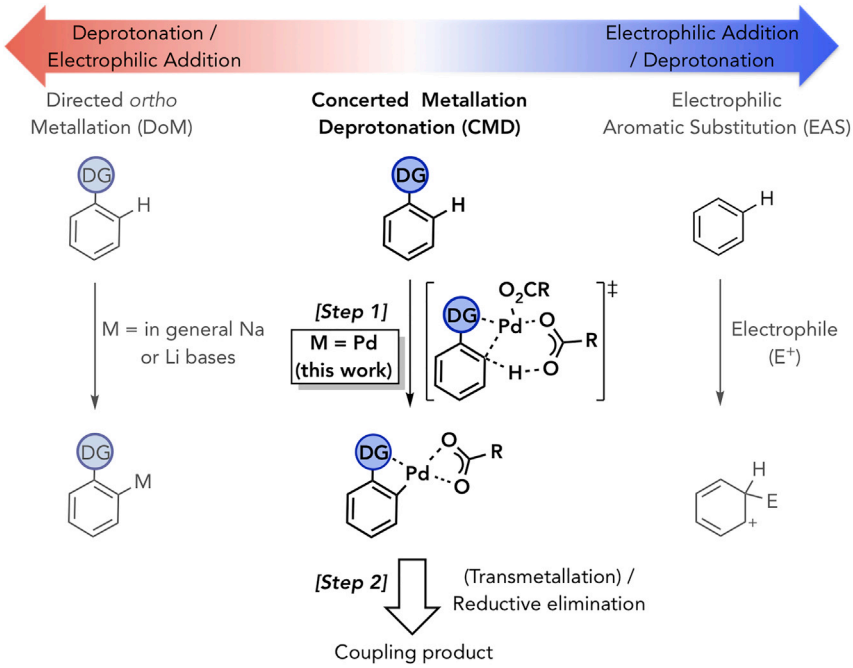

Scheme 1. Classes of C–H Functionalization

The presented work focuses on palladium-catalyzed aromatic C–H activation through the CMD mechanism.

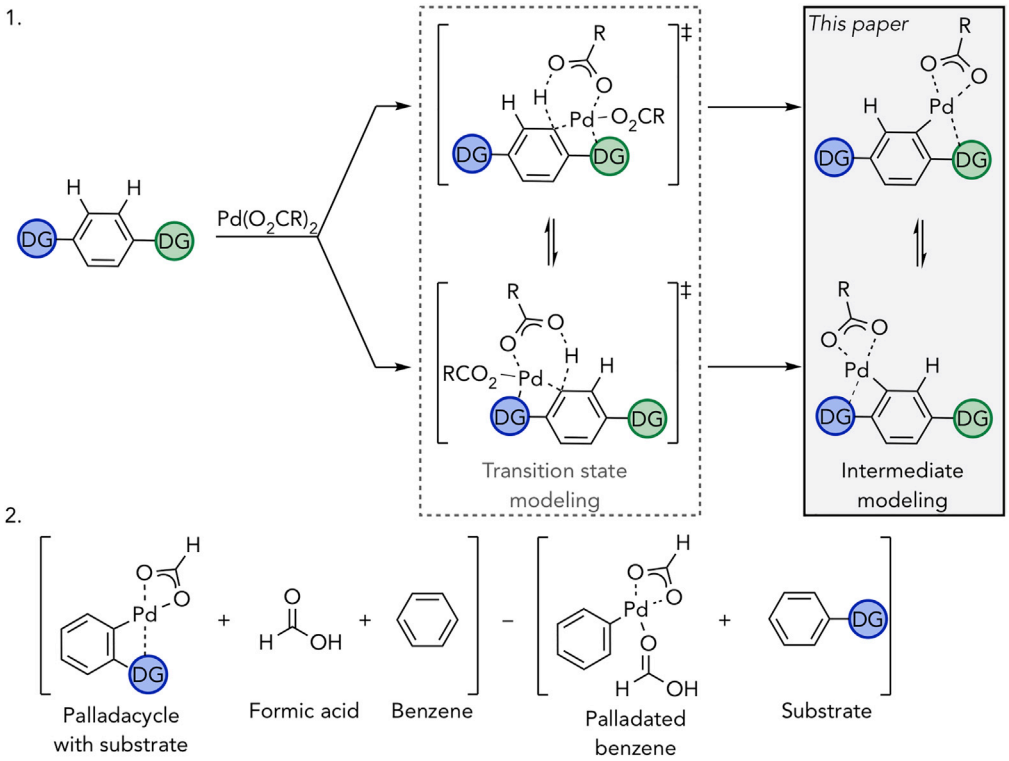

Scheme 2. Palladacycle Intermediates Were Used to Probe Relative DGs Strengths

(1) Isodesmic pseudo-equilibrium between two transition states reflected in the high energy intermediate.

(2) Illustration of the equation used to calculate the relative energies of palladacycles corresponding to DGs. See also Data S17 for coordinates and DFT energies of the compounds and palladacycles studied in this work.

(Gorelsky et al., 2008; Lapointe and Fagnou, 2010), Macgregor (Davies et al., 2005), and others (Davies et al., 2017). As palladium initiates an electrophilic attack on an aromatic carbon, the carboxylate forms a bond with the hydrogen atom on that position. Subsequently, palladium moves into the plane of the aromatic ring, forming a σ-bond to that carbon, while its proton is transferred to the carboxylate (Scheme 1 Step 1). The intrinsic barrier for this reaction is moderately high, but the reaction will be facile if the palladium is stabilized by coordination to a proximal DG. The resulting aryl−palladium complex can then undergo coupling reactions through reductive elimination with another group on palladium, possibly preceded by a transmetallation depending on the exact reaction conditions (Scheme 1 Step 2).

The CMD reaction can be reversible. However, if the forward coupling reaction is favored over the reverse CMD, the reaction will display kinetic selectivity based on the relative stabilities of the plausible C−H activation transition states (TSs). Thus, it has been shown that the reaction selectivity can be predicted by calculating the various possible CMD activation barriers using DFT methods (Davies et al., 2017). However, we are interested in automating the selectivity prediction in a workflow available to bench chemists, as we have previously done for other C−H functionalization reactions (Tomberg et al., 2019; Andersson et al., 2014). To this end, TSs searches are not the method of choice since these calculations are notoriously hard to automate, even though recent approaches show promise (Guan et al., 2018). We therefore wanted to explore if simpler methods show sufficient predictive power for our purposes. Based on the Bell-Evans-Polanyi relationship (Bell and Hinshelwood, 1936; Evans and Polanyi, 1936; Jensen, 1999), and the more specific Hammond postulate (Hammond, 1955), we tested the hypothesis that the selectivity in the CMD TS is reflected in the relative energy of the corresponding palladacycle intermediate in the reaction (Scheme 2.1).

To further simplify the calculations and put each DG on a convenient scale, we compared each potential group with hydrogen, using the equation illustrated in Scheme 2.2. Note that this comparison

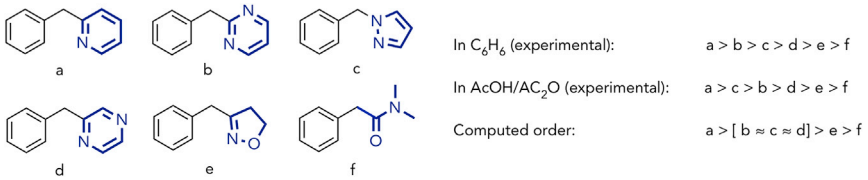

Figure 2. Competition Experiments Reported by Sanford et al. with the Corresponding Calculated Order in 1,2-dicholoroethane

changes molecularity: the DG displaces one carboxylic acid from palladium. Even in cases in which the coordination of the DG is enthalpically disfavored, it may still be favored entropically and thus can outcompete the non-directed CMD reaction. This means that, on a scale based on potential energies, even DGs with moderately positive values will outcompete positions without a DG. The primary use for the scale should be to compare different groups, i.e., only relative numbers should be used.

To the best of our knowledge, the directing abilities of DGs toward palladium electrophiles have never been analyzed in depth and/or in a systematic way. Few experimental studies can be found reporting competition experiments with a handful of DGs, providing only qualitative trends in reactivity (Sun et al., 2013; Desai et al., 2008; Dey et al., 2019). The work presented here aims to quantitatively measure the directing strength of common *ortho*-directing functional groups. Specialized functional groups are able to direct instead to the *meta*-position (Bera et al., 2014; Wan et al., 2013), but the geometry is expected to differ significantly from the CMD intermediate considered here (Yang et al., 2014) and is thus out of the scope of the current study.

We propose a quantum mechanical approach to compute the relative strengths of DGs in palladium-catalyzed aromatic C−H activation. The results have been assembled into a convenient look-up table, featuring 133 DGs, that can be used to quickly compare which DG would yield the major product. The computed relative strengths of DGs were validated by matching results to 150 examples from the literature, where reactant molecules featured two or more non-equivalent potential sites of activation.

RESULTS AND DISCUSSION

We set the goal to develop an approach to quantitatively and systematically score DGs for aromatic C−H activations catalyzed by $Pd(OAc)_2$. Our hypothesis was that there should be a correlation between the stability of the palladacycle formed during CMD and the directing strength of a DG. In other words, if DG_1 prevails over DG_2, then its relative energy according to the equation shown in Scheme 2(2) should be lower than the one from DG_2 (see Transparent Methods section in Supplemental Information). It has to be kept in mind that this approach does not have the capability of predicting a reaction's feasibility but provides a way to score DGs relative to each other.

To probe the validity of our hypothesis, we first tried to reproduce experimental findings from Sanford et al. (Desai et al., 2008). The competition experiments described in their work compared how much of each respective acetoxylation product formed after 12 h in AcOH/Ac_2O and in benzene when using different DGs. Experimentally, the orders observed for the two solvents were almost identical (Figure 2). Using our method, the ranking was similar to experimental data with very small differences (within 1 kcal/mol) for heterocycles b, c, and d. Therefore, although the calculated values were not spot on with experimental findings, the overall trend in reactivity was captured.

Although the competition experiments reported by Sanford investigated separate compounds featuring one DG each, our main goal was to study molecules that bear two different DGs. For example, compound **1** features a pyridine and an ester, as shown in Scheme 3, which can both be *ortho*-directing. Several experiments, taken from different studies (Li et al., 2011; Hull et al., 2006), report that the pyridine group is more strongly directing than the ethyl ester. Indeed, our calculations showed that the coordination through pyridine was over 15 kcal/mol lower in relative energy than the one with directing ethyl ester.

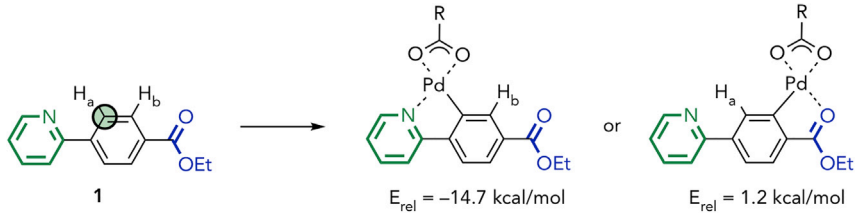

Scheme 3. Compound 1 and the Two Palladacycles Formed with Its DGs Showing that Pyridine Is a Stronger DG Than Ethyl Ester

Experimental C–H activation site is marked by a black circle (Li et al., 2011); predicted site of activation is marked by a green-filled circle; DGs are highlighted with color. See exact energies in Table S1.

The next type of molecules we investigated were compounds that have different DGs that could "help" each other direct reactivity to the same carbon. This is exemplified in compound **2**, in which both the pyridine group and the O-methyl oxime could direct the reaction to position C (Figure 3). Nevertheless, the intermediate directing the reaction onto position A through pyridine was calculated to be more stable (E_{rel} = −14.9 kcal/mol) compared with the two intermediates that direct the reaction to position C (E_{rel} = −11.5 or −7.9 kcal/mol depending on whether pyridine or oxime ether coordinates). Position B, stabilized by only the oxime ether, was also less favored (E_{rel} = −11.6 kcal/mol). Interestingly, the potential synergy between the two DGs was not observed: the relative energy of the palladacycle with both DGs coordinated was much higher than either individual coordination, namely, 4.6 kcal/mol. From this, we can conclude that only the strongest DG coordinates to palladium. For two positions that both can be activated by the strongest group, the least sterically hindered position would be favored. These results are in agreement with experimental data from Kalyani et al. (Kalyani and Sanford, 2005) who also observed that the less sterically hindered position was preferred for palladium-catalyzed C–H activations.

Fragmentation Can Be Used to Compare DGs in a Full Molecule

Encouraged by these results, we sought to simplify the model further: could the regioselectivity of complex molecules be predicted using relevant fragments? In other words, can we compare the relative energies of the metallacycles with fragments featuring only one DG and successfully predict the reaction sites on entire molecules? An example of such fragmentation is illustrated in Scheme 4. Exemplified by compound **1** again, the resulting fragments are methyl benzoate (ethyl was replaced by methyl in the model fragment) and 2-phenylpyridine. When coordinated to palladium, these form metallacycles with relative energies

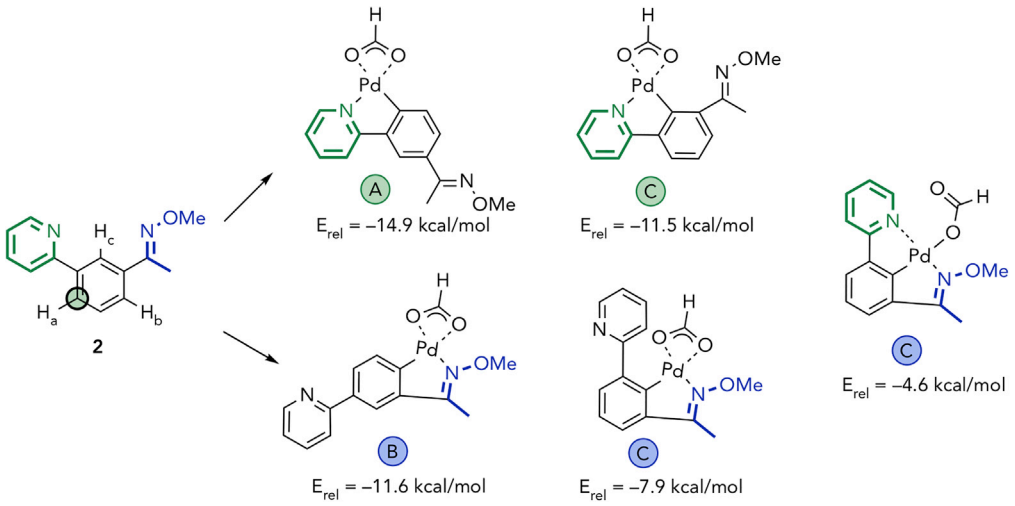

Figure 3. Compound 2 Has Three Positions that Could React

The less hindered position activated by the strongest DG is the preferred reaction site, both computationally and experimentally. Experimental C–H activation site is marked by a black circle; predicted site of activation is marked by a green-filled circle; DGs are highlighted with color. See exact energies in Table S2.

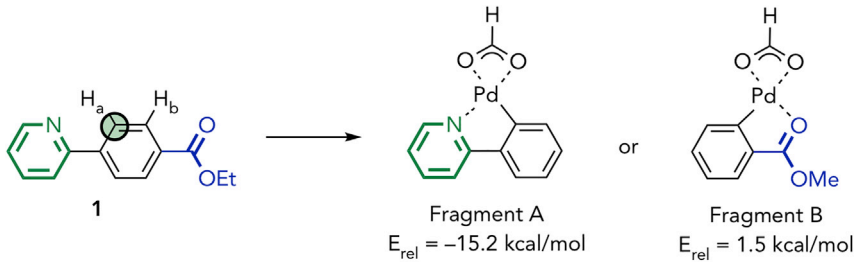

Scheme 4. Compound 1 and the Fragments that Can Be Used to Predict the Site of Reaction

Experimental C–H activation site is marked by a black circle; predicted site of activation is marked by a green-filled circle; DGs are highlighted with color.

of 1.5 and −15.2 kcal/mol, respectively. In agreement with our previous calculations and with literature precedents (Li et al., 2011; Hull et al., 2006), these energies indicate that pyridine is a stronger DG than the ester.

As discussed earlier, certain DGs can in principle direct the catalyst to more than one aromatic carbon. For example, in compound **3**, three positions can potentially be activated (Scheme 5). To investigate these reactive sites, three fragments were created and scored based on the stability of the corresponding organopalladium intermediates. The relative energy obtained for the intermediate leading to the activation at A was −13.3 kcal/mol, whereas palladacycles formed at B and C resulted in E_{rel} = 4.4 and 2.0 kcal/mol, respectively. This indicates that position A is activated by the strongest DG in this case and that positions B and C are much less likely to react, which is in agreement with experimental data (Tredwell et al., 2011).

In the fragmentation of the previous molecule, alkyl chains on the reacting aryl group were removed leaving only a mono-substituted benzene. The validity of this approximation was evaluated empirically by observing experimental results for a variety of DGs. The reactivity of DGs overshadows the impact of substituents: irrespective of their electron donating/withdrawing abilities, they cannot shift the reactivity from a strong DG to a weak one. In the case of two competing DGs, substitution can be used to either block a position *ortho* to a DG (Figure 4.1) or create steric hindrance from a *meta* position that will direct the reaction to a less sterically hindered carbon available to the DG (Figure 4.2).

When the same DG can activate carbons on different rings, strong electron donating or withdrawing groups can be used to impact selectivity: since the reaction has an electrophilic character (Scheme 1), an electron-rich ring is more likely to react than an electron-poor ring. For example, once a nitro group is placed on one ring of a benzophenone (**8** versus **9**), the activation is observed only on the unsubstituted

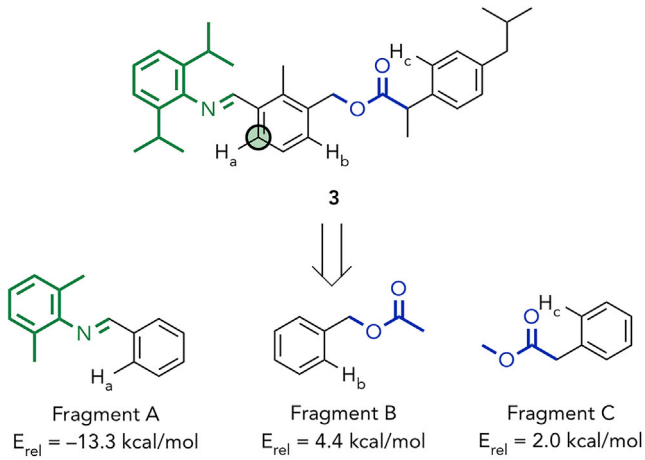

Scheme 5. Compound 3 and the Fragments that can Be Used to Predict the Site of Reaction

Experimental C–H activation site is marked by a black circle; predicted site of activation is marked by a green-filled circle; DGs are highlighted with color.

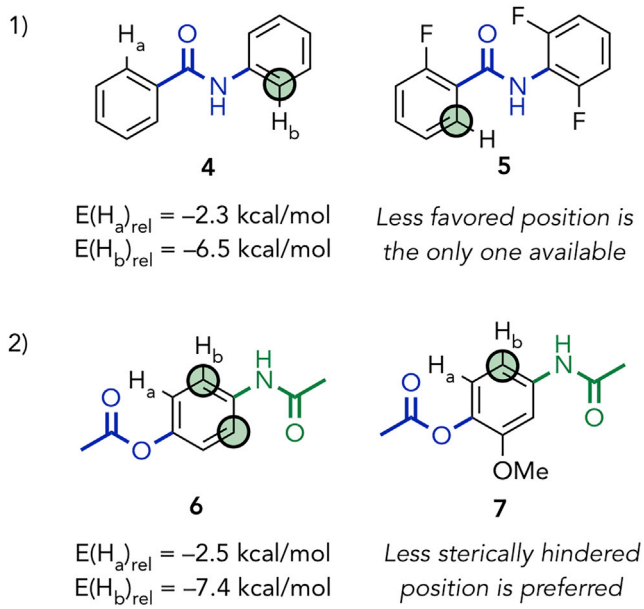

Figure 4. Substituents on Aromatic Rings Cannot Be Used to Shift Reactivity Away from a Strong DG to a Weak One
However, they can be used to block an accessible *ortho*-position (Shan et al., 2012) or to produce steric hindrance at the *meta*-position(Yang et al., 2007).
Experimental C—H activation site is marked by a black circle; predicted site of activation is marked by a green-filled circle; DGs are highlighted with color.

ring (Figure 5) (Xiao et al., 2011; Shan et al., 2012). Similarly, a cyano group on an azobenzene leads to reactivity on only the unsubstituted ring (**10** versus **11**) (Dong et al., 2014). Conversely, the presence of an electron donating group directs the reaction to the same ring, as illustrated by the methoxy substituent on the azobenzene (**10** versus **12**) (Xiong et al., 2013). For these types of compounds, where the directing power is identical for two different positions, selectivity between the two DG-activated positions will be determined by rules similar to EAS.

The same fragmentation approach was used to obtain E_{rel} for DGs in 150 other compounds; the results for six compounds are presented in Figure 6, whereas the rest can be found in the Data S1–S4. The DGs for *ortho*-activation of aromatic carbons were extracted from a review by Chen et al. (2015). To render fragments more transferable, alkyl chains were replaced by methyl groups (e.g., compound **15**) and other substituents on the aromatic rings were removed (e.g., compound **18**). Applying the reactivity patterns described earlier, a simple analysis can be performed on relatively complex molecules with high

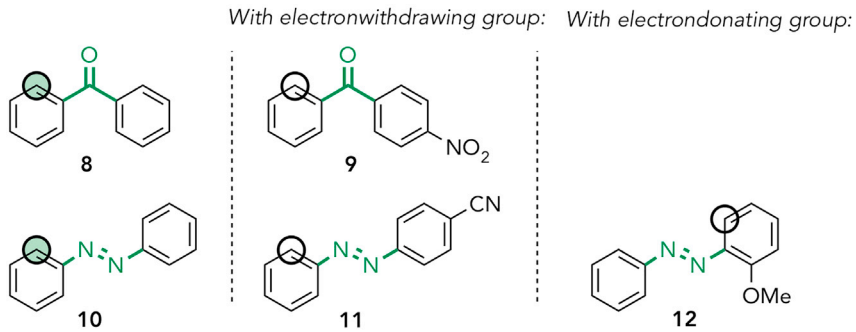

Figure 5. Examples of Compounds in which the DG Activates Two Different Positions: Selectivity Can Be Narrowed Using Ring Substituents
Experimental C—H activation site is marked by a black circle; predicted site of activation is marked by a green-filled circle; DGs are highlighted with color.

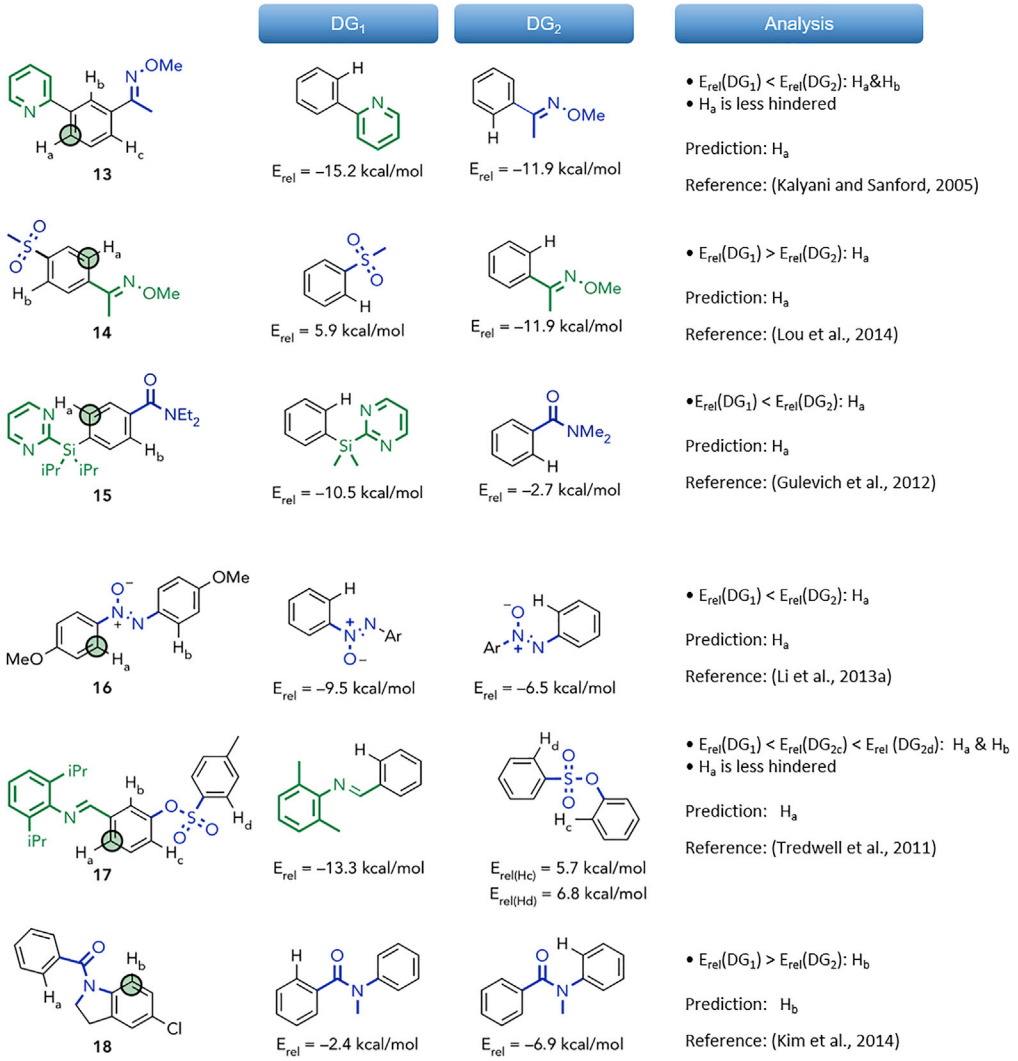

Figure 6. Examples of Fragmentation of Compounds for DGs Strength Comparison

Experimental C–H activation site is marked by a black circle; predicted site of activation is marked by a green-filled circle; DGs are highlighted with color. For experimental results see references Gulevich et al., 2012; Kalyani and Sanford, 2005; Li et al., 2013; Lou et al., 2014; Tredwell et al., 2011, and Kim et al., 2014. See rest of compounds in Data S5.

accuracy in reaction site prediction: of 150 examples collected, only 4 predictions did not match experimental results.

So far, we have considered neither the reaction conditions nor the coupling partner (or its absence). In reality, these are important parameters that can affect the reaction outcome. For example, how does the strength of a directing group depend on the protonation state of the compound? How would our approach perform in such cases?

The DG's Protonation State Influences Regioselectivity

N-phenylbenzamide (**4**) presents a perfect example of a system in which selectivity is highly influenced by reaction conditions (Figure 7). Although experimental studies seem to report contradictory results, some supporting reaction at position A (Boele et al., 2002; Zhu et al., 2018) and others illustrating functionalization at position B (Kametani et al., 2000; Chou et al., 2017), a closer scrutiny at reaction conditions easily rationalizes these divergent reactivity profiles. Under acidic conditions, where the amide is presumably present in its neutral form, transformations take place at position A. In contrast, under mild basic

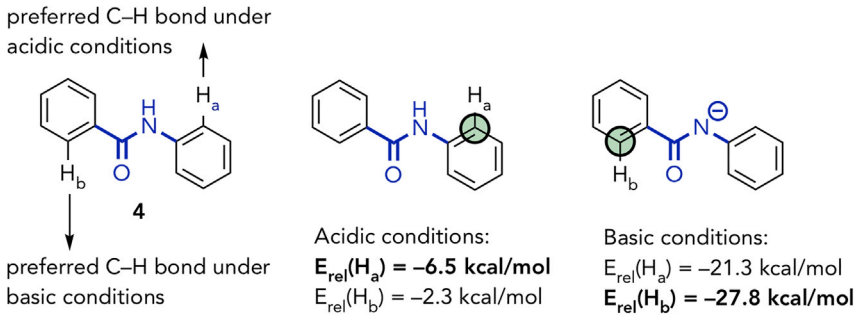

Figure 7. Compound 4, *N*-phenylbenzamide, Shows Acidity-Dependent Reactivity in Palladium-Catalyzed C−H Activation

Experimental C−H activation site is marked by a black circle; predicted site of activation is marked by a green-filled circle; DGs are highlighted with color.

conditions, where the amide may be deprotonated in a kinetically preferred CMD reaction of the N−H group, reactions occur on position B. Using our model, this shifting preference could be captured. In the presence of acid, the neutral DG prefers to coordinate to palladium through the oxygen, leading to a metallacycle intermediate activating position A that is 4.2 kcal/mol more stable than the palladacycle activating B. Under basic conditions, the metallacycle intermediate is generated from deprotonated amide with a formal negative charge on the nitrogen. This coordination is preferred over the cycle with oxygen coordination (E_{rel}(B) = −27.8 kcal/mol versus E_{rel}(A) = −21.3 kcal/mol), leading to activation of position B instead.

To provide a proof of concept and to validate our predictions, we have synthesized substrate **19** featuring both pyridine and acetanilide DGs. According to our model, pyridine is a very strong DG with E_{rel} = −15.2 kcal/mol, whereas the acetamide is significantly weaker (E_{rel} = −7.4 kcal/mol). Using this compound, we wanted to investigate whether it is possible to shift the reactivity away from the pyridine DG by altering the pH of the reaction. On the one hand, we anticipated that by addition of a strong acid, the pyridine moiety should be protonated and under these conditions the acetanilide should become the strongest DG. On the other hand, we envisioned that deprotonation of the acetanilide functionality would result in the formation of a charged amide DG, which according to our model, should coordinate more strongly to palladium than the pyridine fragment does.

The initial conditions of arylation of **19** were inspired by Sanford's seminal report (Kalyani et al., 2005). Under the typical C−H arylation conditions (in acetic acid), we observed mostly arylation *ortho* to the pyridine DG (**19a**-**b**), whereas products of arylation *ortho* to the acetanilide (mono- or bis-arylation products, including **19c** and **d**) could not be detected, confirming and supporting that under these « neutral » conditions, the pyridine fragment is a much stronger binder to palladium than the acetanilide moiety (Scheme 6.1, see also competition experiments in Tables S4 and S5). Performing the same transformation in toluene in the presence of a strong Brønsted acid (HBF_4 as its diethyl ether complex) resulted in an overall poorer reactivity profile; however, in this reaction small amounts of products of arylation *ortho* to the acetanilide (**19c** and **d**) could be isolated and characterized, whereas no trace of products of arylation *ortho* to the pyridine could be detected (Scheme 6.2). Although this approach to switch regioselectivity has not been optimized, the latter experiment provides a proof of concept and supports our model's prediction. The final test was the deprotonation of the acetamide DG under strong basic conditions. Stoichiometric deprotonation of **19** in the presence of freshly prepared lithium diisopropyl amide (LDA), addition of this lithium amide to stoichiometric $Pd(OAc)_2$, and subsequent exposure to Ph_2IBF_4 did not lead to any observable amount of arylation products **19c** or **19d**, and only traces of **19b** were isolated. The identical procedure applied to acetanilide led to much lower reactivity than that typically observed for the same arylation under catalytic and neutral conditions (see Transparent Methods in Supplemental Information). This suggests that most of the palladium presumably forms an unproductive and catalytically inactive complex. Additionally, reproducing the latter experiment in the presence of 2-phenylpyridine led to arylation of 2-phenylpyridine only. Therefore, we can conclude that LDA is not a suitable base to achieve both satisfactory reactivity and a regioselectivity shift under the conditions presented herein.

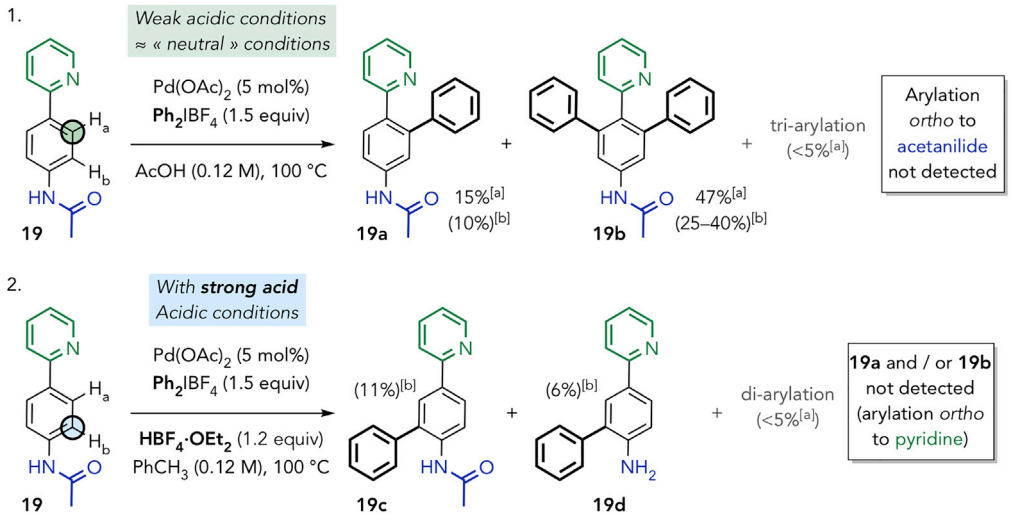

Scheme 6. C–H Arylation of Bifunctional Substrate 19 under a Range of Conditions: Proof of Concept of Control of Regioselectivity via Protonation or Deprotonation of DGs

1. C–H Arylation of **19** under « neutral » conditions.
2. C–H Arylation of **19** under strong acidic conditions.

Experimental C–H activation site is marked by a black circle; predicted site of activation is marked by a green-filled and blue-filled circles; DGs are highlighted with color. Also see Tables S4 and S5 and Data S8–S16. [a]^{1}H NMR yield employing 1,1,2,2-tetrachloroethane as internal standard >; [b] Isolated yield (as measured against 1,1,2,2-tetrachloroethane as internal standard).

Coupling Partners Play a Role if the Energy Difference Is Small

When a DG can activate more than one position with similar strength, the nature of the coupling partner starts playing a role. As exemplified by compound **20**, a triazole DG on the naphthalene can direct the catalyst to either position A or B (Figure 8). Comparing the relative energies of the corresponding metallacycles suggests that the DG would activate both positions to a similar extent. However, from experiment, a mixture of products is not observed. In the paper by Shi and Kuang (2014), *ortho* alkoxylations on this aryl triazole were reported to take place on position A. Alternatively, in the study by Tian et al. who investigated the bromination of similar molecules, compound **20** reacted on position B (Tian et al., 2013). Both alkoxide and bromide will have relatively high barriers to reductive elimination. Thus, it is conceivable that in at least one of the cases, the reductive elimination becomes rate limiting, allowing the two palladium intermediates to equilibrate before the irreversible selectivity-determining step. Since our model does not describe the reaction steps after C–H activation, it cannot be used to predict which of the two positions will be reactive if another step becomes selectivity determining.

Another important aspect of the reaction conditions is the presence or absence of coupling partners. This information is important in biaryls or systems with fused rings. For example, in the compounds shown in Figure 9, the DGs reach two positions, A (on same ring) and B (on neighboring ring). By calculation, the activations on positions A are more favorable and those will react if a coupling partner is available (**21a** [Daugulis and Chiong, 2009; Chiong et al., 2007] and **22a** [Kim et al., 2010]). Alternatively, in the absence of an external coupling partner, there is no energetically accessible pathway from the activation of position A;

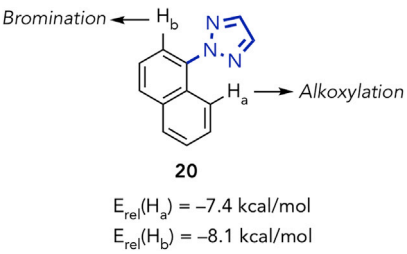

Figure 8. Compound 20: Relative Energies of Metallacycles for Positions A and B Are within the Margin of Error (1 kcal/mol), so the Model Is Unable to Distinguish between the Two

Other factors such as the nature of the coupling partner will determine regioselectivity. DG is highlighted with color.

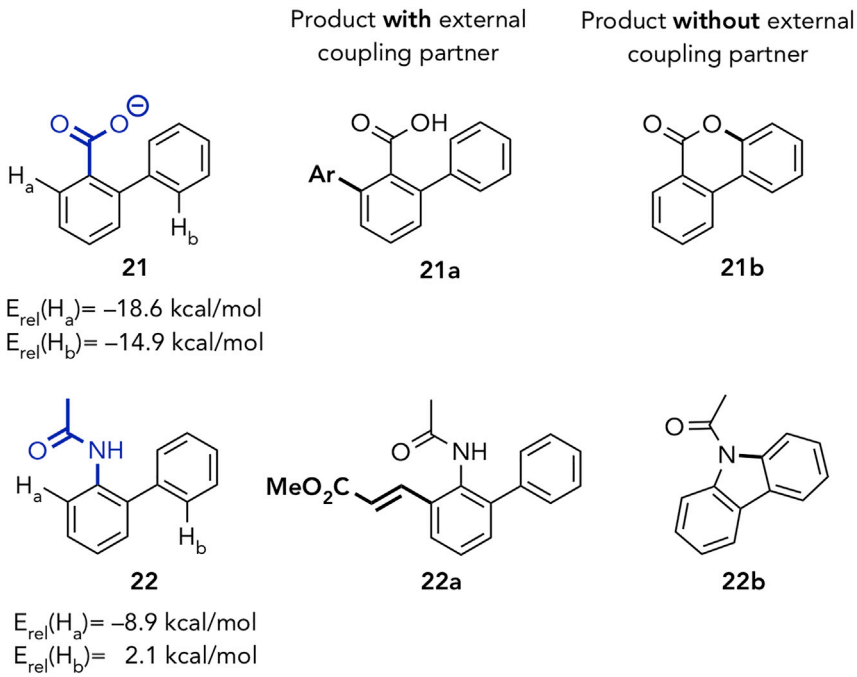

Figure 9. Examples of Compounds where the Absence of a Coupling Agent Changes Selectivity
DGs are highlighted with color. See rest of similar compounds in Data S6.

thus, the system will eventually equilibrate to position B, which allows cyclization (**21b** [Li et al., 2013b] and **22b** [Li et al., 2014]).

Directing Strength Scale Combining the Results for 133 DGs

Combining the observations from the above-mentioned examples and many more, we have demonstrated that our simplified regioselectivity model for palladium-catalyzed C−H activation is predictive (see Data S5–S7). In molecules with multiple competing DGs, the reaction site can be determined by comparing the relative energy of metallacycles consisting of fragments and palladium formate. To validate our approach on as many compounds as possible, we have (1) assembled a testing set featuring a variety of DGs, (2) selected fragments covering the test molecules, and (3) compiled the results into a directing strength scale (see Data S1–S4 in Supplemental Information).

The scale allows one to easily find fragments that correspond to a studied molecule and compare their relative energies: the one with the lowest energy should lead to the major product of the C−H activation α to the DG (Figure 10). As explained earlier, the protonation state of a DG affects strongly its ability to form a stable metallacycle with palladium. As such, the correct fragments must be compared to obtain an accurate prediction. Evidently, the larger the difference between the energies of two DGs, the more likely it is that the model would detect the appropriate reaction site. Our results indicate that DGs within ca. 1 kcal/mol of each other are indistinguishable. In cases in which a molecule bears DGs of similar strength, other electronic and steric factors prevail, as discussed earlier. DGs in their deprotonated form are generally much stronger than the neutral ones. Among the strongest are amines, alcohols, and bidentate (designer) DGs. An example of a bidentate DG is *N*-(quinolin-8-yl)benzamide, which binds to palladium through both nitrogens, becoming one of the strongest directing group on the list. Although this moiety performs better under basic conditions, neutral/mildly acidic conditions can still allow for the deprotonation of the amide due to the effect of palladium (Gou et al., 2009). A wide range of different coupling partners can be used with this DG (Kanyiva et al., 2014; Wang et al., 2015; Li et al., 2016; Liao et al., 2018). In general, in both neutral and charged forms, the strongest coordination to palladium takes place through a nitrogen, whereas groups that bind through an oxygen atom seem to be weaker. This tendency is further illustrated by another bidentate DG, 2-(benzylideneamino)acetic acid. This imine is a transient DG (Liu et al., 2017), generally formed *in situ* from an aldehyde or a ketone and an amino acid (Wang et al., 2018; Xu et al., 2017). In the presence of base, both the carboxylic acid and the imine

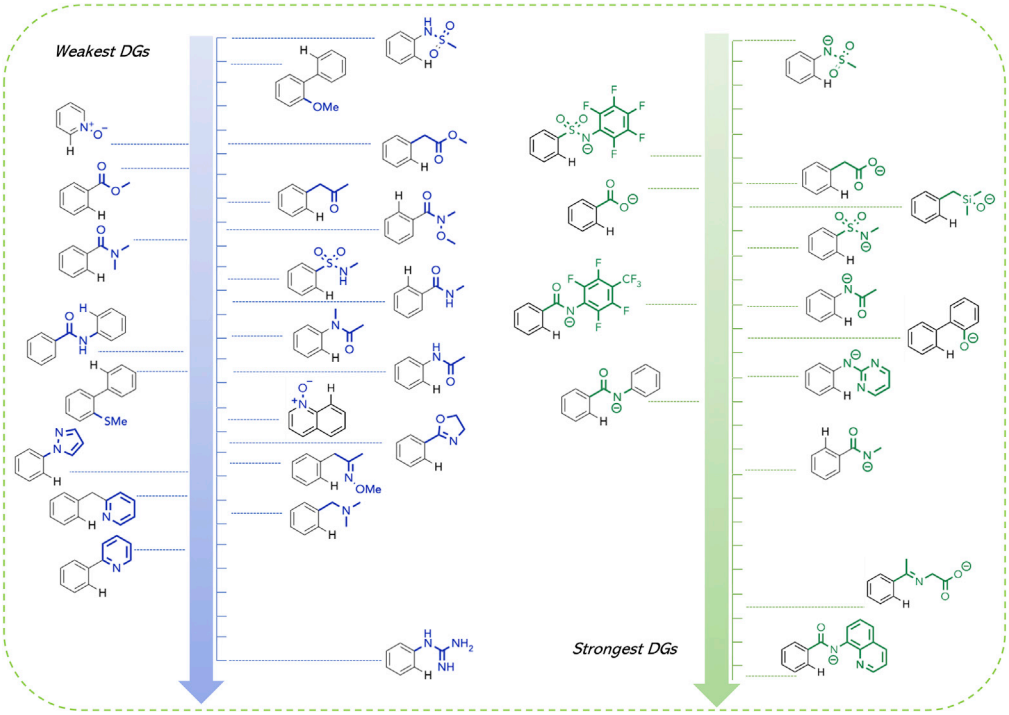

Figure 10. DGs Relative Strength Scale: A Few Key Examples
See all studied DGs in Data S1–S4.

nitrogen coordinate to palladium, with a relative strength slightly weaker than the *N*-(quinolin-8-yl)benzamide. Once the coupling step is completed, the aldehyde or ketone can be recovered by addition of acid (Zhang et al., 2019).

Once all results for the fragments were assembled into an ordered list, interesting patterns started emerging. For example, there is a correlation between the strength of a DG and the size of the ring it forms in the corresponding metallacycle. Expectedly, DGs that form four-member rings are the weakest. As exemplified in Figure 11.1 by compound **23**, the negatively charged oxygen coordinates to palladium leading to two potential activation sites. Reactive site A forms a four-member ring metallacycle and has a relative energy of 1.9 kcal/mol; reactive site B forms a five-member ring with palladium, which leads to a relative energy of

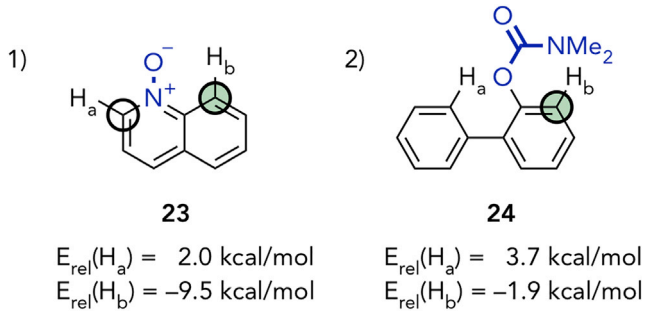

Figure 11. Trends in Reactivity
1: The presence of phosphines alters the reactivity to the less energetically favorable position A (Willis and Smith, 2014; Liu and Tzschucke, 2016; Roudesly et al., 2018; Lehecq et al., 2017).
2: Positions activated through 6-member palladacycles are more favorable than the ones forming larger rings (Bedford et al., 2009; Zhao et al., 2010; Sun et al., 2015).
Experimental C—H activation site is marked by a black circle; predicted site of activation is marked by a green-filled circle; DGs are highlighted with color.

−9.7 kcal/mol. When we examined the experimental results, we were surprised to find that most papers report position A-selective activation. However, all these examples had one thing in common: the presence of phosphines as reagents (Willis and Smith, 2014; Liu and Tzschucke, 2016; Roudesly et al., 2018; Lehecq et al., 2017). As demonstrated by Stephens et al. (2015a), phosphines play an important role in diverting the selectivity from the more energetically favorable reactive site B toward position A. If phosphines are not used, the reactivity is observed on position B, as our model predicted (Stephens et al., 2015a, 2015b). This example highlights that our approach can be used only with palladium ligands with similar reactivity to acetates.

DGs that form large rings have lower energies than four-member rings but still lose to five- or six-member ring forming groups. For example, the carbamate group on compound **24** (Figure 11.2) can direct to both positions A and B, with relative strengths of 3.7 and −1.9 kcal/mol, respectively. This is in line with the observed experimental results showing reactivity on position B (six-member ring palladacycle) (Zhao et al., 2010; Sun et al., 2015).

The majority of DGs form either five- or six-member ring palladacycles. From the analysis of our calculations, we found no strong preference toward either. Several examples collected in Figure 12 demonstrate that the computed relative strengths of these DGs differ by less than 1 kcal/mol. The same trend is observed for the deprotonated form as well.

Examples of Mismatch between Predictions and Experimental Results

Of the 150 examples collected, four predictions did not match experimental results. In this section we will go through these cases and, when possible, rationalize the discrepancies.

The first example is an illustration of the method's limitation: compound **31** was selectively hydroxylated on position A in presence of $Pd(OAc)_2$, TFA/TFAA, and Selectfluor (Shan et al., 2012). The DGs found in this molecule are trifluoroacetamide and benzophenone (Figure 13.1). According to the relative energies corresponding to these DGs, the trifluoroacetamide, activating position C, is slightly stronger than benzophenone. Our model cannot distinguish groups that have relative energies within 1 kcal/mol; thus, the electron richness of each ring should be used to predict which one is the most likely to react. Since the trifluoroacetamide is an electron-withdrawing group (Hansch et al., 1991), we should expect the reaction to take place on the unsubstituted ring of compound **31** on position A. Another possibility that we considered was the influence of TFA on reactivity. A recent paper by Jiří Vaňa et al. highlighted the effect of the carboxylates on different aspects controlling reactivity of

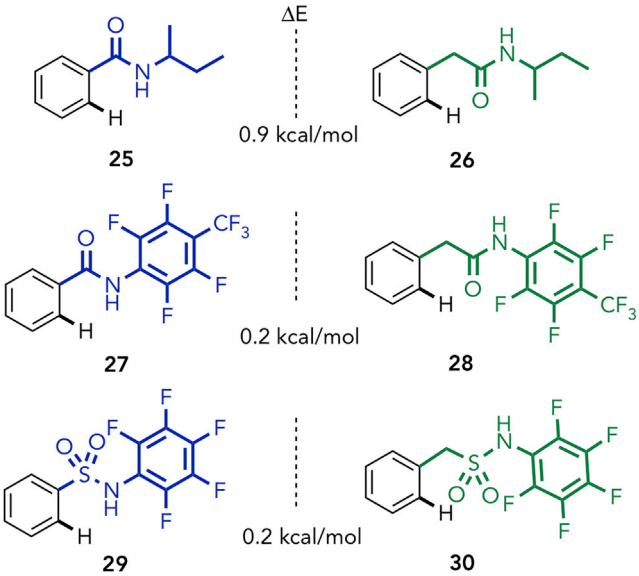

Figure 12. There Is No Clear Preference between DGs Forming Five- and Six-Member Ring Intermediates with Palladium

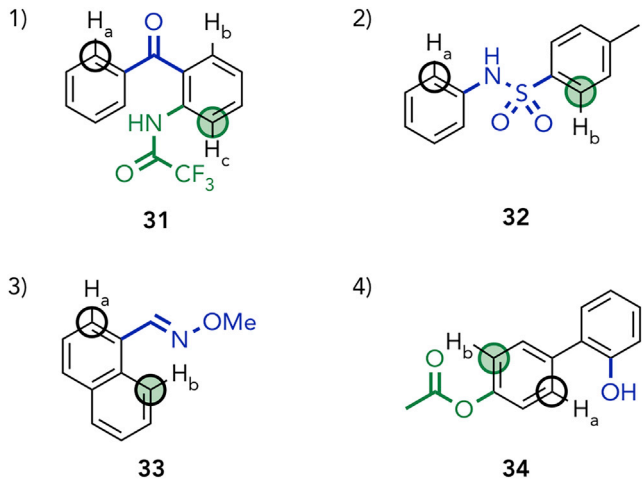

Figure 13. Molecules for which the Predicted Reactive Site Did Not Match Experiment

1. Compound **31** with two competing groups of similar strengths at play: benzophenone and trifluoroacetamide. See exact energies in Table S3.
2. Compound **32** where activation on B is wrongly predicted over experimentally observed activation on A.
3. Compound **33**: in similar conditions, but with different coupling partners, the reactivity shifted from A to B.
4. Compound **34**: the conditions do not seem to allow for deprotonation of the phenol, yet this DG wins over the acetate, which is against predictions.

Experimental C−H activation site is marked by a black circle; predicted site of activation is marked by a green-filled circle; DGs are highlighted with color. See also Data S7.

the palladium-catalyzed C−H activation (Váňa et al., 2019). The authors concluded that TFA can replace acetic acid on the metal, which would change the reactivity of the catalyst by increasing the electrophilicity of the palladium atom. We computed these energies using our approach while replacing the formate ligand by a trifluoroacetate in the palladacycles with the corresponding fragments. Interestingly, the use of TFA as ligand shifted the relative stability of the organopalladium complexes, resulting in the benzophenone fragment being 6.2 kcal/mol lower in energy than the trifluoroacetamide. With this modification of the model, the experimental results are in agreement with the computed values.

Another case in which our predictions were incorrect is illustrated in Figure 13.2, compound **32**. According to the relative energies computed, the position *ortho* to the sulfonyl moiety (B) has a higher chance of being activated in both the neutral and the deprotonated forms: the nitrogen coordinates to palladium forming a five-member intermediate, which is much more stable than the coordination through the sulfonyl's oxygens. However, experimental results show that the activation takes place on the carbon A *ortho* to the nitrogen. A recent computational study on a similar palladium catalyst suggested that the activation does indeed proceed through the nitrogen coordination to palladium (Qiao et al., 2019). The following acetate-mediated N−H deprotonation leads to a four-member transition state that directs the reaction to position A. According to their results, the coordination through an oxygen of the sulfonyl moiety is over 10 kcal/mol higher in energy, which is in line with our predictions. However, the reported reaction mechanism does not proceed to a stable palladacycle intermediate following the C−H activation step. It is possible that, in this case, no such intermediate is formed; thus, our model cannot be used on this DG.

The next example where our model predictions differed from experiment is compound **33** (Figure 13.3). From the literature, we found two studies reporting different regioselectivities (Thirunavukkarasu and Cheng, 2011; Yu et al., 2008). However, the relative energies for positions A and B in this molecule are substantially dissimilar (−10.7 and −15.6 kcal/mol, respectively); thus, we would expect reactivity solely on position B. This is in line with the reported product of arylation of **33**, reported by Thirunavukkarasu et al. (Thirunavukkarasu and Cheng, 2011). Conversely, a study on oxidative ethoxycarbonylation described activation on position A (Yu et al., 2008), using diethyl azodicarboxylate (DEAD) as coupling partner. The authors proposed that this reagent delivers a CO_2Et radical by thermal decomposition

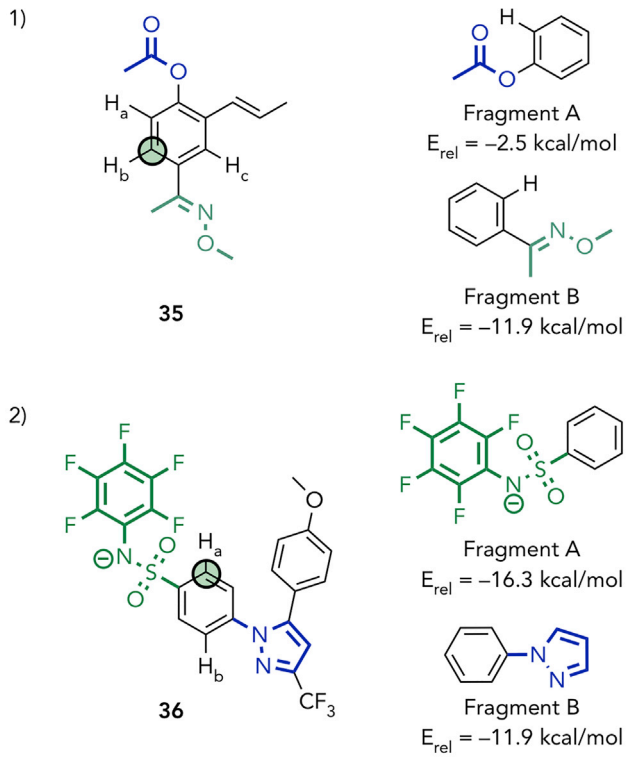

Figure 14. Drug Precursors/Analogues That Were Obtained Using Pd-catalyzed C–H Activation

Experimental C–H activation site is marked by a black circle; predicted site of activation is marked by a green-filled circle; DGs are highlighted with color. See rest of compounds in Data S5.

and promotes the reaction through a Pd^{IV} intermediate, which falls outside of the reactivity predicted by our model.

The last prediction that did not agree with experimental results was for compound **34**. The DGs at play are highlighted in Figure 13.4: phenol and acetate. The reaction was performed in AcOH, with benzoquinone as oxidant, so the phenol is expected to be in its neutral form (Zhang et al., 2014). This suggests that the acetate DG should lead to the major product (position B), since its relative energy is −8.8 kcal/mol lower than the one of the palladacycle with the phenol DG. However, the reported product is the alkenylation at position A exclusively. According to our model, this could be possible only if a portion of the phenol DG was deprotonated, which could explain the low yield observed for this reaction (34%).

Final Test: Regioselectivity on Drug-like Compounds

As a final test for the model, we found examples of drug-like molecules that have a palladium-catalyzed C–H activation step in their synthesis and verified that the correct regioselectivity can be predicted using our directing strength scale.

The first example is a natural product, penchinone A, recently isolated from *Penthorum chinense*, and it was found to have anti-cancer and anti-inflammatory properties (He et al., 2015). The synthesis of this compound and several derivates has since then been achieved through palladium-catalyzed acylation of compound **35** (Oh et al., 2017). In this molecule, two DGs compete: an acetate and an oxime (Figure 14.1). Based on the relative energies of the corresponding fragments' intermediates, the oxime DG is stronger than the acetate, which is in accordance with the reported product of acylation.

The second example is celecoxib **36**, an anti-inflammatory drug, and its analogues (Figure 14.2). The two competing groups are the sulfonamide and the pyrazole, both strong DGs. In the study by

Dai et al. (2011), a variety of couplings were performed under basic conditions, such that the sulfonamide is expected to be deprotonated. Negatively charged groups have a stronger coordination to palladium; thus, the sulfonamide will be the winning DG in this case, which is in line with experimental observations.

As demonstrated by the many examples given earlier, the model described herein yields accurate predictions of reactive sites on complex molecules, which should allow chemists to more readily apply this reaction.

With the introduction of late-stage functionalization into mainstream chemistry, regioselectivity prediction became an even more challenging exercise. In the field of metal-catalyzed C−H activation, one of the most successful approaches to increase regioselectivity is to use DGs. However, when such a group can direct reactivity to several sites or when multiple DGs are present in the reactant, accurately predicting which carbon will be activated can be problematic. With little literature reports that compare different DGs, the experimentalist is left to rely on experience and intuition to make synthetic decisions. In our study of palladium-catalyzed directed C–H activations, we offer a scale of the relative strengths of common functional groups and their relative capacity to *ortho*-direct palladium-catalyzed aromatic C−H activation. We demonstrated that, although the use of fragments and intermediates instead of full molecules and transition states may seem like a dramatic simplification, comparing only the relative energies of corresponding palladacycles allows one to quickly estimate which position is most likely to react. Additionally, our scale is able to capture the shifting reactivity at different pH. With over a hundred common DGs examined, the full scale enables one to make regioselectivity predictions on complex molecules in a flash, as well as encourages to try new unprecedented combinations of functional groups leading to unusual compounds.

Limitation of the Study

The method presented herein was developed to compare the strength of *ortho*-directing groups for the activation of unsubstituted aromatic carbons by $Pd(OAc)_2$ model catalyst. This approach is not directly transferable to *meta*-directing activation or to hydrogens bound to non-aromatic carbons or to heteroatoms. Additionally, although we demonstrate that the strength of a directing group depends on its protonation state, the current model does not compute the pKa of directing groups, and users need to decide by themselves whether the group they are interested in would be deprotonated at the reaction conditions they will use to apply the correct scale. Finally, the sensitivity of the model was found to be around 1 kcal/mol: if the relative energies of two directing groups are within this range, then the model cannot be applied to know which group would lead to the main product of the reaction.

METHODS

All methods can be found in the accompanying Transparent Methods supplemental file.

SUPPLEMENTAL INFORMATION

Supplemental Information can be found online at https://doi.org/10.1016/j.isci.2019.09.035.

ACKNOWLEDGMENTS

We would like to thank Pernilla Korsgren for her support. A.T. and M.E.M. are fellows of the AstraZeneca postdoc program.

AUTHOR CONTRIBUTIONS

Conceptualization, P.-O.N., M.J.J., A.T., and I.T.; Methodology, P.-O.N., M.J.J., M.E.M., and A.T.; Software, A.T.; Validation, A.T., M.E.M., and P.-O.N.; Formal Analysis, A.T. and M.E.M.; Investigation, A.T. and M.E.M.; Data Curation, A.T. and M.E.M.; Writing – Original Draft, A.T., M.E.M., M.J.J., and P.-O.N.; Writing – Review & Editing, A.T., M.E.M., M.J.J., I.T., C.S., and P.-O.N.; Visualization, A.T., M.J.J., and M.E.M.; Supervision, P.-O.N., M.J.J., I.T., and C.S.; Project Administration and Funding, I.T., P.-O.N., and M.J.J.

DECLARATION OF INTERESTS

The authors declare no competing interests.

Received: June 4, 2019
Revised: August 29, 2019
Accepted: September 24, 2019
Published: October 25, 2019

REFERENCES

Abrams, D.J., Provencher, P.A., and Sorensen, E.J. (2018). Recent applications of C–H functionalization in complex natural product synthesis. Chem. Soc. Rev. *47*, 8925–8967.

Andersson, T., Broo, A., and Evertsson, E. (2014). Prediction of drug candidates' sensitivity toward autoxidation: computational estimation of C–H dissociation energies of carbon-centered radicals. J. Organomet. Chem. *103*, 1949–1955.

Bedford, R.B., Webster, R.L., and Mitchell, C.J. (2009). Palladium-catalysed ortho-arylation of carbamate-protected phenols. Org. Biomol. Chem. *7*, 4853–4857.

Bell, R.P., and Hinshelwood, C.N. (1936). The theory of reactions involving proton transfers. Proc. R. Soc. Lond. Ser. A *154*, 414–429.

Bera, M., Modak, A., Patra, T., Maji, A., and Maiti, D. (2014). Meta-selective arene C–H bond olefination of arylacetic acid using a nitrile-based directing group. Org. Lett. *16*, 5760–5763.

Boele, M.D.K., Van Strijdonck, G.P.F., De Vries, A.H.M., Kamer, P.C.J., De Vries, J.G., and Van Leeuwen, P.W.N.M. (2002). Selective Pd-catalyzed oxidative coupling of anilides with olefins through C—H bond activation at room temperature. J. Am. Chem. Soc. *124*, 1586–1587.

Cernak, T., Dykstra, K.D., Tyagarajan, S., Vachal, P., and Krska, S.W. (2016). The medicinal chemist's toolbox for late stage functionalization of drug-like molecules. Chem. Soc. Rev. *45*, 546–576.

Chen, Z., Wang, B., Zhang, J., Yu, W., Liu, Z., and Zhang, Y. (2015). Transition metal-catalyzed C–H bond functionalizations by the use of diverse directing groups. Org. Chem. Front. *2*, 1107–1295.

Chiong, H.A., Pham, Q.-N., and Daugulis, O. (2007). Two methods for direct ortho-arylation of benzoic acids. J. Am. Chem. Soc. *129*, 9879–9884.

Chou, H.-M., Jhou, J.-N., and Hong, F.-E. (2017). Incorporation of norbornene moiety onto the arene of diaryl substituted amides through C–H functionalization. J. Organomet. Chem. *853*, 178–183.

Dai, H.-X., Stepan, A.F., Plummer, M.S., Zhang, Y.-H., and Yu, J.-Q. (2011). Divergent C–H functionalizations directed by sulfonamide pharmacophores: late-stage diversification as a tool for drug discovery. J. Am. Chem. Soc. *133*, 7222–7228.

Davies, H.M.L., and Morton, D. (2017). Collective approach to advancing C–H functionalization. ACS Cent. Sci. *3*, 936–943.

Davies, D.L., Donald, S.M.A., and Macgregor, S.A. (2005). Computational study of the mechanism of cyclometalation by palladium acetate. J. Am. Chem. Soc. *127*, 13754–13755.

Davies, D.L., Macgregor, S.A., and Mcmullin, C.L. (2017). Computational studies of carboxylate-assisted C–H activation and functionalization at group 8–10 transition metal centers. Chem. Rev. *117*, 8649–8709.

Desai, L.V., Stowers, K.J., and Sanford, M.S. (2008). Insights into directing group ability in palladium-catalyzed C—H bond functionalization. J. Am. Chem. Soc. *130*, 13285–13293.

Dey, A., Sinha, S.K., Achar, T.K., and Maiti, D. (2019). Accessing remote meta- and para-C(sp2)—H bonds with covalently attached directing groups. Angew. Chem. Int. Ed. *58*, 10820–10843.

Dong, J., Jin, B., and Sun, P. (2014). Palladium-catalyzed direct ortho-nitration of azoarenes using NO2 as nitro source. Org. Lett. *16*, 4540–4542.

Evans, M.G., and Polanyi, M. (1936). Further considerations on the thermodynamics of chemical equilibria and reaction rates. J. Chem. Soc., Faraday Trans. *32*, 1333–1360, https://doi.org/10.1039/TF9363201333.

Gensch, T., Hopkinson, M.N., Glorius, F., and Wencel-Delord, J. (2016). Mild metal-catalyzed C–H activation: examples and concepts. Chem. Soc. Rev. *45*, 2900–2936.

Gorelsky, S.I., Lapointe, D., and Fagnou, K. (2008). Analysis of the concerted metalation-deprotonation mechanism in palladium-catalyzed direct arylation across a broad range of aromatic substrates. J. Am. Chem. Soc. *130*, 10848–10849.

Gou, F.-R., Wang, X.-C., Huo, P.-F., Bi, H.-P., Guan, Z.-H., and Liang, Y.-M. (2009). Palladium-catalyzed aryl C—H bonds activation/acetoxylation utilizing a bidentate system. Org. Lett. *11*, 5726–5729.

Guan, Y., Ingman, V.M., Rooks, B.J., and Wheeler, S.E. (2018). AARON: an automated reaction optimizer for new catalysts. J. Chem. Theor. Comput. *14*, 5249–5261.

Gulevich, A.V., Melkonyan, F.S., Sarkar, D., and Gevorgyan, V. (2012). Double-fold C–H oxygenation of arenes using PyrDipSi: a general and efficient traceless/modifiable silicon-tethered directing group. J. Am. Chem. Soc. *134*, 5528–5531.

Hammond, G.S. (1955). A correlation of reaction rates. J. Am. Chem. Soc. *77*, 334–338.

Hansch, C., Leo, A., and Taft, R.W. (1991). A survey of Hammett substituent constants and resonance and field parameters. Chem. Rev. *91*, 165–195.

Hartwig, J.F., and Larsen, M.A. (2016). Undirected, homogeneous C–H bond functionalization: challenges and opportunities. ACS Cent. Sci. *2*, 281–292.

He, Y.-C., Peng, C., Xie, X.-F., Chen, M.-H., Li, X.-N., Li, M.-T., Zhou, Q.-M., Guo, L., and Xiong, L. (2015). Penchinones A–D, two pairs of cis-trans isomers with rearranged neolignane carbon skeletons from *Penthorum chinense*. RSC Adv. *5*, 76788–76794.

Hull, K.L., Anani, W.Q., and Sanford, M.S. (2006). Palladium-catalyzed fluorination of carbon—hydrogen bonds. J. Am. Chem. Soc. *128*, 7134–7135.

Jensen, F. (1999). Qualitative Theories. The Bell–Evans–Polanyi Principle/Hammond Postulate/Marcus Theory. Introduction to Computational Chemistry (Chichester: John Wiley & Sons Ltd), pp. 364–368.

Kalyani, D., and Sanford, M.S. (2005). Regioselectivity in palladium-catalyzed C—H activation/oxygenation reactions. Org. Lett. *7*, 4149–4152.

Kalyani, D., Deprez, N.R., Desai, L.V., and Sanford, M.S. (2005). Oxidative C—H activation/C—C bond forming reactions: synthetic scope and mechanistic insights. J. Am. Chem. Soc. *127*, 7330–7331.

Kametani, Y., Satoh, T., Miura, M., and Nomura, M. (2000). Regioselective arylation of benzanilides with aryl triflates or bromides under palladium catalysis. Tetrahedron Lett. *41*, 2655–2658.

Kanyiva, K.S., Kuninobu, Y., and Kanai, M. (2014). Palladium-catalyzed direct C–H silylation and germanylation of benzamides and carboxamides. Org. Lett. *16*, 1968–1971.

Kim, B.S., Jang, C., Lee, D.J., and Youn, S.W. (2010). Highly effective Pd-catalyzed ortho olefination of acetanilides: broad substrate scope and high tolerability. Chem. Asian J. *5*, 2336–2340.

Kim, M., Kumar Mishra, N., Park, J., Han, S., Shin, Y., Sharma, S., Lee, Y., Lee, E.-K., Kwak, J.H., and Kim, I.S. (2014). Decarboxylative acylation of indolines with α-keto acids under palladium catalysis: a facile strategy for the synthesis of 7-substituted indoles. Chem. Commun. *50*, 14249–14252.

Kiser, E.J., Magano, J., Shine, R.J., and Chen, M.H. (2012). Kilogram-lab-scale oxindole synthesis via palladium-catalyzed C–H functionalization. Org. Process. Res. Dev. *16*, 255–259.

Lapointe, D., and Fagnou, K. (2010). Overview of the mechanistic work on the concerted

Metallation–Deprotonation pathway. Chem. Lett. *39*, 1118–1126.

Lehecq, A., Rousee, K., Schneider, C., Levacher, V., Hoarau, C., Pannecoucke, X., Bouillon, J.-P., and Couve-Bonnaire, S. (2017). Metal-catalyzed direct C–H fluoroalkenylation of pyridine N–oxides and related derivatives. Eur. J. Org. Chem. *2017*, 3049–3054.

Li, W., Yin, Z., Jiang, X., and Sun, P. (2011). Palladium-catalyzed direct ortho C–H arylation of 2-arylpyridine derivatives with aryltrimethoxysilane. J. Org. Chem. *76*, 8543–8548.

Li, H., Li, P., Zhao, Q., and Wang, L. (2013a). Unprecedented ortho-acylation of azoxybenzenes with α-oxocarboxylic acids by Pd-catalyzed C–H activation and decarboxylation. Chem. Commun. *49*, 9170–9172.

Li, Y., Ding, Y.-J., Wang, J.-Y., Su, Y.-M., and Wang, X.-S. (2013b). Pd-catalyzed C–H lactonization for expedient synthesis of biaryl lactones and total synthesis of cannabinol. Org. Lett. *15*, 2574–2577.

Li, D., Xu, N., Zhang, Y., and Wang, L. (2014). A highly efficient Pd-catalyzed decarboxylative ortho-arylation of amides with aryl acylperoxides. Chem. Commun. *50*, 14862–14865.

Li, C., Zhang, D., Zhu, W., Wan, P., and Liu, H. (2016). Pd(ii)-catalyzed direct functionalization of C–H bonds of benzamides for synthesis of 1,1-difluoro-1-alkenes. Org. Chem. Front. *3*, 1080–1083.

Liao, G., Chen, H.-M., and Shi, B.-F. (2018). Synthesis of phthalic acid derivatives via Pd-catalyzed alkoxycarbonylation of aromatic C–H bonds with alkyl chloroformates. Chem. Commun. *54*, 10859–10862.

Liu, S., and Tzschucke, C.C. (2016). Palladium-catalyzed regioselective dehydrogenative C–H/C–H cross-coupling of pyrroles and pyridine N–oxides. Eur. J. Org. Chem. *2016*, 3509–3513.

Liu, Y.-J., Xu, H., Kong, W.-J., Shang, M., Dai, H.-X., and Yu, J.-Q. (2014). Overcoming the limitations of directed C–H functionalizations of heterocycles. Nature *515*, 389.

Liu, X.-H., Park, H., Hu, J.-H., Hu, Y., Zhang, Q.-L., Wang, B.-L., Sun, B., Yeung, K.-S., Zhang, F.-L., and Yu, J.-Q. (2017). Diverse ortho-C(sp2)–H functionalization of benzaldehydes using transient directing groups. J. Am. Chem. Soc. *139*, 888–896.

Lou, S.-J., Xu, D.-Q., and Xu, Z.-Y. (2014). Mild and versatile nitrate-promoted C–H bond fluorination. Angew. Chem. Int. Ed. *53*, 10330–10335.

Lyons, T.W., and Sanford, M.S. (2010). Palladium-catalyzed ligand-directed C—H functionalization reactions. Chem. Rev. *110*, 1147–1169.

McMurray, L., O'hara, F., and Gaunt, M.J. (2011). Recent developments in natural product synthesis using metal-catalysed C–H bond functionalisation. Chem. Soc. Rev. *40*, 1885–1898.

Oh, Y., Jang, Y.J., Jeon, M., Kim, H.S., Kwak, J.H., Chung, K.H., Pyo, S., Jung, Y.H., and Kim, I.S. (2017). Total synthesis and anti-inflammatory evaluation of penchinone A and its structural analogues. J. Org. Chem. *82*, 11566–11572.

Qiao, Y., Zhao, J., Chang, J., and Wei, D. (2019). Insights into the oxidative palladium-catalyzed regioselective synthesis of 3-arylindoles from N—Ts–anilines and styrenes: a computational study. ChemCatChem. *11*, 780–789.

Roudesly, F., Veiros, L.F., Oble, J., and Poli, G. (2018). Pd-catalyzed direct C–H alkenylation and allylation of azine N-oxides. Org. Lett. *20*, 2346–2350.

Sambiagio, C., Schönbauer, D., Blieck, R., Dao-Huy, T., Pototschnig, G., Schaaf, P., Wiesinger, T., Zia, M.F., Wencel-Delord, J., Besset, T., et al. (2018). A comprehensive overview of directing groups applied in metal-catalysed C–H functionalisation chemistry. Chem. Soc. Rev. *47*, 6603–6743.

Shan, G., Yang, X., Ma, L., and Rao, Y. (2012). Pd-catalyzed C–H oxygenation with TFA/TFAA: expedient access to oxygen-containing heterocycles and late-stage drug modification. Angew. Chem. Int. Ed. *51*, 13070–13074.

Shi, S., and Kuang, C. (2014). Palladium-catalyzed ortho-alkoxylation of 2-aryl-1,2,3-triazoles. J. Org. Chem. *79*, 6105–6112.

Snieckus, V. (1990). Directed ortho metalation. Tertiary amide and O–carbamate directors in synthetic strategies for polysubstituted aromatics. Chem. Rev. *90*, 879–933.

Stephens, D.E., Lakey-beitia, J., Atesin, A.C., Ateşin, T.A., Chavez, G., Arman, H.D., and Larionov, O.V. (2015a). Palladium-catalyzed C8-selective C–H arylation of quinoline N–oxides: insights into the electronic, steric, and solvation effects on the site selectivity by mechanistic and DFT computational studies. ACS Catal. *5*, 167–175.

Stephens, D.E., Lakey-Beitia, J., Chavez, G., Ilie, C., Arman, H.D., and Larionov, O.V. (2015b). Experimental and mechanistic analysis of the palladium-catalyzed oxidative C8-selective C–H homocoupling of quinoline N–oxides. Chem. Commun. *51*, 9507–9510.

Sun, X., Shan, G., Sun, Y., and Rao, Y. (2013). Regio- and chemoselective C—H chlorination/bromination of electron-deficient arenes by weak coordination and study of relative directing-group abilities. Angew. Chem. Int. Ed. *52*, 4440–4444.

Sun, X., Yao, X., Zhang, C., and Rao, Y. (2015). Pd(ii) catalyzed ortho C–H iodination of phenylcarbamates at room temperature using cyclic hypervalent iodine reagents. Chem. Commun. *51*, 10014–10017.

Thirunavukkarasu, V.S., and Cheng, C.-H. (2011). Pd-catalyzed multiple C—H functionalization to construct biologically active compounds from aryl aldoxime ethers with arenes. Chem. Eur. J. *17*, 14723–14726.

Tian, Q., Chen, X., Liu, W., Wang, Z., Shi, S., and Kuang, C. (2013). Regioselective halogenation of 2-substituted-1,2,3-triazoles via sp2 C–H activation. Org. Biomol. Chem. *11*, 7830–7833.

Tomberg, A., Johansson, M.J., and Norrby, P.-O. (2019). A predictive tool for electrophilic aromatic substitutions using machine learning. J. Org. Chem. *84*, 4695–4703.

Tredwell, M.J., Gulias, M., Gaunt Bremeyer, N., Johansson, C.C.C., Collins, B.S.L., and Gaunt, M.J. (2011). Palladium(II)-catalyzed C–H bond arylation of electron-deficient arenes at room temperature. Angew. Chem. Int. Ed. *50*, 1076–1079.

Váňa, J., Bartáček, J., Hanusek, J., Roithová, J., and Sedlák, M. (2019). C–H functionalizations by palladium carboxylates: the acid effect. J. Org. Chem. https://doi.org/10.1021/acs.joc.9b00462.

Wan, L., Dastbaravardeh, N., Li, G., and Yu, J.-Q. (2013). Cross-coupling of remote meta-C–H bonds directed by a U-shaped template. J. Am. Chem. Soc. *135*, 18056–18059.

Wang, Z., Kuninobu, Y., and Kanai, M. (2015). Palladium-catalyzed oxirane-opening reaction with arenes via C–H bond activation. J. Am. Chem. Soc. *137*, 6140–6143.

Wang, P., Verma, P., Xia, G., Shi, J., Qiao, J.X., Tao, S., Cheng, P.T.W., Poss, M.A., Farmer, M.E., Yeung, K.-S., et al. (2017). Ligand-accelerated non-directed C–H functionalization of arenes. Nature *551*, 489.

Wang, D.-Y., Guo, S.-H., Pan, G.-F., Zhu, X.-Q., Gao, Y.-R., and Wang, Y.-Q. (2018). Direct dehydrogenative arylation of benzaldehydes with arenes using transient directing groups. Org. Lett. *20*, 1794–1797.

Willis, N.J., and Smith, J.M. (2014). An operationally simple, palladium catalysed dehydrogenative cross-coupling reaction of pyridine N–oxides and thiazoles "on water". RSC Adv. *4*, 11059–11063.

Xiao, B., Gong, T.-J., Xu, J., Liu, Z.-J., and Liu, L. (2011). Palladium-catalyzed intermolecular directed C—H amidation of aromatic ketones. J. Am. Chem. Soc. *133*, 1466–1474.

Xiong, F., Qian, C., Lin, D., Zeng, W., and Lu, X. (2013). Palladium-catalyzed cascade oxidation/sp2 C–H acylation of azoarenes with aryl methanes. Org. Lett. *15*, 5444–5447.

Xu, J., Liu, Y., Wang, Y., Li, Y., Xu, X., and Jin, Z. (2017). Pd-catalyzed direct ortho-C–H arylation of aromatic ketones enabled by a transient directing group. Org. Lett. *19*, 1562–1565.

Xue, X.-S., Ji, P., Zhou, B., and Cheng, J.-P. (2017). The essential role of bond energetics in C–H activation/functionalization. Chem. Rev. *117*, 8622–8648.

Yang, S., Li, B., Wan, X., and Shi, Z. (2007). Ortho arylation of acetanilides via Pd(II)-catalyzed C—H functionalization. J. Am. Chem. Soc. *129*, 6066–6067.

Yang, Y.-F., Cheng, G.-J., Liu, P., Leow, D., Sun, T.-Y., Chen, P., Zhang, X., Yu, J.-Q., Wu, Y.-D., and Houk, K.N. (2014). Palladium-catalyzed meta-selective C–H bond activation with a nitrile-containing template: computational study on mechanism and origins of selectivity. J. Am. Chem. Soc. *136*, 344–355.

Yu, W.-Y., Sit, W.N., Lai, K.-M., Zhou, Z., and Chan, A.S.C. (2008). Palladium-catalyzed oxidative ethoxycarbonylation of aromatic C—H bond with diethyl azodicarboxylate. J. Am. Chem. Soc. *130*, 3304–3306.

Zhang, C., Ji, J., and Sun, P. (2014). Palladium-catalyzed alkenylation via sp2 C–H bond

activation using phenolic hydroxyl as the directing group. J. Org. Chem. *79*, 3200–3205.

Zhang, J., Xu, Q., Wu, J., Fan, J., and Xie, M. (2019). Construction of N–C axial chirality through atroposelective C–H olefination of N-arylindoles by palladium/amino acid cooperative catalysis. Org. Lett. *21*, 6361–6365.

Zhao, X., Yeung, C.S., and Dong, V.M. (2010). Palladium-catalyzed ortho-arylation of O-phenylcarbamates with simple arenes and sodium persulfate. J. Am. Chem. Soc. *132*, 5837–5844.

Zhu, R., Lu, S., Wang, Q., Bai, J., Wang, Y., Yu, Q., and Huang, J. (2018). Selectfluor-mediated mono-C–H activation: the syntheses of mono-ortho-substituted anilides. Tetrahedron *74*, 3879–3887.

Daugulis, O. and Chiong, H. 2009. Use of aryl chlorides in palladium-catalyzed arylation of heterocycles, benzoates, and phenols. https://patents.google.com/patent/US20090012293A1/en.

ISCI, Volume *20*

Supplemental Information

Relative Strength of Common Directing Groups in Palladium-Catalyzed Aromatic C–H Activation

Anna Tomberg, Michael Éric Muratore, Magnus Jan Johansson, Ina Terstiege, Christian Sköld, and Per-Ola Norrby

Table S1. DFT calculations on compound **1** (related to Scheme 3): (xyz and energies in Hartrees) of full molecules and the palladacycles corresponding to the activations of their aromatic carbons.

Compound **1** alone:

DFT energy = −746.58594962670

C	1.2902	-0.7822	1.2820
C	-0.0765	-0.5356	1.1985
H	-0.7080	-0.7849	2.0461
C	-0.6326	0.0463	0.0446
C	0.2289	0.3947	-1.0115
H	-0.1891	0.8575	-1.8994
C	1.5952	0.1454	-0.9325
H	2.2428	0.4090	-1.7619
C	2.1388	-0.4511	0.2165
C	3.5934	-0.7502	0.3536
O	4.2932	-0.4223	-0.7450
C	5.7225	-0.6831	-0.7176
C	-2.0959	0.2939	-0.0761
C	-3.0318	-0.4758	0.6359
C	-4.3912	-0.2045	0.4870
C	-4.7847	0.8174	-0.3776
C	-3.7874	1.5209	-1.0574
N	-2.4779	1.2781	-0.9191
H	-4.0561	2.3222	-1.7446
H	-5.8319	1.0649	-0.5278
H	-5.1291	-0.7879	1.0319
H	-2.7057	-1.2844	1.2826
H	1.7151	-1.2299	2.1749
O	4.1029	-1.2444	1.3509
C	6.2756	-0.2516	-2.0626
H	5.8125	-0.8197	-2.8758
H	7.3557	-0.4273	-2.0896
H	6.0941	0.8140	-2.2354
H	5.8818	-1.7497	-0.5279
H	6.1673	-0.1239	0.1120

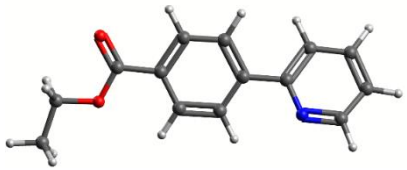

Compound **1a** (palladacycle with pyridine):

DFT energy = −1061.949345548584

Pd	2.3887	-0.5976	2.5174
O	3.8827	-1.3104	4.2168
O	1.7269	-1.8362	4.1026
C	2.8722	-1.9031	4.6765
C	0.8411	0.3948	0.3098
C	0.7342	-0.3888	1.4828
C	-0.2918	0.5958	-0.4935
C	-0.4812	-0.9589	1.8452
C	-1.6128	-0.7503	1.0340
C	-1.5090	0.0257	-0.1304
H	-2.3921	0.1752	-0.7430
H	-0.5614	-1.5597	2.7438
H	2.9481	-2.5051	5.5984
C	2.1759	0.9410	0.0436
N	3.0985	0.5981	0.9914
C	2.5493	1.7382	-1.0413
C	3.8671	2.1805	-1.1478
C	4.7945	1.8213	-0.1670
C	4.3695	1.0244	0.8931
H	5.0492	0.7168	1.6825
H	1.8161	2.0087	-1.7940
H	5.8286	2.1474	-0.2145
H	4.1664	2.8000	-1.9890
H	-0.2322	1.1942	-1.3992
C	-2.9470	-1.3346	1.3726
O	-3.9542	-1.1802	0.6948
O	-2.9211	-2.0503	2.5071
C	-4.1694	-2.6623	2.9312
C	-3.8806	-3.4049	4.2225
H	-3.1224	-4.1789	4.0664
H	-4.7957	-3.8855	4.5833
H	-3.5231	-2.7182	4.9965
H	-4.5197	-3.3317	2.1385
H	-4.9190	-1.8754	3.0650

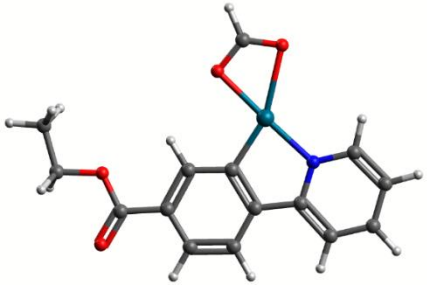

Compound **1b** (palladacycle with ethyl ester):

DFT energy = −1061.92407685699

C	1.3475	-0.7393	1.1561
C	-0.0248	-0.5208	1.1557
H	-0.6087	-0.7722	2.0351
C	-0.6423	0.0582	0.0270
C	0.1440	0.4313	-1.0822
H	-0.3399	0.8859	-1.9399
C	1.5160	0.2109	-1.0883
H	2.1204	0.4861	-1.9484
C	2.1194	-0.3803	0.0305
C	3.5393	-0.6843	0.1708
O	4.3346	-0.3973	-0.8314
O	3.9643	-1.2118	1.2339
Pd	2.3856	-1.5114	2.6230
O	0.8621	-1.7995	4.0164
O	2.8417	-2.4474	4.7905
C	1.6063	-2.2895	4.9445
H	1.1099	-2.5681	5.8898
C	5.7654	-0.7046	-0.7057
C	-2.1156	0.2759	-0.0068
C	-2.9930	-0.5658	0.6973
C	-4.3649	-0.3272	0.6292
C	-4.8254	0.7385	-0.1448
C	-3.8821	1.5142	-0.8237
N	-2.5611	1.3002	-0.7653
H	-4.2052	2.3495	-1.4438
H	-5.8852	0.9631	-0.2304
H	-5.0608	-0.9695	1.1631
H	-2.6118	-1.4092	1.2646
C	6.4121	-0.2836	-2.0096
H	7.4851	-0.4957	-1.9639
H	6.2781	0.7886	-2.1844
H	5.9853	-0.8345	-2.8538
H	5.8660	-1.7767	-0.5128
H	6.1563	-0.1541	0.1551

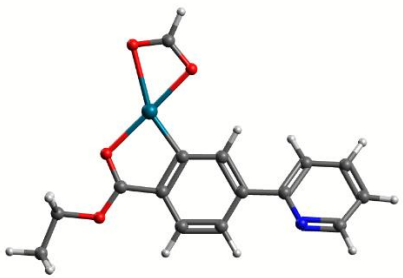

Table S2. DFT calculations on compound **3** (related to Figure 3): (xyz and energies in Hartrees) of full molecules and the palladacycles corresponding to the activations of their aromatic carbons.

Compound **2** alone:

DFT energy = −726.63721261580

C	1.6543	0.2787	0.6623
C	1.6508	-0.0014	2.0402
C	0.4223	0.4052	-0.0001
C	0.4570	-0.1641	2.7509
C	-0.7638	-0.0556	2.0604
C	-0.7751	0.2327	0.6988
H	-1.7222	0.3281	0.1737
H	-1.6933	-0.1866	2.6046
H	0.3863	0.6230	-1.0628
C	2.9354	0.4268	-0.0825
N	3.9846	-0.0462	0.5024
O	5.1583	0.1268	-0.2431
C	6.2644	-0.3967	0.4993
H	6.1497	-1.4726	0.6800
H	6.3832	0.1215	1.4590
H	7.1444	-0.2213	-0.1256
H	2.6040	-0.1079	2.5450
C	2.9317	1.0889	-1.4373
H	3.9420	1.3601	-1.7392
H	2.3052	1.9858	-1.4229
H	2.5193	0.4093	-2.1932
C	0.4602	-0.4372	4.2150
C	1.4750	0.0610	5.0505
N	-0.5710	-1.1614	4.7006
C	1.4284	-0.2121	6.4162
C	0.3670	-0.9681	6.9170
C	-0.6038	-1.4109	6.0167
H	-1.4499	-1.9986	6.3710
H	0.2843	-1.2041	7.9743
H	2.2016	0.1695	7.0785
H	2.2721	0.6748	4.6420

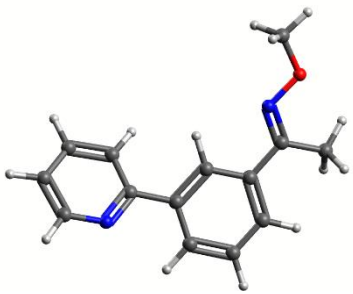

Compound **2a** (palladacycle activating H_a through pyridine):

DFT energy = −1042.00102758899

C	1.6121	0.0683	0.7599
C	1.7437	-0.2132	2.1330
C	0.3183	0.1808	0.2205
C	0.6190	-0.3710	2.9428
C	-0.6748	-0.2416	2.3815
C	-0.8192	0.0302	1.0254
H	-1.8078	0.1278	0.5863
H	0.1779	0.3944	-0.8347
C	2.8176	0.2441	-0.0977
N	3.9467	0.2985	0.5272
O	5.0496	0.4524	-0.3200
C	6.2385	0.5374	0.4726
H	6.3795	-0.3651	1.0801
H	6.2179	1.4163	1.1289
H	7.0601	0.6335	-0.2426
H	2.7416	-0.3072	2.5476
C	2.6580	0.3475	-1.5935
H	3.6275	0.3793	-2.0872
H	2.1029	1.2553	-1.8575
H	2.0911	-0.5077	-1.9771
C	0.6494	-0.6739	4.3777
C	1.7857	-0.8647	5.1694
N	-0.5948	-0.7667	4.9343
C	1.6375	-1.1468	6.5260
C	0.3560	-1.2357	7.0763
C	-0.7412	-1.0389	6.2431
H	-1.7596	-1.0975	6.6167
H	0.2014	-1.4535	8.1282
H	2.5153	-1.2962	7.1489
H	2.7753	-0.7949	4.7283
Pd	-2.1680	-0.4697	3.6300
O	-4.4005	-0.5927	4.4508
O	-3.8269	-0.1728	2.3443
C	-4.7103	-0.3359	3.2591
H	-5.7702	-0.2422	2.9663

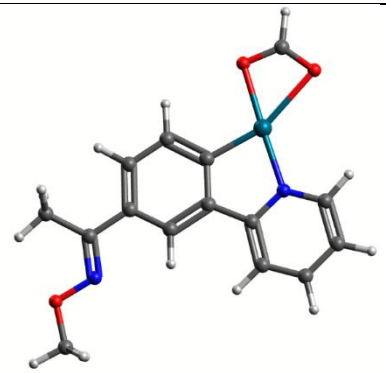

Compound **2b** (palladacycle activating H_b through *O*-methyl oxime):

DFT energy = −1041.99564016815

Pd	3.6164	-0.3661	2.1825
O	5.3671	-0.9179	3.6819
O	3.2018	-0.9261	4.1825
C	4.4322	-1.0841	4.5081
C	1.7597	0.3482	0.1232
C	1.8139	-0.0122	1.4901
C	0.5304	0.6090	-0.4859
C	0.6423	-0.1060	2.2312
C	-0.5848	0.1762	1.6156
C	-0.6583	0.5385	0.2596
H	-1.4945	0.0850	2.2038
H	0.6709	-0.3951	3.2776
H	0.4742	0.8720	-1.5373
C	3.0536	0.4348	-0.5597
N	4.0486	0.1925	0.2470
C	3.1971	0.7569	-2.0119
O	5.3189	0.1482	-0.3164
C	6.2619	0.9106	0.4661
H	6.3117	0.5384	1.4950
H	5.9980	1.9742	0.4637
H	7.2229	0.7603	-0.0302
H	2.6298	1.6640	-2.2438
H	2.7728	-0.0580	-2.6104
H	4.2404	0.8961	-2.2907
H	4.6512	-1.3728	5.5505
C	-1.9582	0.8452	-0.3964
C	-3.0450	1.3606	0.3315
N	-2.0307	0.6258	-1.7270
C	-3.1834	0.9002	-2.3518
C	-4.3177	1.3960	-1.7067
C	-4.2390	1.6334	-0.3333
H	-5.0899	2.0351	0.2112
H	-2.9492	1.5693	1.3926
H	-5.2264	1.5949	-2.2681
H	-3.2032	0.7104	-3.4243

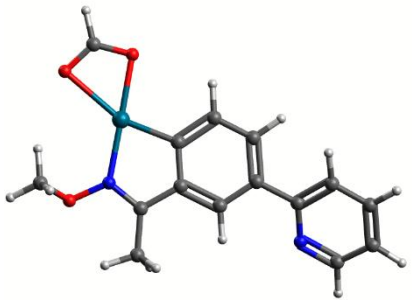

Compound **2c** (palladacycle activating H_c through pyridine):

DFT energy = −1041.99549684683

C	1.6606	0.0052	0.9296
C	1.5930	-0.2099	2.3140
C	0.4613	0.0289	0.1907
C	0.3570	-0.5478	2.9180
C	-0.8229	-0.5459	2.1597
C	-0.7678	-0.2272	0.8012
H	-1.6794	-0.2082	0.2104
H	0.5011	0.2211	-0.8799
C	2.9633	0.1477	0.2259
N	3.8349	-0.7594	0.5063
O	5.0413	-0.5408	-0.1742
C	6.0095	-1.4884	0.2795
H	5.6895	-2.5184	0.0758
H	6.1997	-1.3705	1.3525
H	6.9222	-1.2711	-0.2823
C	3.2156	1.2847	-0.7285
H	4.0250	1.9043	-0.3254
H	2.3256	1.9024	-0.8592
H	3.5523	0.9120	-1.7019
C	0.4472	-0.9428	4.3276
C	-0.5880	-1.4233	5.1352
N	1.7144	-0.8606	4.8291
C	-0.3108	-1.8266	6.4399
C	0.9973	-1.7462	6.9262
C	1.9884	-1.2487	6.0868
H	3.0210	-1.1534	6.4103
H	1.2518	-2.0585	7.9339
H	-1.1092	-2.2059	7.0721
H	-1.5973	-1.4886	4.7421
Pd	3.0841	0.0230	3.5907
O	4.9926	0.5948	4.7171
O	4.6207	1.2096	2.6183
C	5.3557	1.1888	3.6579
H	-1.7782	-0.7876	2.6191
H	6.3310	1.7040	3.6230

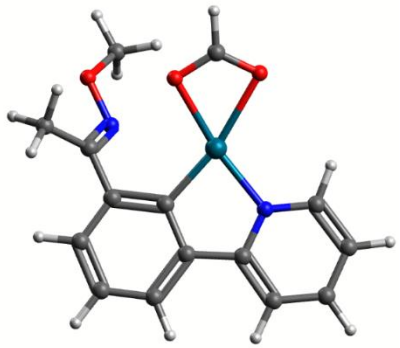

Compound **2c** (palladacycle activating H_c through *O*-methyl oxime):

DFT energy = −1041.98977547828

Compound **2** bidentate coordination with both DGs activating H_c:

DFT energy = −1042.466044312955

Pd	3.5502	-0.4020	2.3026
O	5.3322	-1.1326	3.5968
O	3.2062	-1.3506	4.1965
C	4.4506	-1.5058	4.4246
C	1.7468	0.1673	0.1652
C	1.7610	0.0205	1.5726
C	0.5318	0.2653	-0.5278
C	0.5682	0.1001	2.2987
C	-0.6448	0.1876	1.5846
C	-0.6662	0.2456	0.1895
H	-1.5773	0.2469	2.1419
H	0.5180	0.3549	-1.6108
C	3.0650	0.2789	-0.4659
N	4.0314	0.2051	0.4063
C	3.2686	0.4868	-1.9317
O	5.3318	0.2463	-0.0805
C	6.1503	1.1267	0.7200
H	6.1721	0.7972	1.7640
H	5.7859	2.1579	0.6578
H	7.1491	1.0543	0.2852
H	2.6036	1.2779	-2.2908
H	3.0101	-0.4339	-2.4683
H	4.3019	0.7470	-2.1569
H	4.7505	-1.9807	5.3744
C	0.5637	0.1790	3.7863
C	-0.2734	-0.6402	4.5551
N	1.3845	1.0973	4.3371
C	1.4018	1.1954	5.6732
C	0.6106	0.4168	6.5198
C	-0.2499	-0.5187	5.9438
H	-0.8858	-1.1463	6.5633
H	-0.9145	-1.3684	4.0663
H	0.6672	0.5499	7.5969
H	2.0749	1.9433	6.0894
H	-1.6146	0.3128	-0.3359

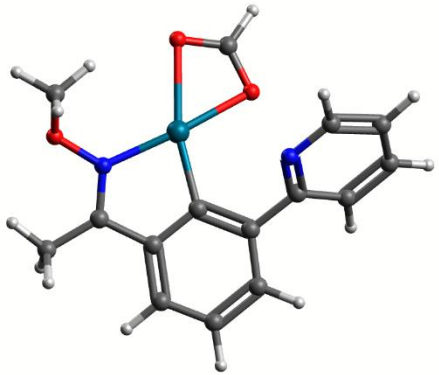

C	1.4697	0.3850	0.5293
C	1.4355	-0.0202	1.8675
C	0.2593	0.4277	-0.1798
C	0.2602	-0.3423	2.5491
C	-0.9434	-0.3038	1.8213
C	-0.9292	0.0722	0.4728
H	-1.8651	0.1063	-0.0776
H	0.2316	0.7497	-1.2179
C	2.7966	0.7958	0.0474
N	3.7268	0.6781	0.9607
O	4.9751	1.1863	0.6257
C	6.0294	0.2819	1.0099
H	5.9916	0.0736	2.0840
H	5.9668	-0.6515	0.4401
H	6.9536	0.8107	0.7676
C	3.0253	1.3393	-1.3251
H	4.0872	1.4145	-1.5542
H	2.5787	2.3391	-1.3992
H	2.5302	0.7008	-2.0634
C	0.4514	-0.6356	3.9782
C	-0.5444	-0.9877	4.8895
N	1.7537	-0.5145	4.3959
C	-0.2069	-1.2168	6.2242
C	1.1237	-1.0950	6.6293
C	2.0790	-0.7404	5.6795
H	3.1279	-0.6322	5.9371
H	1.4245	-1.2673	7.6581
H	-0.9782	-1.4879	6.9404
H	-1.5736	-1.0781	4.5575
Pd	3.0763	0.0675	2.8729
O	4.8458	0.6387	4.2327
O	4.1313	2.7832	4.4329
C	4.9621	1.7839	4.6676
H	-1.8898	-0.5521	2.2965
H	5.7960	2.0868	5.3137
H	3.3812	2.5095	3.8614

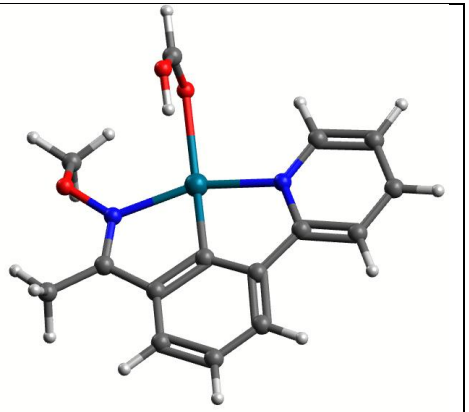

Table S3. DFT calculations on palladacycles of compound **31** with TFA (related to Figure 13): (xyz and energies in Hartrees) of the two palladacycles formed from fragments of compound **31**. The influence of TFA as Pd ligand was investigated. Energy difference between intermediates A and B is 6.2 kcal/mol.

Palladacycle A with TFA				DFT energy = -1229.03672570826
C	1.2332	-0.6405	0.9082	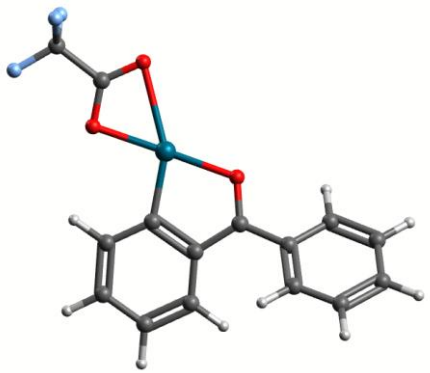
C	-0.1160	-0.4038	1.1448	
H	-0.6022	-0.8013	2.0305	
C	-0.8373	0.3733	0.2266	
H	-1.8921	0.5674	0.4085	
C	-0.2160	0.9193	-0.9049	
H	-0.7855	1.5418	-1.5887	
C	1.1331	0.6755	-1.1485	
H	1.6205	1.1256	-2.0074	
C	1.8663	-0.1327	-0.2583	
Pd	2.4250	-1.6048	2.1066	
O	1.0093	-2.1925	3.5285	
O	3.0020	-3.0428	4.0698	
C	1.7845	-2.8848	4.2692	
C	1.1441	-3.5699	5.4979	
C	4.1495	-0.1884	-1.5079	
C	3.6869	-0.3032	-2.8316	
C	5.4964	0.1406	-1.2646	
C	6.3561	0.3878	-2.3302	
C	5.8889	0.2813	-3.6455	
C	4.5599	-0.0741	-3.8939	
H	2.6668	-0.6173	-3.0295	
H	7.3908	0.6592	-2.1385	
H	6.5642	0.4675	-4.4767	
H	4.2043	-0.1803	-4.9152	
H	5.8503	0.2140	-0.2405	
C	3.2770	-0.4771	-0.3576	
O	3.7952	-1.0743	0.6377	
F	-0.1746	-3.3540	5.5714	
F	1.7098	-3.1095	6.6277	
F	1.3517	-4.8998	5.4459	

Palladacycle B with TFA				DFT energy = -1390.36205842841
C	1.8712	-1.1077	1.1563	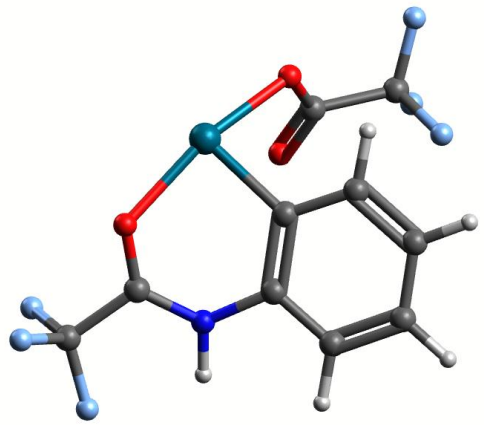
C	0.4904	-1.0961	1.3863	
H	0.1103	-0.8855	2.3784	
C	-0.4140	-1.4094	0.3643	
H	-1.4808	-1.4025	0.5747	
C	0.0479	-1.7539	-0.9079	
H	-0.6503	-2.0083	-1.7013	
C	1.4167	-1.7630	-1.1577	
H	1.7953	-2.0086	-2.1495	
C	2.3214	-1.4325	-0.1344	
N	3.6933	-1.4136	-0.4935	
C	4.6377	-0.7089	0.1196	
O	4.5250	-0.0506	1.1805	
Pd	3.1300	-0.7282	2.6491	
O	1.8907	-1.9870	3.7941	
O	2.8443	-3.8101	2.8040	
C	1.9509	-3.2189	3.4022	
C	0.6340	-4.0040	3.6733	
C	6.0204	-0.7232	-0.5577	
F	5.9777	-1.3241	-1.7645	
F	6.8928	-1.3892	0.2125	
F	6.4593	0.5288	-0.7218	
H	3.9520	-1.9186	-1.3391	
F	0.0620	-3.6890	4.8509	
F	0.8371	-5.3332	3.6547	
F	-0.2616	-3.7193	2.6967	

Table S4. Conditions screening for the arylation of 2-phenylpyridine and acetanilide (in the absence or presence of acids) (related to Scheme 6):

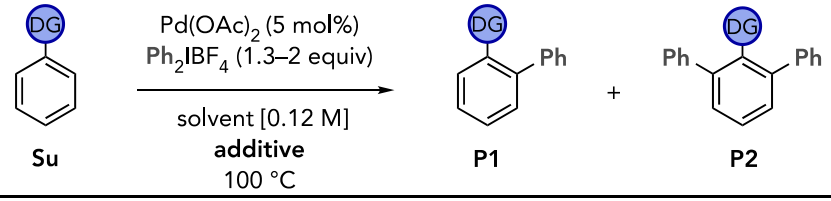

Entry	DG	Solvent	Additive (eq)	%yield[a] Su / P1 / P2
1		AcOH	–	15 / 41 / 35
2		$PhCH_3$	–	89 / 3 / n.d.
3		$PhCH_3$ / Ac_2O (1:1)		65 / 17 / n.d.
4		$PhCH_3$	AcOH (5)	40 / 29 / 23
5		$PhCH_3$	AcOH (5) + AcONa (5)	50 / 29 / 7
6		$PhCH_3$	AcOH (5) + DIPEA (5)	74 / 20 / n.d.
7		AcOH	**Tf_2NH (5)**	100 / n.d. / n.d.
8	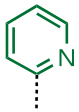	$PhCH_3$	**Tf_2NH (5)**	100 / n.d. / n.d.
9		$PhCH_3$	AcOH (5) + **Tf_2NH (5)**	93 / n.d. / n.d.
10		AcOH	**Tf_2NH (1.1)**	76 / 3 / 13
11		AcOH	**TFA (5)**	57 / 28 / 27
12		AcOH	**CSA (1.1)**	64 / 5 / 10
13		AcOH	**$TsOH{\cdot}H_2O$ (1.1)**	75 / 7 / 11
14		AcOH	**MsOH (1.1)**	78 / 5 / 9
15		$PhCH_3$	AcOH (5) + **$HBF_4{\cdot}OEt_2$ (1.1)**	95 / <1 / n.d.
16	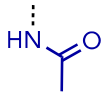	AcOH	–	54 / 28 / n.d.
17[c]		AcOH	–	42 / 50 / n.d.

18	$PhCH_3$	–	25 / 46 / 11
19	$PhCH_3$ / Ac_2O (1:1)		Complex mixture
20	$PhCH_3$	AcOH (5)	29 / 45 / 7
21	AcOH	**$TsOH{\cdot}H_2O$ (0.2)**	64 / 22 / –
22	AcOH	**MsOH (0.2)**	62 / 23 / –
23	$PhCH_3$	AcOH (5) + **CSA (0.2)**	33 / 48 / 7
24	$PhCH_3$	AcOH (5) + **CSA (1.2)**	73 / 15 / n.d.
25	$PhCH_3$	AcOH (5) + **Tf_2NH (0.2)**	36 / 48 / 6
26	$PhCH_3$	AcOH (5) + **Tf_2NH (1.2)**	55 / 40 / <1
27	$PhCH_3$	AcOH (5) + **$HBF_4{\cdot}OEt_2$ (0.1)**	30 / 55 / 7
28	$PhCH_3$	**$BF_3{\cdot}OEt_2$ (0.1)**	–[b] / 49 / 12

[a] Crude NMR yields against 1,1,2,2-tetrachloroethane as internal standard; [b] using 10 mol% of $Pd(OAc)_2$; n.d. = not detected (<1% in NMR); DIPEA = diisopropylethylamine; [c]Cannot be quantified because diagnostic peak overlaps with other signals.

Discussion of Table S4 (related to Scheme 6):

It is worth noting that the C–H arylation reaction reported by Sanford and co-workers[29] with 2-phenylpyridine (**S2,** below) as substrate requires a source of proton (e.g. acetic acid) in order for the catalyst to be turned over. Hence, in toluene, approximately a single catalyst turnover is observed (ca. 5% NMR yield of arylation product, compare Table S4 entries 1 & 4–6 *vs* entry 2). Interestingly, although this arylation is more efficient in acetic acid as solvent (Table S4, entry 1), the addition of 5 equivalents of acetic acid to toluene as solvent leads to >50% conversion of the substrate into arylation products (Table S4, entry 4). The acid may even be buffered by addition of 5 equivalents of a base such as sodium acetate or diisopropylethylamine (DIPEA), resulting in moderate observable reactivity. The use of a strong acid additive, in particular Tf_2NH and $HBF_4{\cdot}OEt_2$, generally led to reactivity shutdown, presumably by protonation of the pyridine nitrogen, thereby preventing further coordination to palladium and *ortho*-directed C–H arylation (Table S4, entries 9 & 15).

In contrast, the arylation of acetanilide proved to be more efficient in toluene than in acetic acid (Table S4, entries 16 & 17 vs entry 18). Furthermore, the addition of 5 equivalents of acetic acid did not seem to have a significant detrimental effect on the arylation efficiency (Table S4, entry 20). In this case the addition of catalytic amount of a strong acid (reasoning that only this excess amount would remain after reaction of one equivalent of the acid with a basic residue in a bifunctional substrate such as **19**) did not significantly alter the reactivity (Table S4, entries 23, 25 & 27); even the addition of stoichiometric Tf_2NH did not seem to dramatically affect how the reaction proceeded (Table S4, entry 26).

Therefore, conditions employing toluene as solvent, in the presence or absence of 5 equivalents of acetic acid and with strong acid additives (Tf_2NH or $HBF_4{\cdot}OEt_2$) seem to be viable options to study the effect of the protonation state of substrate **19** on its C–H arylation outcome.

Table S5: Competition experiments for the arylation of 2-phenylpyridine and acetanilide (related to Scheme 6)

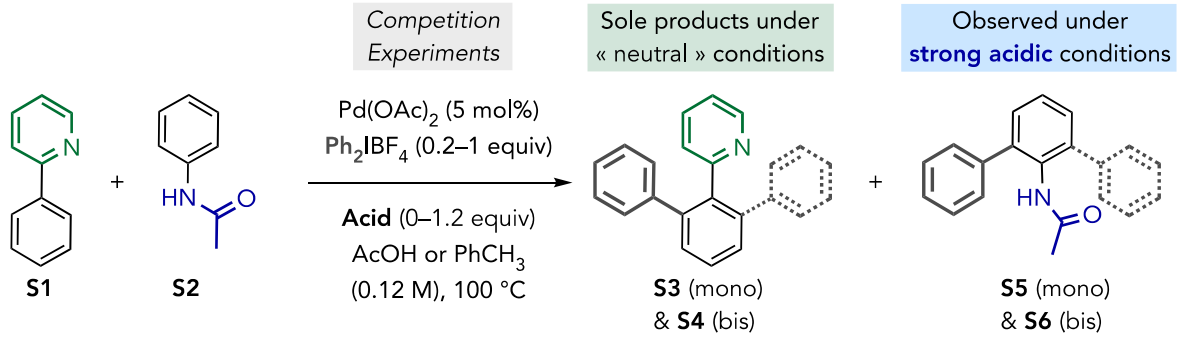

Entry	Solvent	Equivalents Ph_2IBF_4	Additive (eq)	%yield[a] S1 / S2 / S3 / S4 / S5 / S6
1	AcOH	1	–	28 / –[b] / 48 / 27 / n.d. / n.d.
2	AcOH	0.2	–	76 / –[b] / 15 / 3 / n.d. / n.d.
3	$PhCH_3$	1	AcOH (5)	59 / –[b] / 24 / 9 / n.d. / n.d.
4	$PhCH_3$	1	–	90 / –[b] / 6 / 1 / n.d. / n.d.
5	$PhCH_3$	1.5	AcOH (5)	62 / –[b] / 27 / 10 / n.d. / n.d.
6	$PhCH_3$	1	**$HBF_4{\cdot}OEt_2$ (1.2)**	93 / –[b] / 4 / n.d. / 5[c] / n.d.
7	$PhCH_3$	**1**	**Tf_2NH (1.2)**	82 / –[b] / 2 / n.d. / 2 / n.d.
8	$PhCH_3$	1	AcOH (5) + **Tf_2NH (1.2)**	75 / –[b] / 15 / 7 / <3 / n.d.

[a] Crude NMR yields against 1,1,2,2-tetrachloroethane as internal standard; [b] Cannot be quantified because all peaks overlap; n.d. = not detected (<1% in NMR); [c] 2-Phenylaniline might also have been formed in small amounts.

Discussion of Table S5:

These competition experiments confirm that pyridine is a much stronger DG than the acetanilide moiety and only C–H arylation on 2-phenylpyridine is observed under neutral conditions (in acetic acid or toluene/acetic acid, Table S5, entries 1–3). In addition, in the absence of a proton source to turn the catalyst over, the pyridine

coordinates to palladium preventing efficient arylation to take place, and a single catalyst turnover is observed by arylation of 2-phenylpyridine only (Table S5, entry 4; also observed in Table S4, entry 2). Interestingly, the addition of strong acid additives decreased dramatically the reactivity of 2-phenylpyridine and the product of arylation of acetanilide could be observed in small amounts under these conditions (Table S5, entries 6 & 7), confirming that they may be suitable to study the effect of the protonation state of substrate **19** on its C–H arylation outcome.

Data S1. Relative strengths of *ortho*-Directing Groups (DGs) of format 1. (Related to Figure 9)

Directing strength is defined as the energy of the corresponding metallacycle with Pd(OAc) relative to the same intermediate with benzene.
All the xyz coordinates and the corresponding DFT energies of the molecules necessary to compute the directing strengths listed below can be found in the sdf file name Data S17.

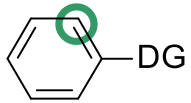

DG	SMILES	SMARTS	Directing Strength (kcal/mol)
—N(H)C(=O)CH_3	CC(=O)Nc1ccccc1	[C]C(=O)[NH1]c[cH1]	−7.4
—N^-C(=O)CH_3	CC(=O)[N-]c1ccccc1	[C]C(=O)[N-]c[cH1]	−22.9
—N(H)C(=O)H	O=CNc1ccccc1	[H][C](=O)[NH1]c[cH1]	−6.2
—N^-C(=O)H	O=C[N-]c1ccccc1	[H][C](=O)[N-]c[cH1]	−21.2
—C(=O)N(H)CH_3	CNC(=O)c1ccccc1	[C][NH1]C(=O)c[cH1]	−4.3
—C(=O)N^-CH_3	C[N-]C(=O)c1ccccc1	[C][N-]C(=O)c[cH1]	−31.7
—N(H)C(=O)CH_2CH_3	CCC(=O)Nc1ccccc1	[C][C]C(=O)[NH1]c[cH1]	−7.3
—N^-C(=O)CH_2CH_3	CCC(=O)[N-]c1ccccc1	[C][C]C(=O)[N-]c[cH1]	−21.8
—N(CH_3)C(=O)CH_3	CN(C(=O)C)c1ccccc1	[C]C(=O)N([C])c[cH1]	−6.0
—N(H)C(=O)CF_3	FC(F)(F)C(=O)Nc1ccccc1	C(F)(F)(F)C(=O)[NH1]c[cH1]	−2.2
—N^-C(=O)CF_3	FC(F)(F)C(=O)[N-]c1ccccc1	C(F)(F)(F)C(=O)[N-]c[cH1]	−17.7

—N(H)SO_2CH_3	CS(=O)(=O)Nc1ccccc1	[C]S(=O)(=O)[NH1]c[cH1]	6.29
—$N^-SO_2CH_3$	CS(=O)(=O)[N-]c1ccccc1	[C]S(=O)(=O)[N-]c[cH1]	−4.46
—$SO_2N(H)CH_3$	CNS(=O)(=O)c1ccccc1	[C][NH1]S(=O)(=O)c[cH1]	−3.5
—$SO_2N^-CH_3$	C[N-]S(=O)(=O)c1ccccc1	[C][N-]S(=O)(=O)c[cH1]	−20.1
—N(H)C(=O)-*tert*-Butyl	CC=C(NC(=O)C(C)(C)C)C=C	[C]C([C])([C])C(=O)[NH1]c[cH1]	−7.0
—N^-C(=O)-*tert*-Butyl	CC(C)(C)C(=O)[N-]c1ccccc1	[C]C([C])([C])C(=O)[N-]c[cH1]	−23.2
—N(Et)C(=O)CH_3	CCN(C(=O)CC)c1ccccc1	CC(=O)N([C][C])c[cH1]	−4.9
—C(=O)N$(CH_3)_2$	CN(C)C(=O)c1ccccc1	[C]N([A])C(=O)c[cH1]	−2.7
—C(=O)N(H)-*sec*-Butyl	CCC(C)NC(=O)c1ccccc1	[C][C][C]([C])[NH1]C(=O)c[cH1]	−3.0
—C(=O)N^--*sec*-Butyl	CCC(C)[N-]C(=O)c1ccccc1	[C][C][C]([C])[N]C(=O)c[cH1]	−34.0
—C(=O)CH_2N(H)-*sec*-Butyl	CCC(C)NC(=O)Cc1ccccc1	[C][C][C]([C])[NH1]C(=O)[C]c[cH1]	−3.9
—C(=O)CH_2N^--*sec*-Butyl	CCC(C)[N-]C(=O)Cc1ccccc1	[C][C][C]([C])[N-]C(=O)[C]c[cH1]	−33.6
—N(H)C(=O)N$(CH_3)_2$	CN(C)C(=O)Nc1ccccc1	[C]N([C])C(=O)[NH1]c[cH1]	−7.5
—N^-C(=O)N$(CH_3)_2$	CN(C)C(=O)[N-]c1ccccc1	[C]N([C])C(=O)[N-]c[cH1]	−21.1
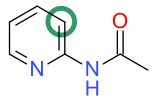 —C(=O)N(H)(2-pyridyl)	CC(=O)Nc1ccccn1	[C]C(=O)[NH1]c1[cH1][c][c][c]n1	−6.8
 —C(=O)N^--(2-pyridyl)	CC(=O)[N-]c1ccccn1	[C]C(=O)[N-]c1[cH1][c][c][c]n1	−21.1
—pyridine	c1ccc(cc1)c2ccccn2	[cH1][c]c2[c][c][c][c][nX2]2	−15.2

—C(=O)N(H)PhF$_4$CF$_3$	Fc1c(F)c(c(F)c(F)c1NC(=O)c2ccccc2)C(F)(F)F	[cH1]cC(=O)[NH1]c2c(c(c(c(c2F)F)C(F)(F)F)F)F	1.34
—C(=O)N$^-$PhF$_4$CF$_3$	Fc1c(F)c(c(F)c(F)c1[N-]C(=O)c2ccccc2)C(F)(F)F	[cH1]cC(=O)[N-]c2c(c(c(c(c2F)F)C(F)(F)F)F)F	−25.1
—CH$_2$C(=O)N(H)PhF$_4$CF$_3$	Fc1c(F)c(c(F)c(F)c1NC(=O)Cc2ccccc2)C(F)(F)F	[cH1]c[C]C(=O)[NH1]c2c(c(c(c(c2F)F)C(F)(F)F)F)F	1.5
—CH$_2$C(=O)N$^-$PhF$_4$CF$_3$	Fc1c(F)c(c(F)c(F)c1[N-]C(=O)Cc2ccccc2)C(F)(F)F	[cH1]c[C]C(=O)[N-]c2c(c(c(c(c2F)F)C(F)(F)F)F)F	−22.5
—CH$_2$N(H)SO$_2$CF$_3$	FC(F)(F)S(=O)(=O)NCc1ccccc1	[cH1]c[C][NH1]S(=O)(=O)C(F)(F)F	0.8
—CH$_2$N$^-$SO$_2$CF$_3$	FC(F)(F)S(=O)(=O)[N-]Cc1ccccc1	[cH1]c[C][N-]S(=O)(=O)C(F)(F)F	−15.5
—C(=O)NH$_2$	NC(=O)c1ccccc1	[cH1]cC(=O)[NH2]	−4.3
—C(=O)N$^-$H	[NH-]C(=O)c1ccccc1	[cH1]cC(=O)[NH-]	−29.5
—C(=O)N(H)OCH$_3$	CONC(=O)c1ccccc1	[C]O[NH1]C(=O)c[cH1]	−2.1
—C(=O)N$^-$OCH$_3$	CO[N-]C(=O)c1ccccc1	[C]O[N-]C(=O)c[cH1]	−28.5
—N(H)-pyrimidine	N(c1ccccc1)c2ncccn2	[cH1]c[NH1]c2n[c][c][c]n2	−15.1
—N$^-$-pyrimidine	[N-](c1ccccc1)c2ncccn2	[cH1]c[N-]c2n[c][c][c]n2	−26.2
—SO$_2$N(H)PhF$_5$	Fc1c(F)c(F)c(NS(=O)(=O)c2ccccc2)c(F)c1F	[cH1]cS(=O)(=O)[NH1]c2c(c(c(c(c2F)F)F)F)F	2.2
—SO$_2$N$^-$PhF$_5$	Fc1c(F)c(F)c([N-]S(=O)(=O)c2ccccc2)c(F)c1F	[cH1]cS(=O)(=O)[N-]c2c(c(c(c(c2F)F)F)F)F	−16.3
—CH$_2$SO$_2$N(H)PhF$_5$	Fc1c(F)c(F)c(NS(=O)(=O)Cc2ccccc2)c(F)c1F	[cH1]c[C]S(=O)(=O)[NH1]c2c(c(c(c(c2F)F)F)F)F	2.4

—$CH_2SO_2N^-PhF_5$	Fc1c(F)c(F)c([N-]S(=O)(=O)Cc2ccccc2)c(F)c1F	[cH1]c[C]S(=O)(=O)[N-]c2c(c(c(c(c2F)F)F)F)F	−17.0
—(1-pyrazole) 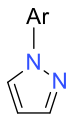	c1ccc(cc1)n2cccn2	[cH1]c-n2[c][c][c]n2	−11.9
—OCH_2-pyridine	C(Oc1ccccc1)c2ccccn2	[cH1]cO[C]c2[c][c][c][c]n2	−5.8
—(2-(1-methylimidazole)) 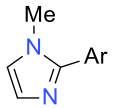	Cn1ccnc1c2ccccc2	[C]n1[c][c]nc1c[cH1]	−13.7
— (2-pyrimidyl) 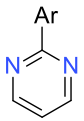	c1ccc(cc1)c2ncccn2	[cH1]c-c2n[c][c][c]n2	−12.5
—C(H)=$NOCH_3$	CON=Cc1ccccc1	[C][O][N]=[C]c[cH1] and [C][O][N]=[C][C]c[cH1]	−8.2
—$CH_2C(CH_3)$=NO CH_3	CON=C(C)Cc1ccccc1	[C]C(=NO[C])[C]c[cH1]	−11.5
—$Si(CH_3)_2$-pyrimidine	C[Si](C)(c1ccccc1)c2ncccn2	[C][Si]([C])(c2n[c][c][c]n2)c[cH1]	−10.5
—triazole	c1ccc(cc1)n2nccn2	[cH1][c]n2n[c][c]n2	−7.3
—$SO_2N(CH_3)_2$	CN(C)S(=O)(=O)c1ccccc1	[C]N([C])S(=O)(=O)c[cH1]	−2.7

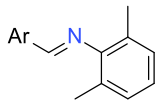	Cc1cccc(C)c1\N=C\c2ccccc2	[C]c1[c][c][c]c([C])c1N=[C]c[cH1]	−13.3
—$CH_2N(CH_3)_2$	CN(C)Cc1ccccc1	[C]N([C])[C]c[cH1]	−14.3
—$CH_2CH_2N(CH_3)_2$	CN(C)CCc1ccccc1	[C]N([C])[C][C]c[cH1]	−16.1
—N(H)C(=NH)NH_2	NC(=N)Nc1ccccc1	[cH1]c-[NH1]C(=[N])[NH2]	−22.9
—N^-C(=NH)NH_2	NC(=N)[N-]c1ccccc1	[cH1]c-[N-]C(=[N])[NH2]	−35.4
—C(=O)N(CH_3)OCH_3	CON(C)C(=O)c1ccccc1	[C]N(O[C])C(=O)c[cH1]	−1.22
—CH_2C(=O)N$(CH_3)_2$	CN(C)C(=O)Cc1ccccc1	[C]N([C])C(=O)[C]c[cH1]	4.2
—CH_2C(H)=NOCH_3	CON=CCc1ccccc1	[C]ON=[C][C]c[cH1]	−10.1
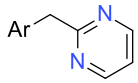	C(c1ccccc1)c2ncccn2	[cH1]c-[C]c2n[c][c][c]n2	−10.0
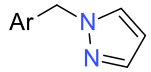	C(c1ccccc1)n2cccn2	[cH1]c-[C]n2[c][c][c]n2	−11.3
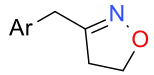	C(C1=NOCC1)c2ccccc2	[cH1]c-[C]-[C]2=[N][O][C][C]2	−9.01
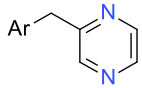	C(c1ccccc1)c2cnccn2	[cH1]c-[C]c2[c]n[c][c]n2	−10.7
—C(=O)OH	OC(=O)c1ccccc1	[cH1]c-C(=O)[OH]	1.6
—C(=O)O^-	[O-]C(=O)c1ccccc1	[cH1]c-C(=O)[O-]	−17.1
—CH_2C(=O)OH	OC(=O)Cc1ccccc1	[cH1]c-[C]C(=O)[OH]	0.8
—CH_2C(=O)O^-	[O-]C(=O)Cc1ccccc1	[cH1]c-[C]C(=O)[O-]	−17.7

—$CH_2CH_2C(=O)OH$	OC(=O)CCc1ccccc1	[cH1]c[C][C]C(=O)[OH]	1.1
—$CH_2CH_2C(=O)O^-$	[O-]C(=O)CCc1ccccc1	[cH1]c[C][C]C(=O)[O-]	−12.8
—$C(=O)CH_3$	CC(=O)c1ccccc1	[C]C(=O)c[cH1]	−1.8
—$CH_2C(=O)CH_3$	CC(=O)Cc1ccccc1	[C]C(=O)[C]c[cH1]	−0.2
—$CH_2C(=O)OCH_3$	COC(=O)Cc1ccccc1	[C]OC(=O)[C]c[cH1]	2.0
—$OC(=O)CH_3$	CC(=O)Oc1ccccc1	[C]C(=O)Oc[cH1]	−2.5
—$C(=O)OCH_3$	COC(=O)c1ccccc1	[C]OC(=O)c[cH1]	1.5
—OC(=O)-*tert*-Butyl	CC(C)(C)C(=O)Oc1ccccc1	[C]C([C])([C])C(=O)Oc[cH1]	−1.5
—$CH=CHC(=O)OCH_3$	COC(=O)C=Cc1ccccc1	[C]OC(=O)[C]=[C]c[cH1]	1.0
—oxazole 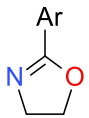	C1CN=C(O1)c2ccccc2	[cH1]c-C2=N[C][C]O2	−10.7
—CH_2-pyridine	C(c1ccccc1)c2ccccn2	[cH1]c-[C]c2[c][c][c][c]n2	−13.2
—$CH_2N(H)CH_3$	CNCc1ccccc1	[CX4][NH1][C]c[cH1]	−15.4
—$CH_2N^-CH_3$	C[N-]Cc1ccccc1	[CX4][N-][C]c[cH1]	−49.4
—pyridine N-oxide	[O-][n+]1ccccc1	[cH1][n+][O-]	2.31
—SO_2NH_2	NS(=O)(=O)c1ccccc1	[cH1]c-S(=O)(=O)[NH2]	−1.7
—SO_2N^-H	[NH-]S(=O)(=O)c1ccccc1	[cH1]c-S(=O)(=O)[N-H]	−20.2
—$OC(=O)N(CH_3)_2$	CN(C)C(=O)Oc1ccccc1	[C]N([C])C(=O)Oc[cH1]	−2.9

—SO_2CH_3	CS(=O)(=O)c1ccccc1	[C]S(=O)(=O)c[cH1]	6.0
—O^-	[O-]c1ccccc1	[cH1]c-[O^-]	−4.9
—CH_2CH_2OH	OCCc1ccccc1	[cH1]c-[C][C][OH]	2.5
—$CH_2CH_2O^-$	[O-]CCc1ccccc1	[cH1]c-[C][C][O^-]	−37.7
—$OSi(CH_3)_2OH$	C[Si](C)(O)Oc1ccccc1	[C][Si]([C])([OH])Oc[cH1]	5.9
—$OSi(CH_3)_2O^-$	C[Si](C)([O-])Oc1ccccc1	[C][Si]([C])([O^-])Oc[cH1]	−19.6
—$CH_2CH_2OCH_3$	COCCc1ccccc1	[C]O[C][C]c[cH1]	0.4
—$CH_2Si(CH_3)_2OH$	C[Si](C)(O)Cc1ccccc1	[C][Si]([C])([OH])[C]c[cH1]	5.0
—$CH_2Si(CH_3)_2O^-$	C[Si](C)([O-])Cc1ccccc1	[C][Si]([C])([O^-])[C]c[cH1]	−18.4
—CH_2SCH_3	CSCc1ccccc1	[C]S[C]c[cH1]	−6.4
—$CH_2CH_2S(=O)CH_3$	CS(=O)CCc1ccccc1	[C,c]S(=O)[C][C]c[cH1]	−3.7
—$CH_2S(=O)CH_3$	CS(=O)Cc1ccccc1	[C]S(=O)[C]c[cH1]	−4.1
—$N(H)SO_2$-iPr	CC(C)S(=O)(=O)Nc1ccccc1	[C][C]([C])S(=O)(=O)[NH1]c[cH1]	6.0
—N^-SO_2-iPr	CC(C)S(=O)(=O)[N-]c1ccccc1	[C][C]([C])S(=O)(=O)[N^-]c[cH1]	−6.7
—$SO_2N(H)$-iPr	CC(C)NS(=O)(=O)c1ccccc1	[C][C]([C])[NH1]S(=O)(=O)c[cH1]	−2.7
—SO_2N^--iPr	CC(C)[N-]S(=O)(=O)c1ccccc1	[C][C]([C])[N^-]S(=O)(=O)c[cH1]	−20.2
—$N(CH_3)SO_2$-iPr	CC(C)S(=O)(=O)N(C)c1ccccc1	[C]N(S(=O)(=O)[C])c[cH1]	4.4
—$CH_2P(=O)(OCH_3)_2$	COP(=O)(Cc1ccccc1)OC	[C]OP(=O)(O[C])[C]c[cH1]	0.3
—$CH_2P(=O)(OCH_3)OH$	COP(=O)(O)Cc1ccccc1	[C]OP(=O)([OH])[C]c[cH1]	0.8
—$CH_2P(=O)(OCH_3)O^-$	COP(=O)([O-])Cc1ccccc1	[C]OP(=O)([O^-])[C]c[cH1]	−9.5
—$OP(=O)(OCH_3)OH$	COP(=O)(O)Oc1ccccc1	[C]OP(=O)([OH])Oc[cH1]	5.2

—OP(=O)(OCH_3)O^-	COP(=O)([O-])Oc1ccccc1	[C]OP(=O)([O^-])Oc[cH1]	−9.2
—P(=O)(OCH_3)OH	COP(=O)(O)c1ccccc1	[C]OP(=O)([OH])c[cH1]	1.9
—P(=O)(OCH_3)O^-	COP(=O)([O-])c1ccccc1	[C]OP(=O)([O^-])c[cH1]	−11.8
—N(H)P(=O)(OCH_3)$_2$	COP(=O)(Nc1ccccc1)OC	[C]OP(=O)(O[C])[NH1]c[cH1]	0.6
—N^-P(=O)(OCH_3)$_2$	COP(=O)([N-]c1ccccc1)OC	[C]OP(=O)(O[C])[N^-]c[cH1]	−9.2
—N(CH_3)P(=O)(OCH_3)$_2$	COP(=O)(OC)N(C)c1ccccc1	[C]N(P(=O)(O[C])O[C])c[cH1]	1.0
—P(=O)(CH_3)$_2$	CP(=O)(C)c1ccccc1c2ccccc2	[C,c]P(=O)([C,c])c1[c][c][c][c]c1-c[cH1]	−3.6
—CH_2CH=$CHCH_3$	C-C=C-Cc1ccccc1	[C][C]=[C][C]c[cH1]	−5.0
—OC≡CSi(CH_3)$_3$	C[Si](C)(C)C#COc1ccccc1	[C][Si]([C])([C])C#COc[cH1]	−3.3
—CH_2CH_2N(H)C(=O)C(=O)N(CH_3)$_2$	CN(C)C(=O)C(=O)NCCc1ccccc1	[C]N([C])C(=O)C(=O)[NH1][C][C]c[cH1]	5.7
—$CH_2CH_2N^-$C(=O)C(=O)N(CH_3)$_2$	CN(C)C(=O)C(=O)[N-]CCc1ccccc1	[C]N([C])C(=O)C(=O)[N^-][C][C]c[cH1]	−28.0
—C(CH_3)=NOCH_3	CO-N=C(C)-c1ccccc1	[C]C(=NO[C])c[cH1]	−11.9
—CH_2CH_2C(=O)OCH_3	COC(=O)CCc1ccccc1	[C]OC(=O)[C][C]c[cH1]	5.2
—CH_2OC(=O)CH_3	CC(=O)OCc1ccccc1	[C]C(=O)O[C]c[cH1]	4.4
—C=N-CH_2C(=O)OH	C=NCC(=O)[OH]	[cH1][c]-[C]=N[C]C(=O)[OH]	-13.8
—C=N-CH_2C(=O)O^-	C=NCC(=O)[O-]	[cH1][c]-[C]=N[C]C(=O)[O-]	-37.1
—C(CH_3)=N-CH_2C(=O)OH	C(C)=NCC(=O)[OH]	[cH1][c]-[C](C)=N[C]C(=O)[OH]	-18.1
—C(CH_3)=N-CH_2C(=O)O^-	C(C)=NCC(=O)[O-]	[cH1][c]-[C](C)=N[C]C(=O)[O-]	-29.8
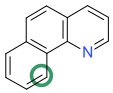	c1ccc2c(c1)ccc3cccnc23	[c]1[c][cH1]c2c([c]1)[c][c]c3c2[nX2][c][c][c]3	−12.2

Data S2. Relative strengths of *ortho*-Directing Groups (DGs) of format 2. (Related to Figure 9)

Directing strength is defined as the energy of the corresponding metallacycle with Pd(OAc) relative to the same intermediate with benzene.

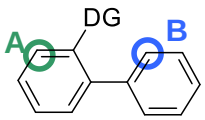

DG	SMILES	SMARTS	Directing Strength A (kcal/mol)	Directing Strength B (kcal/mol)
—CH=NOCH$_3$	CON=Cc1ccccc1c2ccccc2	A: [C]ON=[C]-[c][c]-c[cH1] B: [C]ON=[C]c([cH1])[c]-[c]	−9.1	−4.8
—NH$_2$	Nc1ccccc1c2ccccc2	[cH1]c-c2[c][c][c][c]c2[NH2]	N/A	−8.1
—N$^-$H	[NH-]c1ccccc1c2ccccc2	[cH1]c-c2[c][c][c][c]c2[NH-]	N/A	−37.8
—N(H)CH$_3$	CNc1ccccc1c2ccccc2	[C3][NH1]c1[c][c][c][c]c1-c[cH1]	N/A	−9.5
—N$^-$CH$_3$	C[N-]c1ccccc1c2ccccc2	[C3][N-]c1[c][c][c][c]c1-c[cH1]	N/A	−38.0
—CH$_2$NH$_2$	NH1Cc1ccccc1c2ccccc2	A: [NH2,NH1][C]-c1[cH1]cccc1-[c] B: [NH2,NH1][C]-[c][c]-[c][cH1]	−16.1	−14.9
—CH$_2$N$^-$H	N$^-$Cc1ccccc1c2ccccc2	A: [N$^-$][C]-c1[cH1]cccc1-[c] B: [N$^-$][C]-[c][c]-[c][cH1]	−49.8	−48.0
—C(=O)OH	OC(=O)c1ccccc1c2ccccc2	A: [c]-c2[c][c][c][cH1]c2-C(=O)[OH] B: [cH1]c-[c][c]-C(=O)[OH]	0.4	3.6
—C(=O)O$^-$	[O-]C(=O)c1ccccc1c2ccccc2	A: [c]-c2[c][c][c][cH1]c2-C(=O)[O-] B: [cH1]c-[c][c]-C(=O)[O-]	−18.6	−14.9

—N(H)SO_2CH_3	CS(=O)(=O)Nc1ccccc1c2ccccc2	A: [C,c]S(=O)(=O)[NH1]c1[cH1][c][c][c]c1-c B: [C,c]S(=O)(=O)[NH1]-cc-c2[cH1][c][c][c][c]2	4.3	−4.4
—$N^-SO_2CH_3$	CS(=O)(=O)[N-]c1ccccc1c2ccccc2	A: [C,c]S(=O)(=O)[N-]c1[cH1][c][c][c]c1-c B: [C,c]S(=O)(=O)[N-]-cc-c2[cH1][c][c][c][c]2	−6.8	−20.6
—N(H)C(=O)CH_3	CC(=O)Nc1ccccc1c2ccccc2	A: [C,c]C(=O)[NH1]c1[cH1][c][c][c]c1-c B: [C,c]C(=O)[NH1]-cc-c[cH1]	−8.9	2.1
—N^-C(=O)CH_3	CC(=O)[N-]c1ccccc1c2ccccc2	A: [C,c]C(=O)[N-]c1[cH1][c][c][c]c1-c B: [C,c]C(=O)[N-]-cc-c[cH1]	−22.7	−29.3
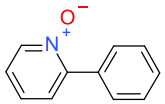	[O-][n+]1ccccc1c2ccccc2	A: c-c2[c][c][c][cH1][n+]2[O-] B: [cH1]c-c2[c][c][c][c][n+]2[O-]	0.1	−9.45
—C(=O)CH_3	CC(=O)c1ccccc1c2ccccc2	A: [C]C(=O)c1[cH1][c][c][c]c1-c B: [C]C(=O)cc-c[cH1]	−4.3	0.8
—OC(=O)N$(CH_3)_2$	CN(C)C(=O)Oc1ccccc1c2ccccc2	A: [C]N([C])C(=O)O-c1[cH1][c][c][c]c1-c B: [C]N([C])C(=O)O-[c][c]-c[cH1]	−1.9	3.7
—OH	Oc1ccccc1c2ccccc2	[OH]-c1ccccc1-c[cH1]	N/A	6.3
—O^-	[O-]c1ccccc1c2ccccc2	[O^-]-c1ccccc1-c[cH1]	N/A	−22.6
—OCH_3	COc1ccccc1c2ccccc2	[C]Oc1[c][c][c][c]c1-c[cH1]	N/A	4.8
—SCH_3	CSc1ccccc1c2ccccc2	[C]Sc1[c][c][c][c]c1-c[cH1]	N/A	−7.6
—SO_2CH_3	CS(=O)(=O)c1ccccc1c2ccccc2	A: [C,c]S(=O)c1[cH1][c][c][c]c1-c	−6.5	−6.6

		B: [C,c]S(=O)[c][c]-c[cH1]		
—C(=O)N(H)OCH_3	CONC(=O)c1ccccc1c2ccccc2	A: [C]O[NH1]C(=O)c1[cH1][c][c][c]c1-c B: [C]O[NH1]C(=O)-[c][c]-c[cH1]	−2.5	−0.6
—C(=O)N^-OCH_3	CO[N-]C(=O)c1ccccc1c2ccccc2	A: [C]O[N^-]C(=O)c1[cH1][c][c][c]c1-c B: [C]O[N^-]C(=O)-[c][c]-c[cH1]	−27.5	−23.9
—P(=O)H(CH_3)	CP(=O)c1ccccc1c2ccccc2	A: [C,c][PH1](=O)c1[cH1][c][c][c]c1-c B: [C,c][PH](=O)cc-c[cH1]	−2.9	−2.0
—P^-(=O)(CH_3)	C[P-](=O)c1ccccc1c2ccccc2	A: [C,c][P^-](=O)c1[cH1][c][c][c]c1-c B: [C,c][P^-](=O)cc-c[cH1]	−23.0	−18.3
—C=CCH_3		[C][C]=[C]-c1[c][c][c][c]c1-c[cH1]	N/A	−5.8
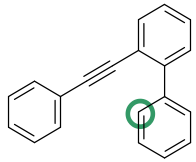	c1ccc(cc1)C#Cc2ccccc2c3ccccc3	c-C#C-c2[c][c][c][c]c2-c[cH1]	N/A	0.4

Data S3. Relative strengths of *ortho*-Directing Groups (DGs) of format 3. (Related to Figure 9)

Directing strength is defined as the energy of the corresponding metallacycle with Pd(OAc) relative to the same intermediate with benzene.

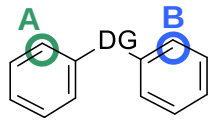

DG	SMILES	SMARTS	Directing Strength A (kcal/mol)	Directing Strength B (kcal/mol)
A—C(=O)—B	O=C(c1ccccc1)c2ccccc2	[cH1]c-C(=O)c	−1.7	N/A

A—S(=O)—B	O=S(c1ccccc1)c2ccccc2	[cH1]cS(=O)c	−2.8	N/A
A—C(=O)S—B	O=C(Sc1ccccc1)c2ccccc2	A: [cH1]c-C(=O)Sc B: c-C(=O)Sc[cH1]	−1.9	1.8
A—C(=O)N(H)—B	O=C(NH1c1ccccc1)c2ccccc2	A: [cH1] [c]-C(=O)[NH1]-[c] B: [c]-C(=O)[NH1]-[c] [cH1]	−2.3	−6.5
A—C(=O)N⁻—B	O=C(N⁻c1ccccc1)c2ccccc2	A: [cH1] [c]-C(=O)[N⁻]-[c] B: [c]-C(=O)[N⁻]-[c] [cH1]	−27.8	−21.3
A—SO_2N(H)—B	O=S(=O)(Nc1ccccc1)c2ccccc2	A: [c]S(=O)(=O)[NH1]c[cH1] B: [c][NH1]S(=O)(=O)c[cH1]	7.0	−0.02
A—SO_2N^-—B	O=S(=O)([N-]c1ccccc1)c2ccccc2	A: [c]S(=O)(=O)[N⁻]c[cH1] B: [c][N⁻]S(=O)(=O)c[cH1]	−5.4	−16.8
A—N(CH_3)SO_2—B	CN(c1ccccc1)S(=O)(=O)c2ccccc2	A: cN([C,c])S(=O)(=O)c[cH1] B: [cH1]cN([C,c])S(=O)(=O)c	2.0	5.0
A—C(=O)N(CH_3) —B	CN(C(=O)c1ccccc1)c2ccccc2	A: [C,c]N([C,c])C(=O)c[cH1] B: [cH1][c]N([C,c])C(=O)c	−2.5	−6.9
A—OSO_2—B	O=S(=O)(Oc1ccccc1)c2ccccc2	A: [cH1]c-OS(=O)(=O)c B: cOS(=O)(=O)c[cH1]	5.7	6.8
A—N=N—B	c1ccc(cc1)N=Nc2ccccc2	[cH1][c]N=N[c]	−14.6	N/A
A—$N^+(O^-)$=N—B	[O-][N+](=Nc1ccccc1)c2ccccc2	A: cN=[N+]([O-])-c[cH1] B: [cH1]c-N=[N+]([O-])-c	-9.5	-6.49
A—C(=O)O—B	O=C(Oc1ccccc1)c2ccccc2	A: cC(=O)Oc[cH1] B: [cH1][c]C(=O)Oc	−1.5	2.2

A—C(=O)N(H)SO_2—B	O=C(NS(=O)(=O)c1ccccc1)c2ccccc2	A: [cH1][c]C(=O)[NH1]S(=O)(=O)c B: cC(=O)[NH1]S(=O)(=O)c[cH1]	0.3	6.0
A—C(=O)N^-SO_2—B	O=C([N-]S(=O)(=O)c1ccccc1)c2ccccc2	A: [cH1][c]C(=O)[N-]S(=O)(=O)c B: cC(=O)[N-]S(=O)(=O)c[cH1]	−19.6	−14.0
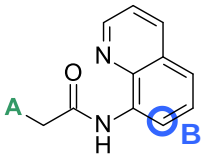	O=C(Cc1ccccc1)Nc2cccc3cccnc23	A: [cH1][c]-[C]C(=O)[NH1]-[c][c&R2][nX2] B: c-[C]C(=O)[NH1]c2[cH1][c][c]c3c2n[c][c][c]3	1.6	-5.6
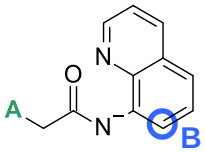	O=C(Cc1ccccc1)[N-]c2cccc3cccnc23	A: [cH1][c]-[C]C(=O)[N^-]-[c][c&R2][nX2] B: c-[C]C(=O)[N^-]c2[cH1][c][c]c3c2n[c][c][c]3	−27.6	−20.9

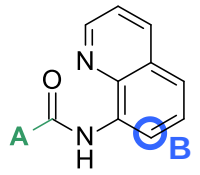	O=C(Nc1cccc2cccnc12)c3ccccc3	A: [cH1]cC(=O)[NH1]-[c][c&R2][nX2] B: cC(=O)[NH1]c2[cH1][c][c]c3c2n[c][c][c]3	5.9	−7.1
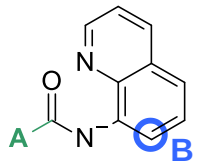	O=C([N-]c1cccc2cccnc12)c3ccccc3	A: [cH1]cC(=O)[N-]-[c][c&R2][nX2] B: cC(=O)[N-]c2[cH1][c][c]c3c2n[c][c][c]3	−44.2	−20.5

Data S4. Relative strengths of *ortho*-Directing Groups (DGs) of format 4. (Related to Figure 9)

Directing strength is defined as the energy of the corresponding metallacycle with Pd(OAc) relative to the same intermediate with benzene.

DG	SMILES	SMARTS	Directing Strength A (kcal/mol)	Directing Strength B (kcal/mol)
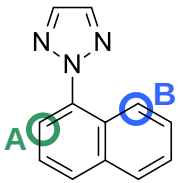	c1ccc2c(cccc2c1)n3nccn3	A: n3[a][a][n]n3-c([cH1])[c&R2] B: n3[a][a][n]n3-c[c&R2][cH1]	−8.06	−7.4
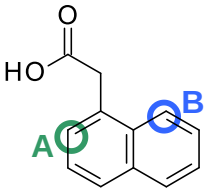	OC(=O)Cc1cccc2ccccc12	A: [OH]C(=O)[C]-c([cH1])[c&R2] B: [OH]C(=O)[C]-c[c&R2][cH1]	0.6	9.0

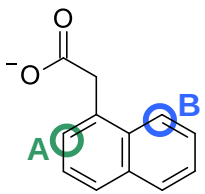	[O-]C(=O)Cc1cccc2ccccc12	A: [O⁻]C(=O)[C]-c([cH1])[c&R2] B: [O⁻]C(=O)[C]-c[c&R2][cH1]	−17.3	−15.0
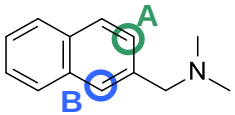	CN(C)Cc1ccc2ccccc2c1	A: [C]N([C])[C]c[cH1][c][c&R2] B: [C]N([C])[C]c[cH1][c&R2]	−13.8	−12.1
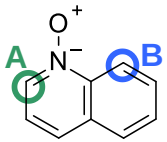	[O-][n+]1cccc2ccccc12	A: [cH1][n+]([O-])[c&R2] B: [cH1][c&R2][n+]([O-])	1.97	−9.5
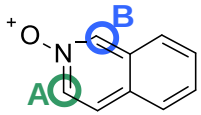	[O-][n+]1ccc2ccccc2c1	A: [c&R2][c][cH1][n+]([O-]) B: [c&R2][cH1][n+]([O-])	1.9	0.5
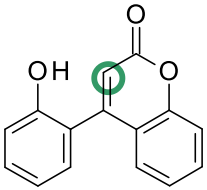	Oc1ccccc1C2=CC(=O)Oc3ccccc23	[c]1[c][c]c2c([c]1)c([cH1]c(=O)o2)c3[c][c][c][c]c3[OH]	6.4	N/A
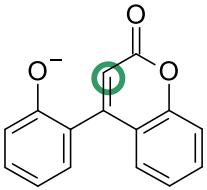	CC=C(C[O-])C1=CC(=O)Oc2ccccc12	[c]1[c][c]c2c([c]1)c([cH1]c(=O)o2)c3[c][c][c][c]c3[O⁻]	−7.71	N/A
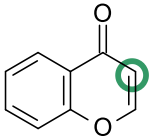	O=C1C=COc2ccccc12	[c]1[c][c]c2c([cH1]1)c(=O)[c][c]o2	−1.62	N/A

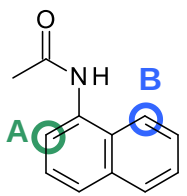	CC(=O)Nc1cccc2ccccc12	A: [C]C(=O)[NH1]c([cH1])[c&R2] B: [C]C(=O)[NH1]c[c&R2][cH1]	−7.21	5.52
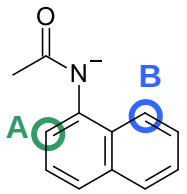	CC(=O)Nc1cccc2ccccc12	A: [C]C(=O)[N⁻]c([cH1])[c&R2] B: [C]C(=O)[N⁻]c[c&R2][cH1]	−23.8	−30.2
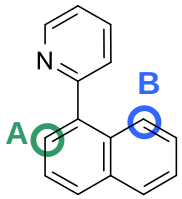	c1ccc(nc1)c2cccc3ccccc23	A: n3[c][c][c][c]c3-c([cH1])[c&R2] B: n3[c][c][c][c]c3-c[c&R2][cH1]	−13.0	−12.7
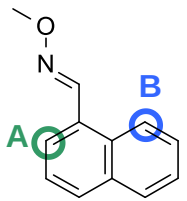	CON=Cc1cccc2ccccc12	A: [C]ON=[CH1]-c([cH1])[c&R2] B: [C]ON=[CH1]-c[c&R2][cH1]	−10.7	−15.6
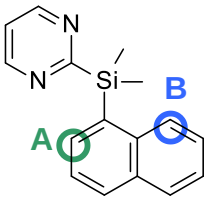	C[Si](C)(c1cccc2ccccc12)c3ncccn3	A: n1[c][c][c][n]c1-[Si]([C])([C])-c([cH1])[c&R2] B: n1[c][c][c][n]c1-[Si]([C])([C])-c[c&R2][cH1]	−10.5	−4.5

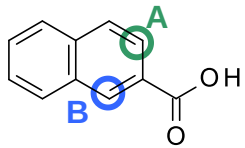	OC(=O)c1ccc2ccccc2c1	A: [OH]C(=O)-c[cH1][c&R1][c&R2] B: [OH]C(=O)-c[cH1][c&R2]	−2.31	−3.51
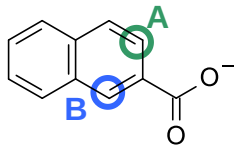	[O-]C(=O)c1ccc2ccccc2c1	A: [O-]C(=O)-c[cH1][c&R1][c&R2] B: [O-]C(=O)-c[cH1][c&R2]	−15.9	−17.0
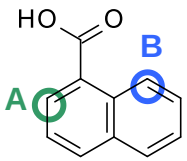	OC(=O)c1cccc2ccccc12	A: [OH]C(=O)-c([cH1])[c&R2] B: [OH]C(=O)-c[c&R2][cH1]	−1.3	−3.2
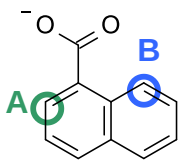	[O-]C(=O)c1cccc2ccccc12	A: [O-]C(=O)-c([cH1])[c&R2] B: [O-]C(=O)-c[c&R2][cH1]	−19.2	−18.5

Examples from literature with competing DGs

Here are collected examples pulled out from many different publications where molecules containing more than one DG were subjected to a palladium-catalyzed C—H activation with a variety of coupling partners (or lack of thereof). The exact reaction conditions can be found in the corresponding articles (see references); we only highlight whether the reaction was performed under generally acidic or basic conditions to save space. The experimentally observed reactive sites are highlighted in red in the compound (in first column). The predicted activated positions are shown in the last two columns, where the second to last column displays the predicted reactive site under acidic conditions, and the last column, under basic conditions. If the molecule cannot be deprotonated, then the predicted reaction position will be the same for both. In certain cases, the difference in energies between the fragments is less or very close to 1 kcal/mol; this is within the margin of error of the model, and the reactive site will then depend mostly on the reagents used and/or the electron-richness of the aromatic system in question. These examples are collected together in the later section of this table. Bicyclic compounds that underwent the reaction without a coupling partner are listed later, otherwise there is a notice in the reaction conditions. The examples that were predicted incorrectly are listed starting at the end of the table.

Data S5. Examples of compounds where our predictions were correct (related to Figure 6 and 14)

In the first column, the experimental site is shown as a red circle. In columns “DG1” to “DG3”, the substructures that matched patterns of the corresponding fragments are highlighted in red.

Structure	Reaction Conditions/ References	DG1	DG2	DG3	Predicted if protonated	Predicted if deprotonated
A:  B: 	A: in acid[1; 2] B: in base [3; 4]	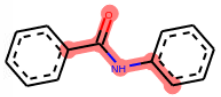 1 : FG_110A (P: -6.49 D: -21.3)	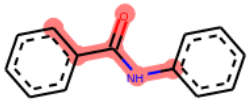 2 : FG_110C (P: -2.33 D: -27.8)		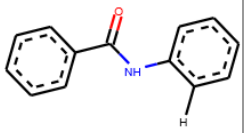	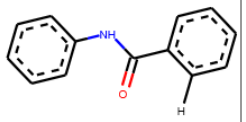
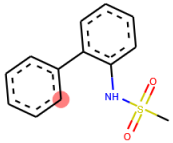	In acid[5-7] In base[8]	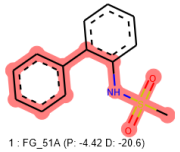 1 : FG_51A (P: -4.42 D: -20.6)	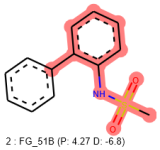 2 : FG_51B (P: 4.27 D: -6.8)		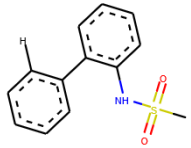	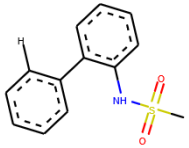
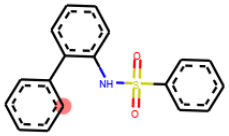	In acid[6] Neutral[9] Without coupling partner - cyclization[10]	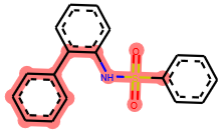 1 : FG_51A (P: -4.42 D: -20.6)	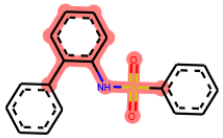 2 : FG_51B (P: 4.27 D: -6.8)	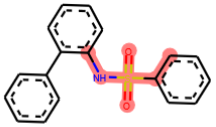 : FG_111A (P: -0.0184 D: -16.8)	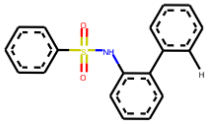 NOTE: in [11], the authors report alkylation on carbon ortho to nitrogen, but in [12], using the exact same conditions, the same authors report the	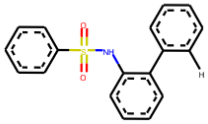

					reactivity we predict here. We can only speculate that in the first publication there must have been a mistake.	
A: 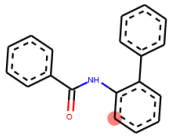 B: 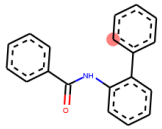	A: In acid[11] B: Without coupling partner - cyclization[13]	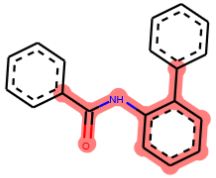 1 : FG_52A (P: -8.89 D: -22.7) 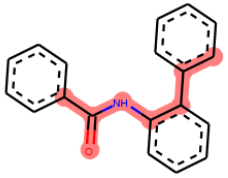 2 : FG_52B (P: 2.13 D: -29.3)	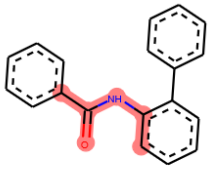 3 : FG_110A (P: -6.49 D: -21.3) 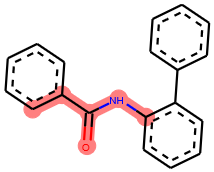 4 : FG_110C (P: -2.33 D: -27.8)		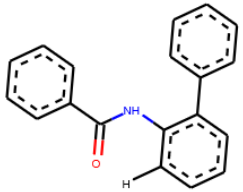 NOTE: in [12], the authors report alkylation on carbon ortho to nitrogen, but in[11], using the exact same conditions, the same authors report the reactivity we predict here. We can only speculate that in the first publication there must have been a mistake.	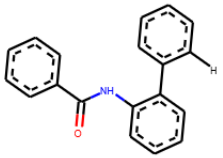

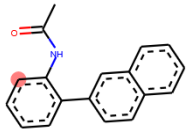	In acid[11]	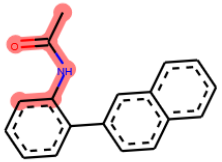 1 : FG_01 (P: -7.41 D: -22.9)	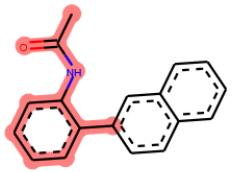 2 : FG_52A (P: -8.89 D: -22.7)	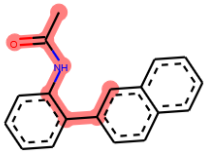 3 : FG_52B (P: 2.13 D: -29.3)	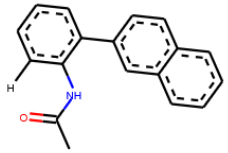	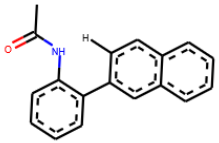
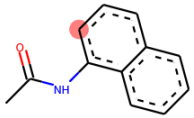	In acid[11; 14] 15; 16	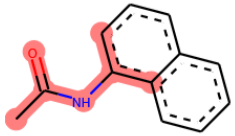 1 : FG_123A (P: -7.21 D: -23.8)	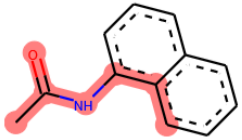 2 : FG_123B (P: 5.52 D: -30.2)		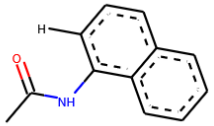	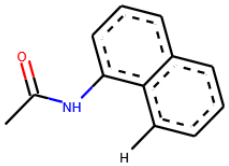
	In acid[11]	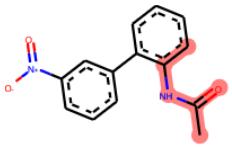 1 : FG_01 (P: -7.41 D: -22.9)	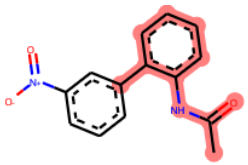 2 : FG_52A (P: -8.89 D: -22.7)	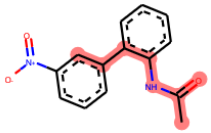 3 : FG_52B (P: 2.13 D: -29.3)	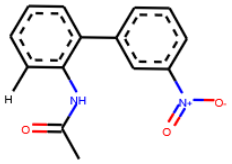	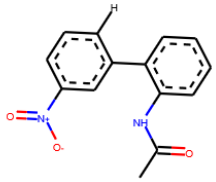
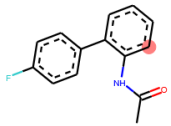	In acid[11]	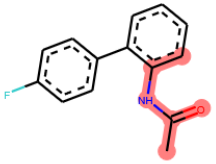 1 : FG_01 (P: -7.41 D: -22.9)	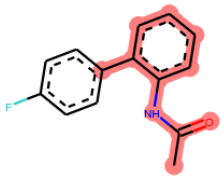 2 : FG_52A (P: -8.89 D: -22.7)	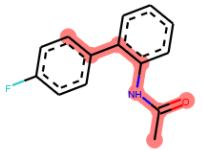 3 : FG_52B (P: 2.13 D: -29.3)	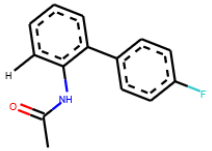	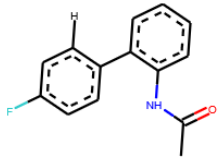
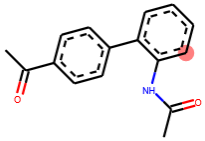	In acid[11]	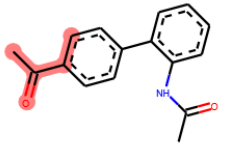 2 : FG_48 (P: -1.82 D: na)	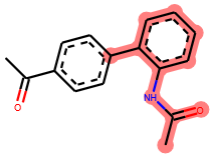 3 : FG_52A (P: -8.89 D: -22.7)	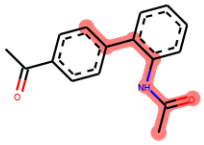 4 : FG_52B (P: 2.13 D: -29.3)	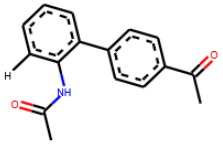	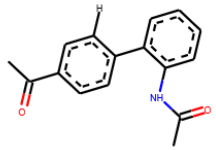

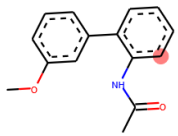	In acid[11]	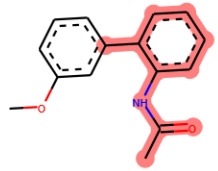 2 : FG_52A (P: -8.89 D: -22.7)	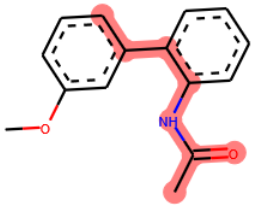 3 : FG_52B (P: 2.13 D: -29.3)		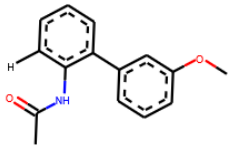	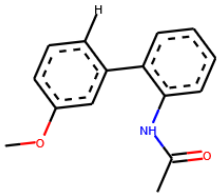
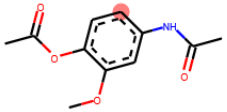	17	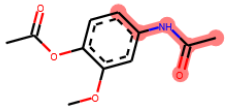 1 : FG_01 (P: -7.41 D: -22.9)	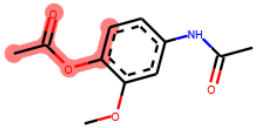 2 : FG_53 (P: -2.51 D: na)		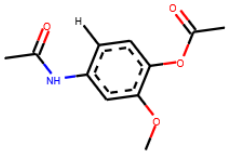	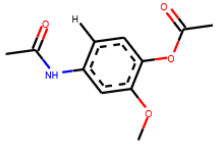
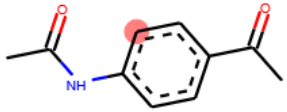	17	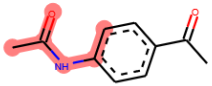 1 : FG_01 (P: -7.41 D: -22.9)	 2 : FG_48 (P: -1.82 D: na)		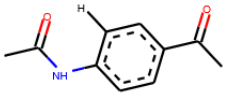	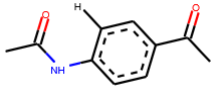
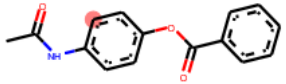	17	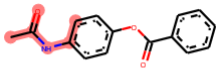 1 : FG_01 (P: -7.41 D: -22.9)	 2 : FG_124A (P: 2.24 D: na)	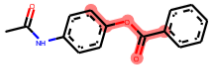 3 : FG_124B (P: -1.47 D: na)	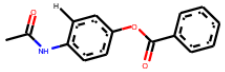	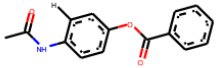
	17	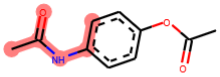 1 : FG_01 (P: -7.41 D: -22.9)	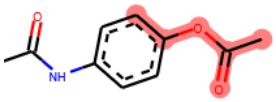 2 : FG_53 (P: -2.51 D: na)		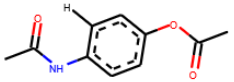	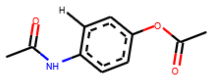

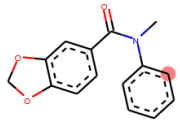	18	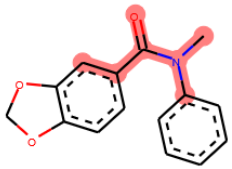 1 : FG_115A (P: -2.45 D: na)	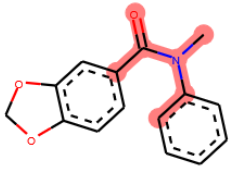 2 : FG_115C (P: -6.89 D: na)		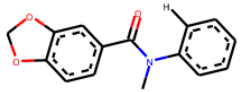	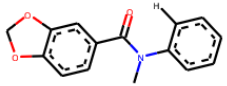
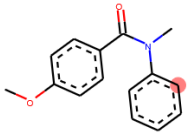	18	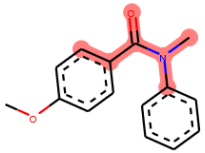 1 : FG_115A (P: -2.45 D: na)	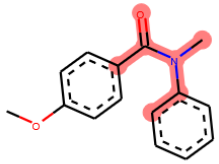 2 : FG_115C (P: -6.89 D: na)		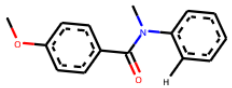	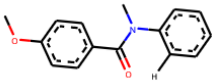
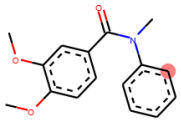	18	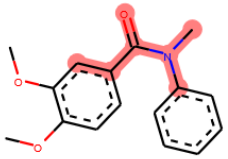 1 : FG_115A (P: -2.45 D: na)	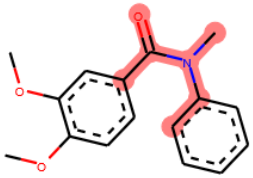 2 : FG_115C (P: -6.89 D: na)		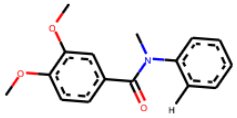	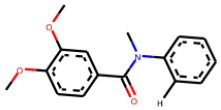
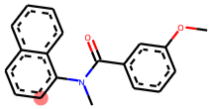	18	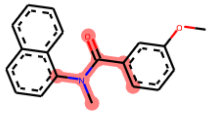 1 : FG_115A (P: -2.45 D: na)	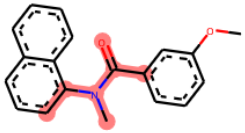 2 : FG_115C (P: -6.89 D: na)		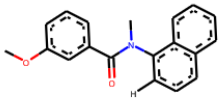	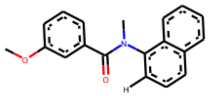
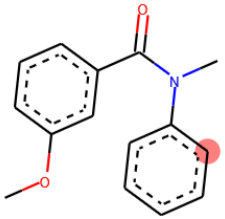	18	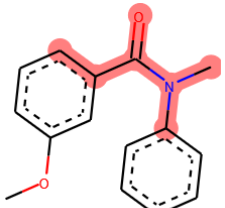 1 : FG_115A (P: -2.45 D: na)	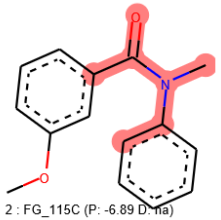 2 : FG_115C (P: -6.89 D: na)		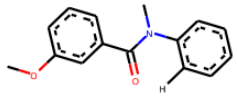	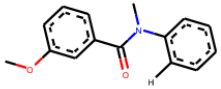

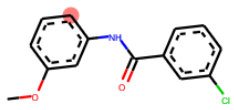	A: in acid[19]	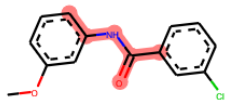 1 : FG_110A (P: -6.49 D: -21.3)	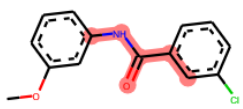 2 : FG_110C (P: -2.33 D: -27.8)		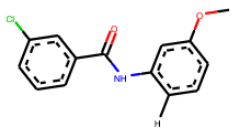	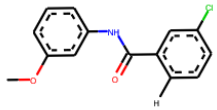
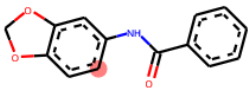	A: in acid[19]	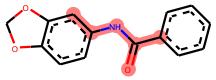 1 : FG_110A (P: -6.49 D: -21.3)	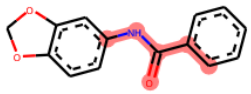 2 : FG_110C (P: -2.33 D: -27.8)		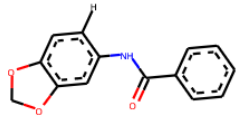	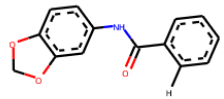
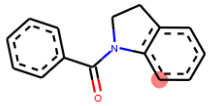	20	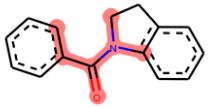 1 : FG_115A (P: -2.45 D: na)	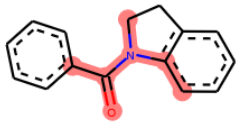 2 : FG_115C (P: -6.89 D: na)		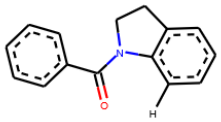	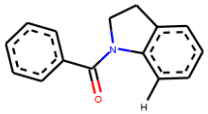
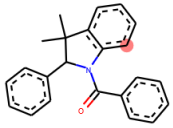	20	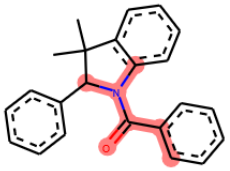 1 : FG_115A (P: -2.45 D: na)	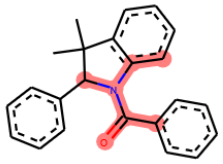 2 : FG_115C (P: -6.89 D: na)		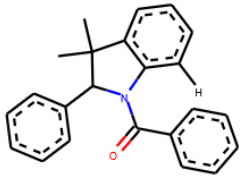	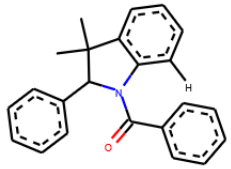
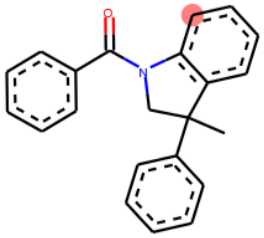	20	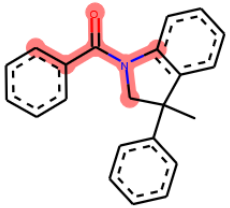 1 : FG_115A (P: -2.45 D: na)	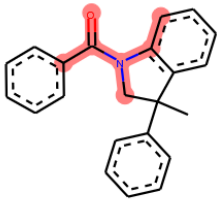 2 : FG_115C (P: -6.89 D: na)		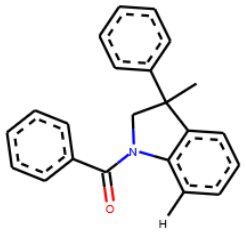	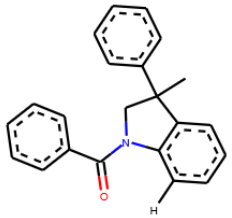

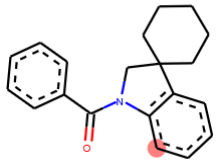	20	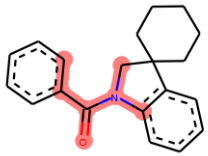 1 : FG_115A (P: -2.45 D: na)	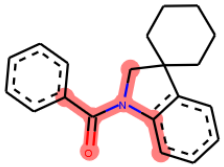 2 : FG_115C (P: -6.89 D: na)		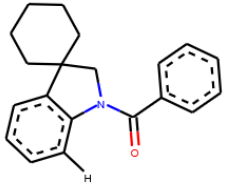	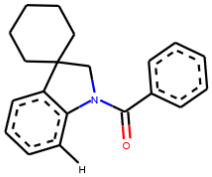
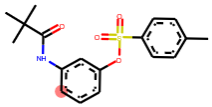	In acid[21]	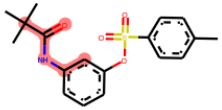 1 : FG_01 (P: -7.41 D: -22.9)	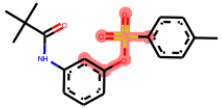 4 : FG_121A (P: 5.67 D: na)	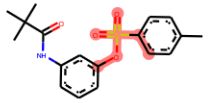 5 : FG_121B (P: 6.82 D: na)	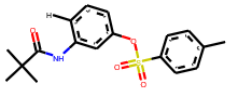	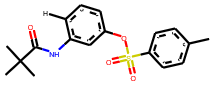
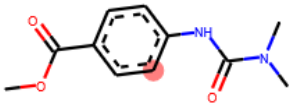	$Pd(OTs)_2(MeCN)_2$[2] 2	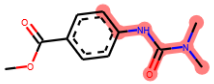 1 : FG_13 (P: -7.52 D: -21.1)	 2 : FG_55 (P: 1.45 D: na)		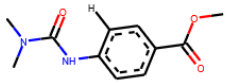	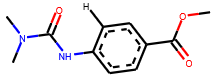
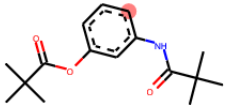	$Pd(OTs)_2(MeCN)_2$[2] 3	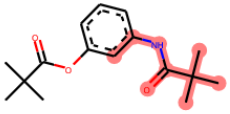 3 : FG_08 (P: -6.98 D: -23.2)	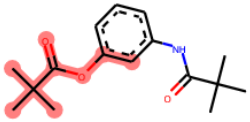 5 : FG_56 (P: -1.49 D: na)		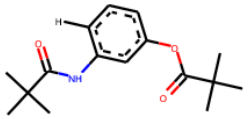	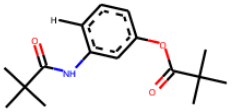
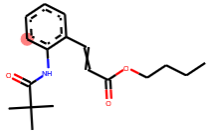	$Pd(OTs)_2(MeCN)_2$[2] 3	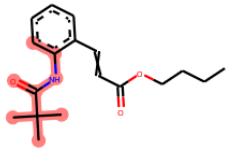 3 : FG_08 (P: -6.98 D: -23.2)	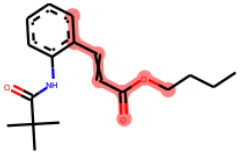 4 : FG_57 (P: 0.974 D: na)		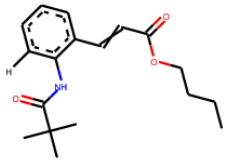	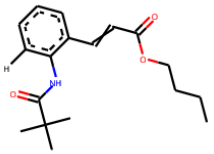

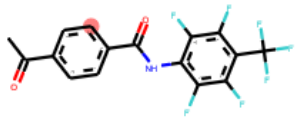	In base[24]	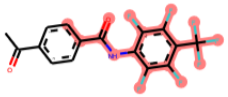 1 : FG_16 (P: 1.34 D: -25.1)	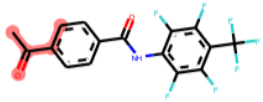 2 : FG_48 (P: -1.82 D: na)		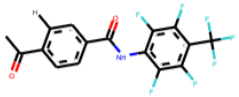	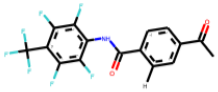
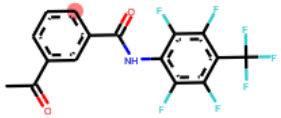	In base[24]	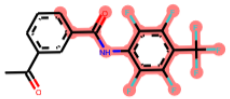 1 : FG_16 (P: 1.34 D: -25.1)	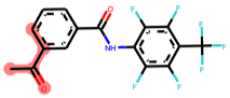 2 : FG_48 (P: -1.82 D: na)		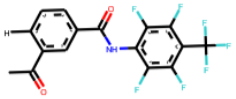	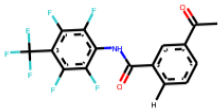
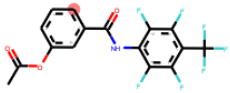	In base[24]	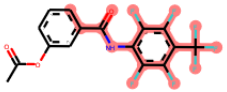 1 : FG_16 (P: 1.34 D: -25.1)	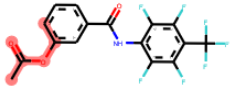 2 : FG_53 (P: -2.51 D: na)			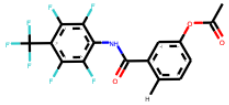
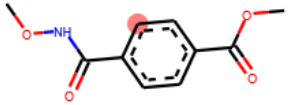	25 In base[26]	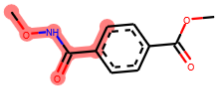 1 : FG_20 (P: -2.06 D: -28.5)	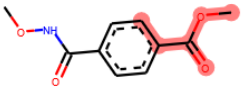 2 : FG_55 (P: 1.45 D: na)		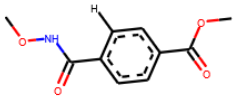	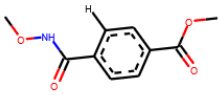
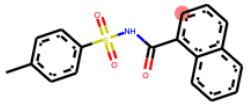	With bathophenanthroline as Pd ligand[27]	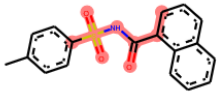 1 : FG_131A (P: 0.331 D: -19.6)	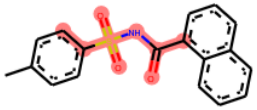 2 : FG_131B (P: 5.99 D: -14)		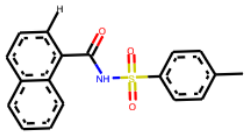	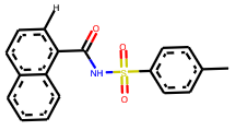

	With bathophenanthroline as Pd ligand[27]	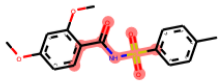 1 : FG_131A (P: 0.331 D: -19.6)	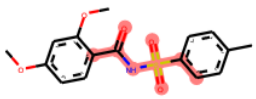 2 : FG_131B (P: 5.99 D: -14)		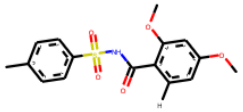	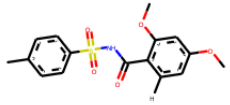
	With bathophenanthroline as Pd ligand[27]	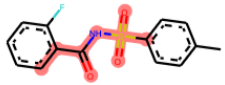 1 : FG_131A (P: 0.331 D: -19.6)	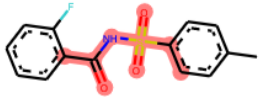 2 : FG_131B (P: 5.99 D: -14)		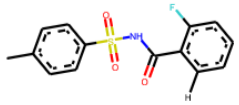	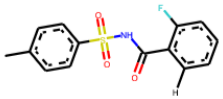
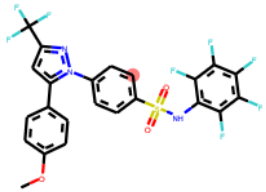	In base[28]	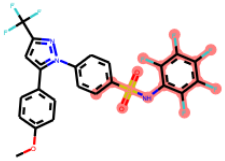 1 : FG_22 (P: 2.17 D: -16.3)	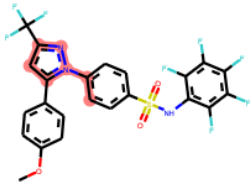 2 : FG_24 (P: -11.9 D: na)		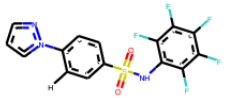	
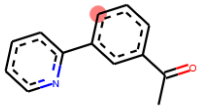	29	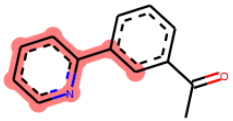 1 : FG_15 (P: -15.2 D: na)	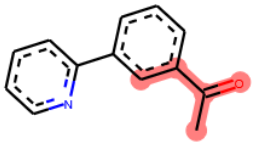 2 : FG_48 (P: -1.82 D: na)		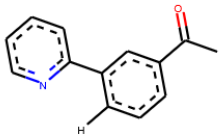	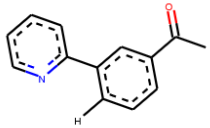
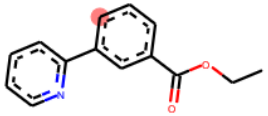	30	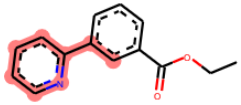 1 : FG_15 (P: -15.2 D: na)	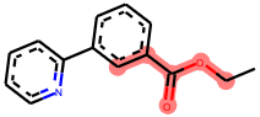 2 : FG_55 (P: 1.45 D: na)		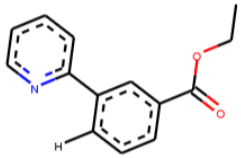	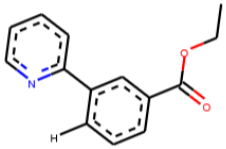

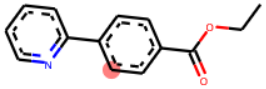	31	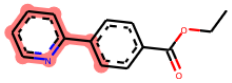 1 : FG_15 (P: -15.2 D: na)	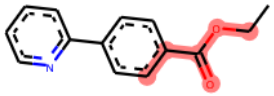 2 : FG_55 (P: 1.45 D: na)		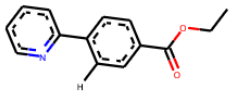	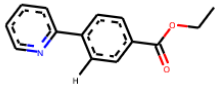
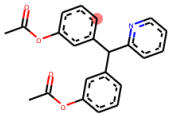	32	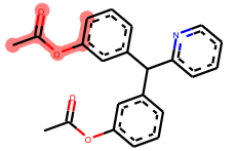 1 : FG_53 (P: -2.51 D: na)	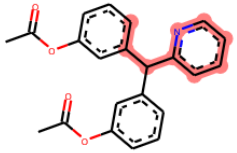 2 : FG_59 (P: -13.2 D: na)		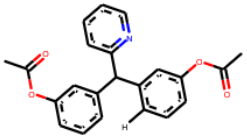	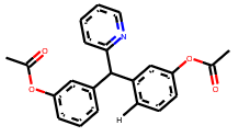
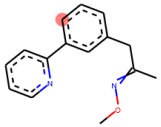	33	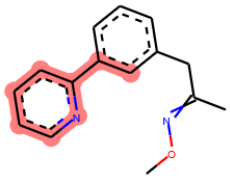 1 : FG_15 (P: -15.2 D: na)	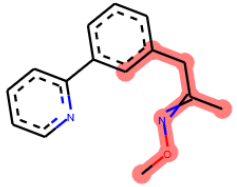 3 : FG_128 (P: -11.5 D: na)		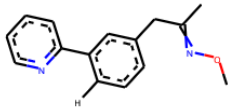	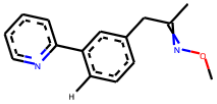
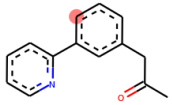	33	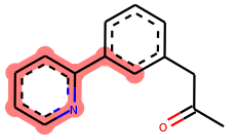 1 : FG_15 (P: -15.2 D: na)	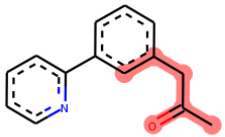 2 : FG_126 (P: -0.207 D: na)		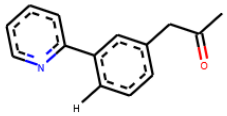	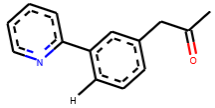
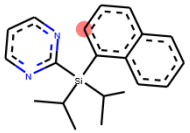	34	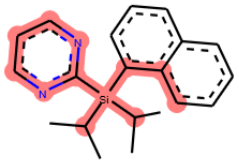 1 : FG_132A (P: -4.46 D: na)	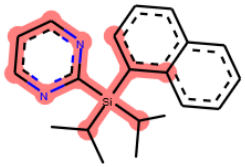 2 : FG_132B (P: -10.5 D: na)		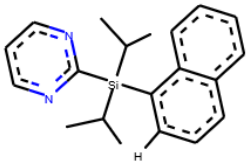	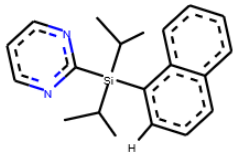

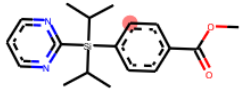	34	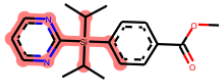 1 : FG_29 (P: -10.5 D: na)	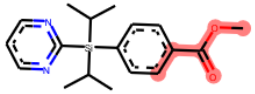 2 : FG_55 (P: 1.45 D: na)		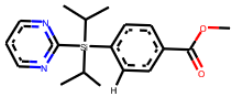	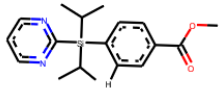
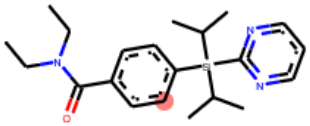	34	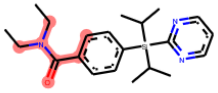 1 : FG_10 (P: -2.71 D: na)	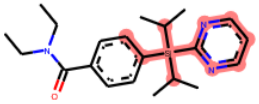 2 : FG_29 (P: -10.5 D: na)		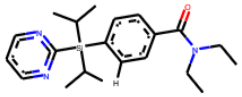	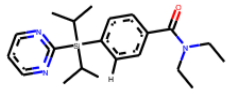
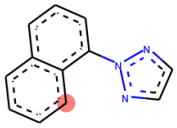	35	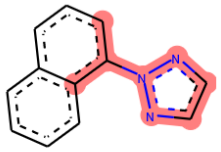 1 : FG_60A (P: -8.06 D: na)	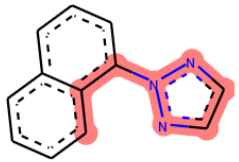 2 : FG_60B (P: -7.4 D: na)		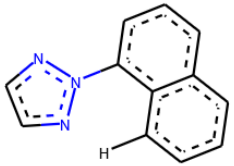 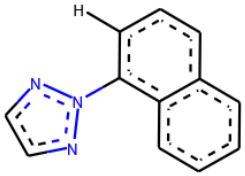	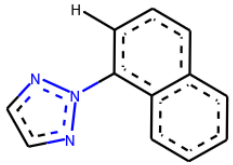 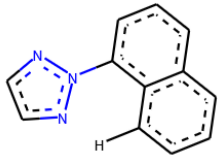
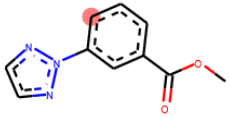	35	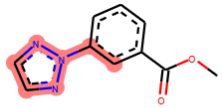 1 : FG_30 (P: -7.29 D: na)	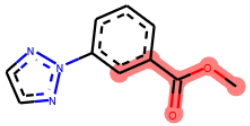 2 : FG_55 (P: 1.45 D: na)		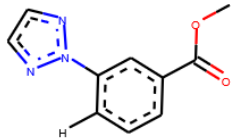	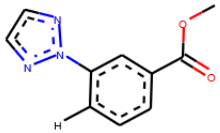

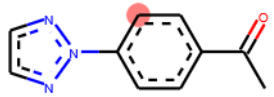	35	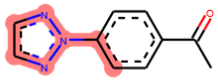 1 : FG_30 (P: -7.29 D: na)	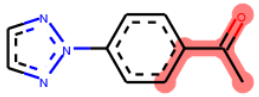 2 : FG_48 (P: -1.82 D: na)		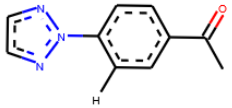	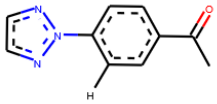
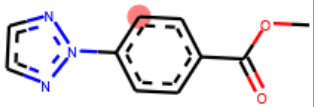	35	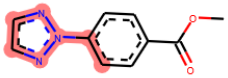 1 : FG_30 (P: -7.29 D: na)	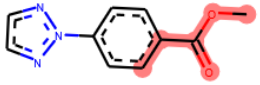 2 : FG_55 (P: 1.45 D: na)		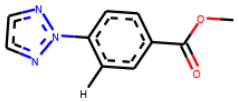	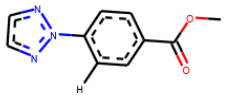
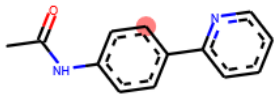	In acid[36]	 1 : FG_01 (P: -7.41 D: -22.9)	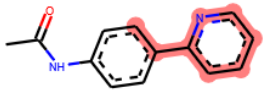 2 : FG_15 (P: -15.2 D: na)		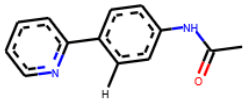	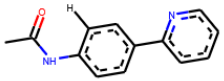
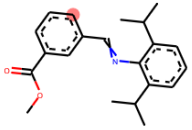	36	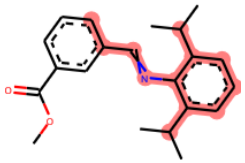 1 : FG_33 (P: -13.3 D: na)	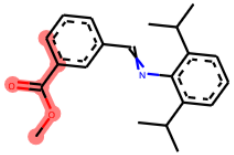 2 : FG_55 (P: 1.45 D: na)		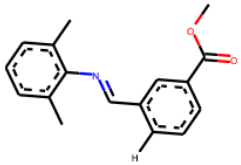	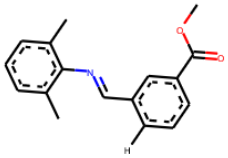
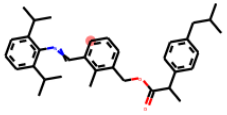	36	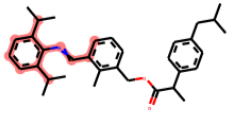 1 : FG_33 (P: -13.3 D: na)	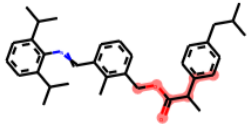 2 : FG_50 (P: 2.02 D: na)	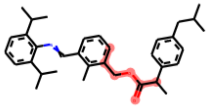 3 : FG_119 (P: 4.39 D: na)	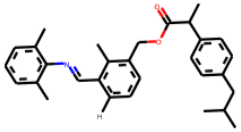	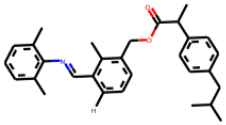

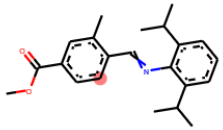	36	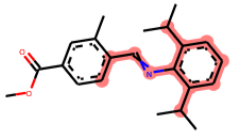 1 : FG_33 (P: -13.3 D: na)	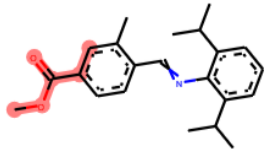 2 : FG_55 (P: 1.45 D: na)		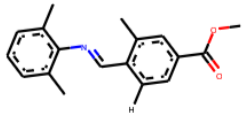	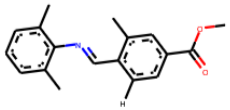
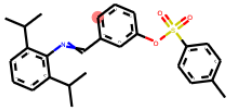	36	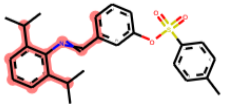 1 : FG_33 (P: -13.3 D: na)	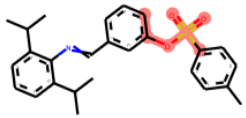 2 : FG_121A (P: 5.67 D: na)	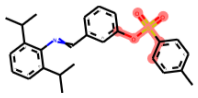 3 : FG_121B (P: 6.82 D: na)	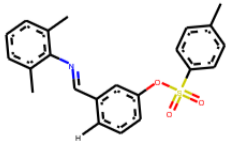	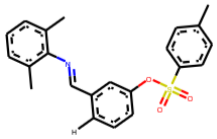
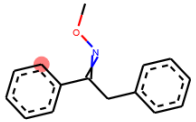	37	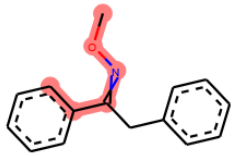 1 : FG_28 (P: -8.24 D: na)	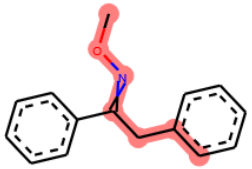 4 : FG_137 (P: -10.1 D: na)		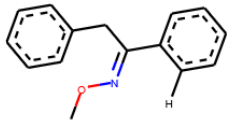	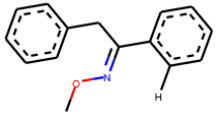
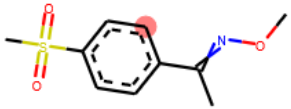	$Pd_2(dba)_3$ [38]	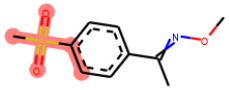 2 : FG_76 (P: 5.97 D: na)	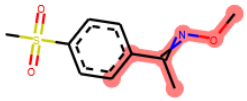 3 : FG_109 (P: -11.9 D: na)		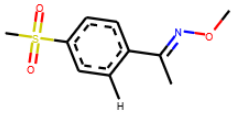	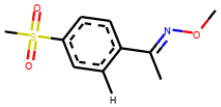
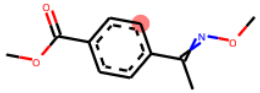	$Pd_2(dba)_3$ [38]	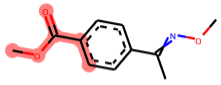 2 : FG_55 (P: 1.45 D: na)	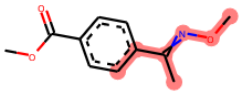 3 : FG_109 (P: -11.9 D: na)		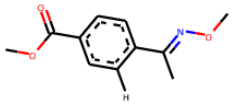	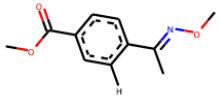

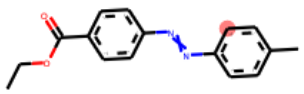	39	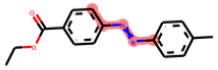 1 : FG_35 (P: -14.6 D: na)	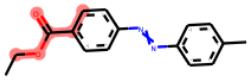 2 : FG_55 (P: 1.45 D: na)		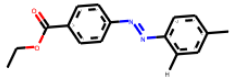	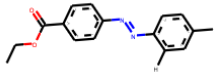
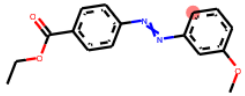	39	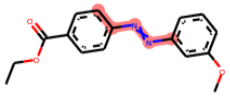 1 : FG_35 (P: -14.6 D: na)	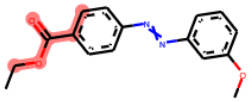 2 : FG_55 (P: 1.45 D: na)		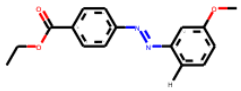	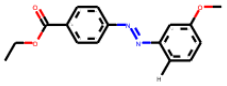
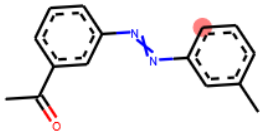	39	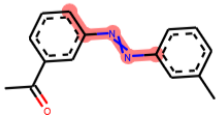 1 : FG_35 (P: -14.6 D: na)	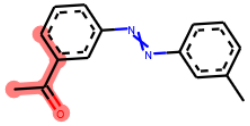 2 : FG_48 (P: -1.82 D: na)		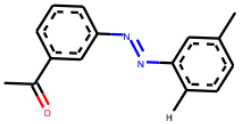	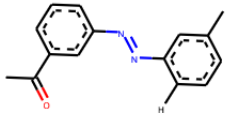
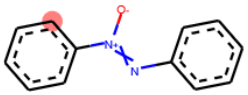	40	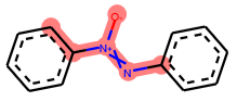 1 : FG_36A (P: -9.5 D: na)	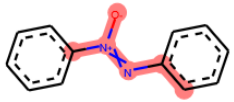 2 : FG_36C (P: -6.51 D: na)		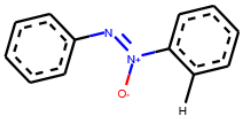	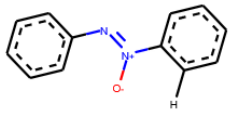
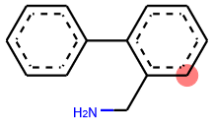	In acid[41]	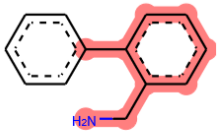 1 : FG_130A (P: -16.1 D: -49.8)	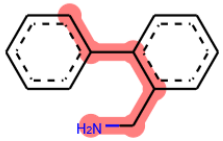 2 : FG_130B (P: -14.9 D: -48)		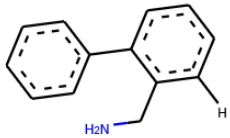	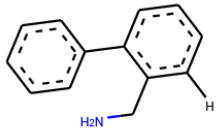

A: 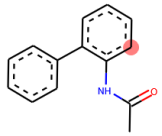 B: 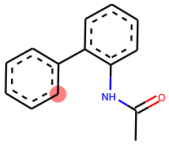	A: in acid[11] B: in base,[42] with 1,10-phenanthroline.[42] Without coupling partner - cyclization[43]	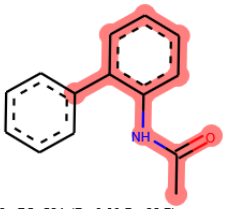 2 : FG_52A (P: -8.89 D: -22.7)	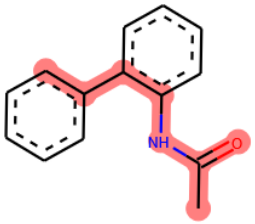 3 : FG_52B (P: 2.13 D: -29.3)		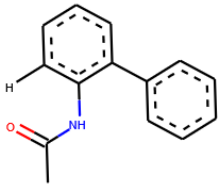	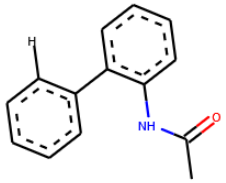
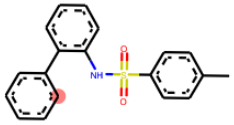	44	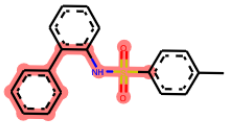 1 : FG_51A (P: -4.42 D: -20.6)	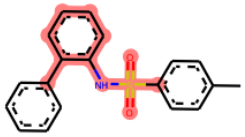 2 : FG_51B (P: 4.27 D: -6.8)	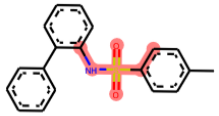 : FG_111A (P: -0.0184 D: -16.8)	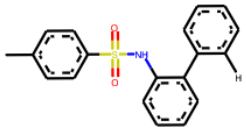	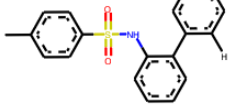
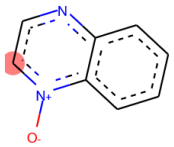	A: with phosphines[45] Please see main text for explanation on the impact of phosphines	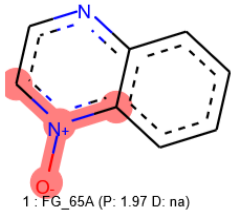 1 : FG_65A (P: 1.97 D: na)	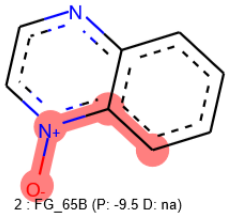 2 : FG_65B (P: -9.5 D: na)		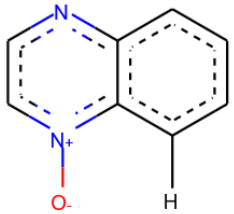	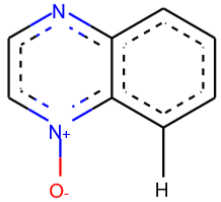
A: 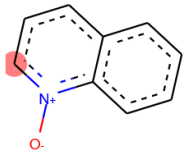	A: with phosphines[45] B: Without phosphines[46]	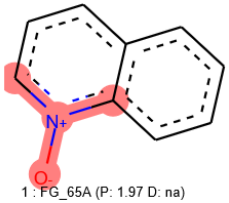 1 : FG_65A (P: 1.97 D: na)	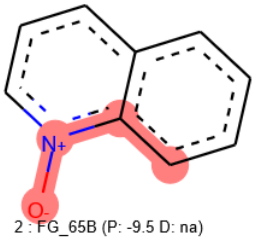 2 : FG_65B (P: -9.5 D: na)		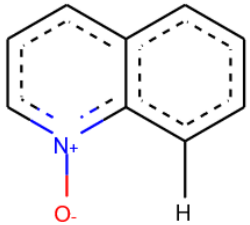	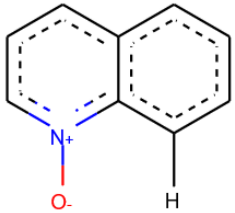

B: 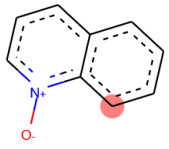						
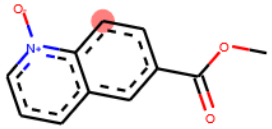	47	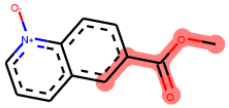 2 : FG_55 (P: 1.45 D: na)	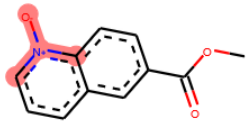 2 : FG_65A (P: 1.97 D: na)	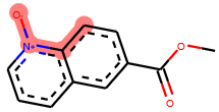 3 : FG_65B (P: -9.5 D: na)	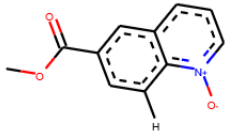	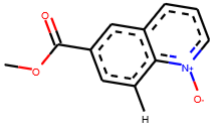
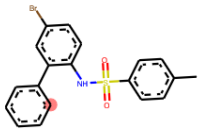	8	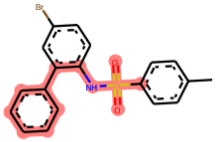 1 : FG_51A (P: -4.42 D: -20.6)	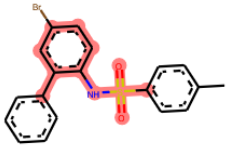 2 : FG_51B (P: 4.27 D: -6.8)	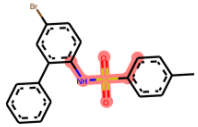 : FG_111A (P: -0.0184 D: -16.8)	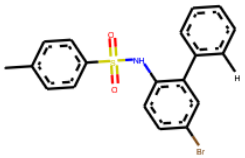	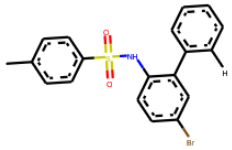
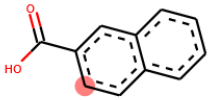	In base[8]	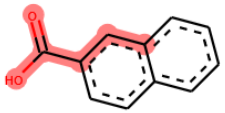 1 : FG_133A (P: -3.51 D: -17)	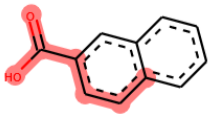 2 : FG_133B (P: -2.31 D: -15.9)		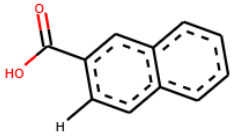	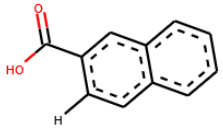
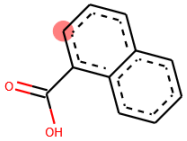	In base[8]	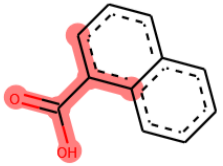 1 : FG_134A (P: -1.3 D: -19.2)	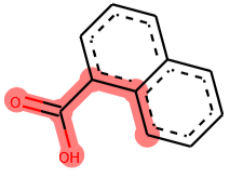 2 : FG_134B (P: -3.24 D: -18.5)		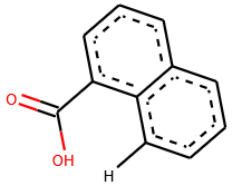	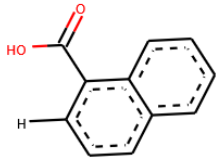

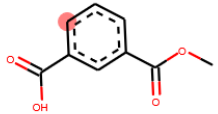	In base[48] Start from salt (deprot.)[49]	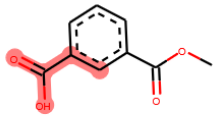 1 : FG_43 (P: 1.63 D: -17.1)	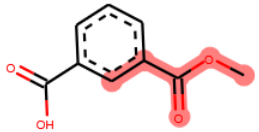 2 : FG_55 (P: 1.45 D: na)		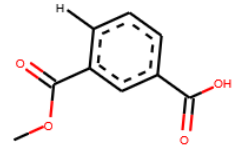 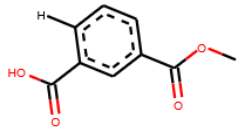 >1kcal/mol diff	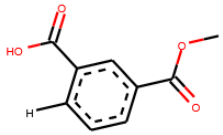
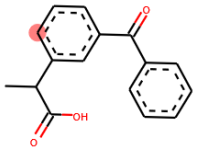	Start from salt (deprot.)[50]	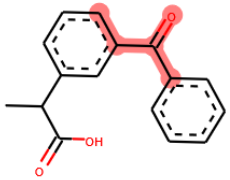 2 : FG_49 (P: -1.68 D: na)	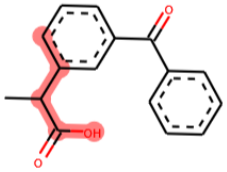 3 : FG_80 (P: 2.48 D: -37.7)		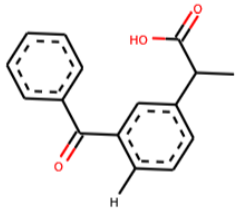	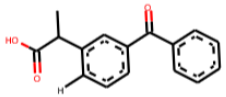
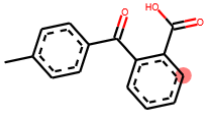	Start from salt (deprot.)[50]	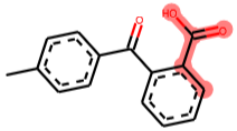 1 : FG_43 (P: 1.63 D: -17.1)	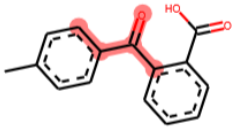 2 : FG_49 (P: -1.68 D: na)		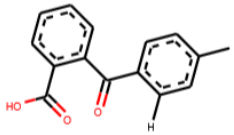	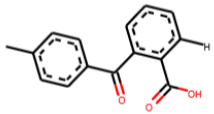
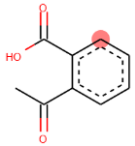	Start from carboxylic salt (deprot.)[50]	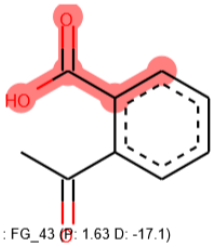 1 : FG_43 (P: 1.63 D: -17.1)	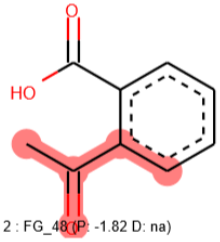 2 : FG_48 (P: -1.82 D: na)		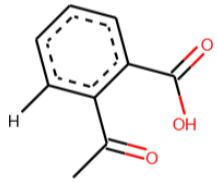	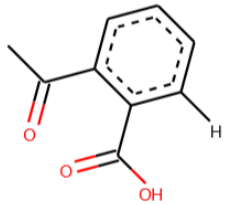

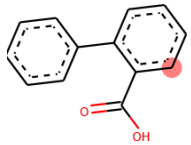	In base[51]	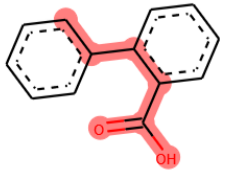 1 : FG_47A (P: 3.59 D: -14.9)	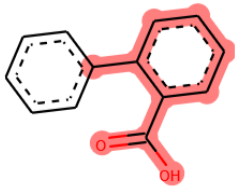 2 : FG_47B (P: 0.419 D: -18.6)		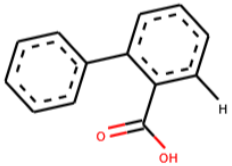	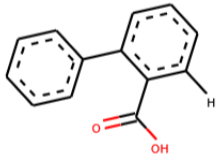
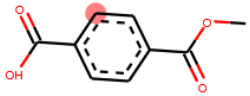	In base[51]	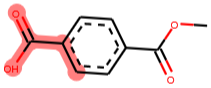 1 : FG_43 (P: 1.63 D: -17.1)	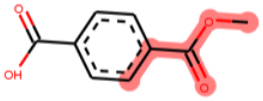 2 : FG_55 (P: 1.45 D: na)		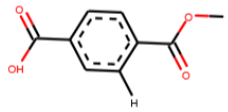 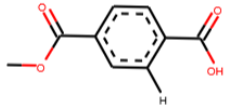	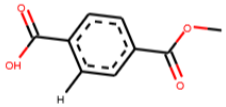
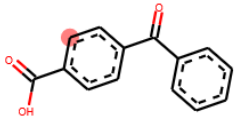	Start from carboxylic salt[52]	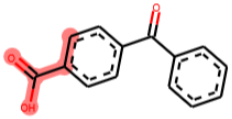 1 : FG_43 (P: 1.63 D: -17.1)	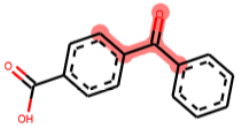 2 : FG_49 (P: -1.68 D: na)		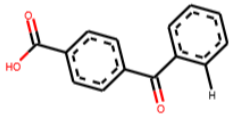	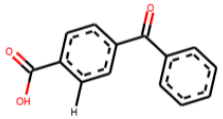
	Start from carboxylic salt[53]	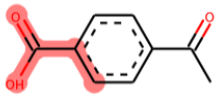 1 : FG_43 (P: 1.63 D: -17.1)	 2 : FG_48 (P: -1.82 D: na)		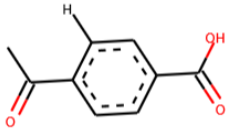	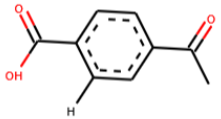
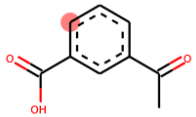	Start from carboxylic salt[53]	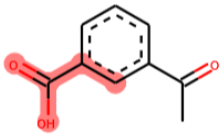 1 : FG_43 (P: 1.63 D: -17.1)	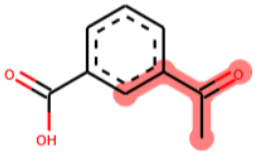 2 : FG_48 (P: -1.82 D: na)		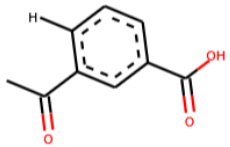	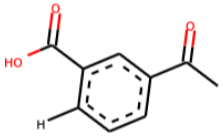

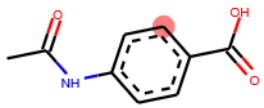	Start from carboxylic salt[53]	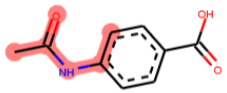 1 : FG_01 (P: -7.41 D: -22.9)	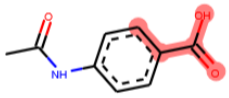 2 : FG_43 (P: 1.63 D: -17.1)	At these conditions, FG_01 will be protonated, while FG_43 is already deprotonated. Therefore, we are comparing (P: -7.41) to (D: -17.1) and **FG_43 wins.**	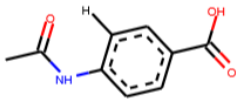	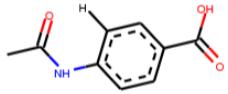
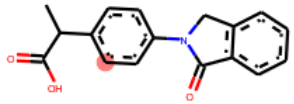	In basic[54]	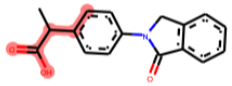 1 : FG_45A (P: 0.804 D: -17.7)	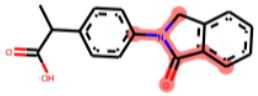 3 : FG_115A (P: -2.45 D: na)	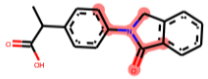 4 : FG_115C (P: -6.89 D: na)		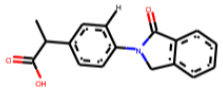
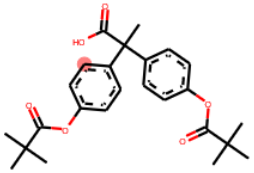	Start from carboxylic salt[55]	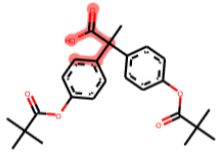 1 : FG_45A (P: 0.804 D: -17.7)	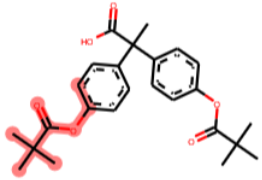 3 : FG_56 (P: -1.49 D: na)		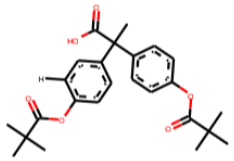	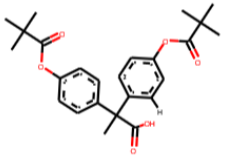
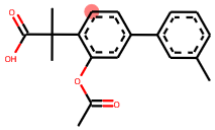	In base[56]	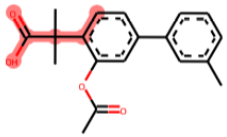 1 : FG_45A (P: 0.804 D: -17.7)	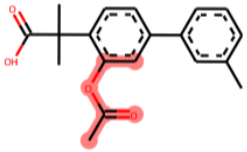 2 : FG_53 (P: -2.51 D: na)		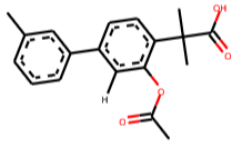	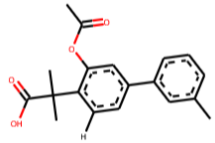

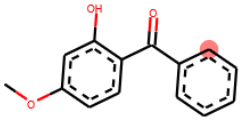	In acid[57]	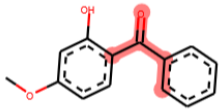 1 : FG_49 (P: -1.68 D: na)	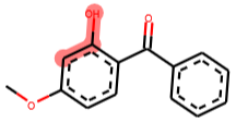 2 : FG_79H (P: na D: -4.9)		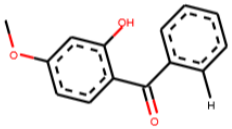	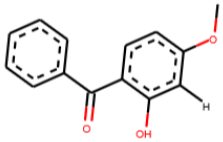
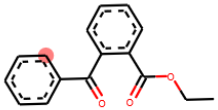	In acid[57]	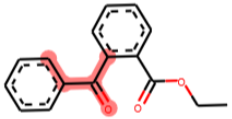 1 : FG_49 (P: -1.68 D: na)	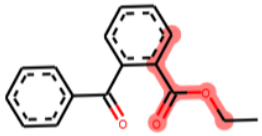 2 : FG_55 (P: 1.45 D: na)		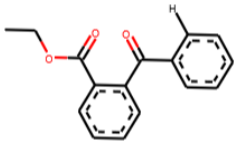	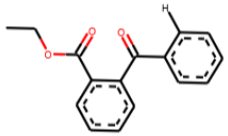
	In acid[58]	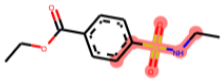 1 : FG_07C (P: -3.5 D: -20.1)	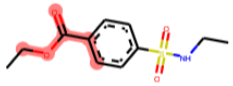 2 : FG_55 (P: 1.45 D: na)		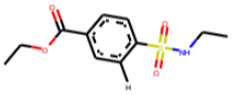	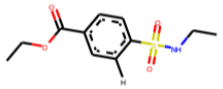
	In acid[58]	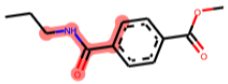 1 : FG_03 (P: -4.31 D: -31.7)	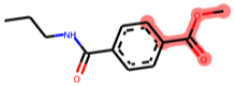 2 : FG_55 (P: 1.45 D: na)		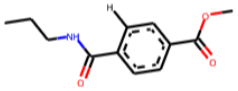	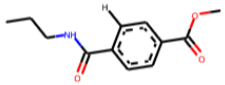
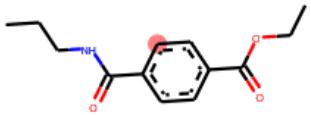	In acid[58]	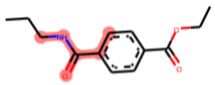 1 : FG_03 (P: -4.31 D: -31.7)	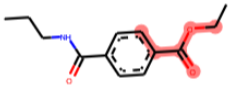 2 : FG_55 (P: 1.45 D: na)		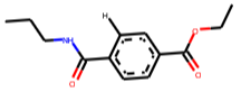	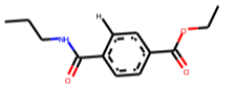

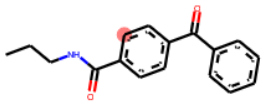	In acid[58]	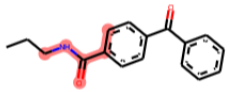 1 : FG_03 (P: -4.31 D: -31.7)	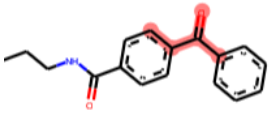 2 : FG_49 (P: -1.68 D: na)		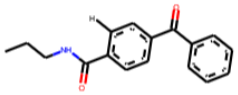	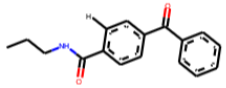
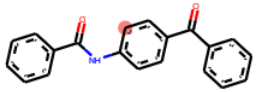	In acid[58]	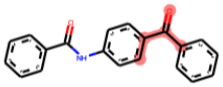 1 : FG_49 (P: -1.68 D: na)	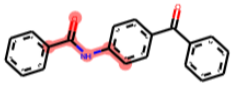 2 : FG_110A (P: -6.49 D: -21.3)	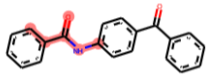 3 : FG_110C (P: -2.33 D: -27.8)	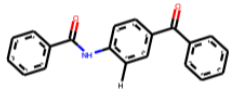	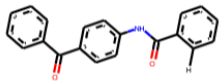
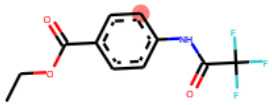	In acid[58]	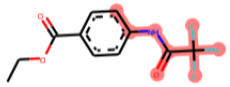 2 : FG_06 (P: -2.22 D: -17.7)	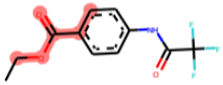 3 : FG_55 (P: 1.45 D: na)		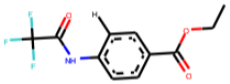	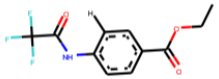
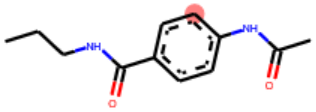	In acid[58]	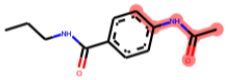 1 : FG_01 (P: -7.41 D: -22.9)	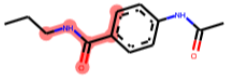 2 : FG_03 (P: -4.31 D: -31.7)		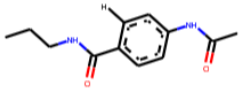	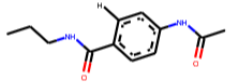
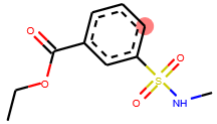	In acid[58]	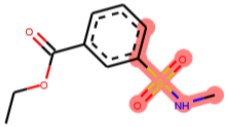 1 : FG_07C (P: -3.5 D: -20.1)	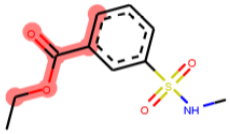 2 : FG_55 (P: 1.45 D: na)		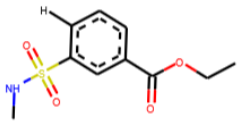	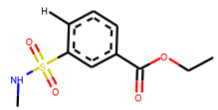

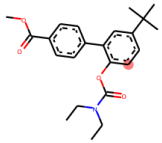	59	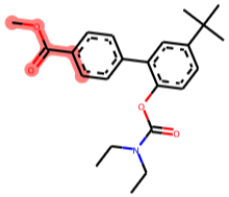 1 : FG_55 (P: 1.45 D: na)	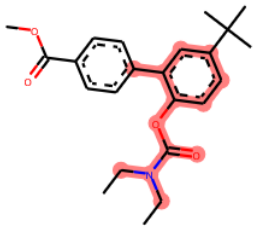 2 : FG_75A (P: -1.93 D: na)	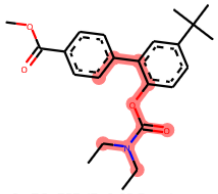 3 : FG_75B (P: 3.65 D: na)	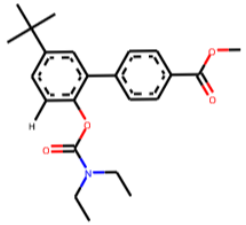	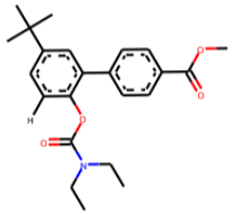
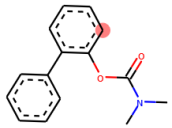	60	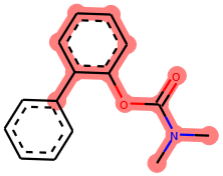 1 : FG_75A (P: -1.93 D: na)	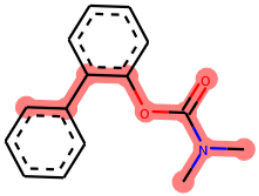 2 : FG_75B (P: 3.65 D: na)		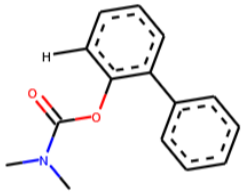	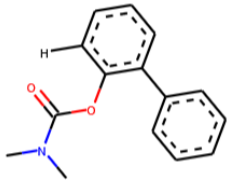
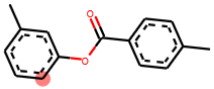	61	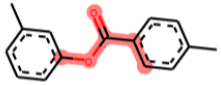 1 : FG_124A (P: 2.24 D: na)	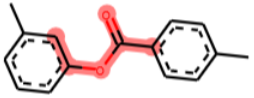 2 : FG_124B (P: -1.47 D: na)		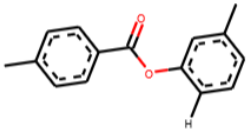	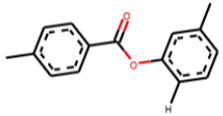
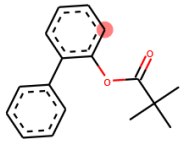	61	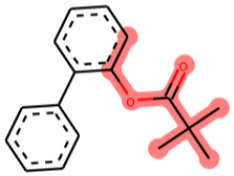 2 : FG_56 (P: -1.49 D: na)	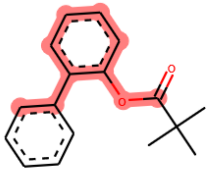 2 : FG_86 (P: 4.78 D: na)		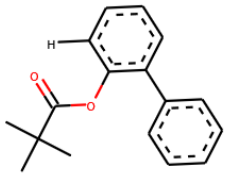	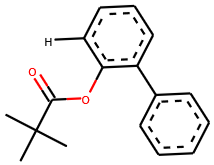
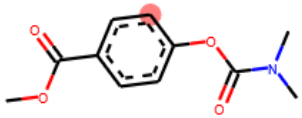	62	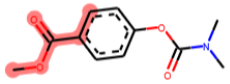 1 : FG_55 (P: 1.45 D: na)	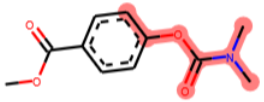 2 : FG_74 (P: -2.93 D: na)		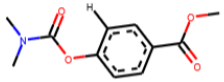	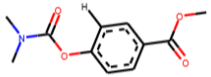

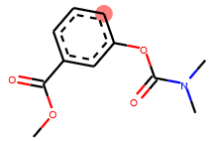	63	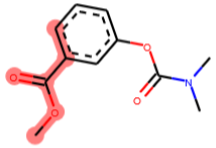 1 : FG_55 (P: 1.45 D: na)	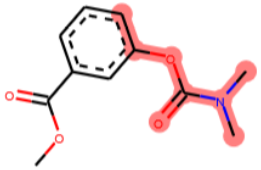 2 : FG_74 (P: -2.93 D: na)		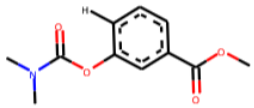	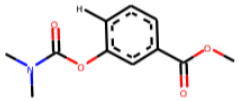
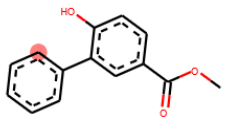	In base[64]	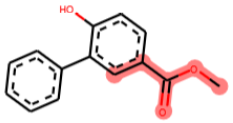 1 : FG_55 (P: 1.45 D: na)	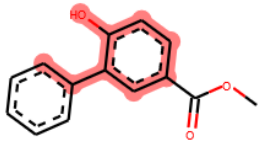 2 : FG_78 (P: 6.29 D: -22.6)		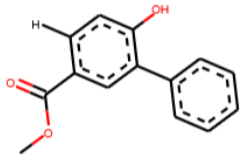	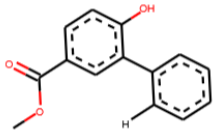
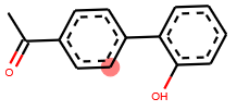	In base[64]	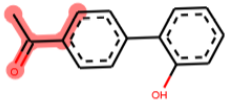 1 : FG_48 (P: -1.82 D: na)	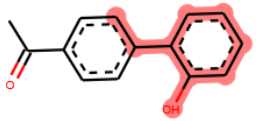 2 : FG_78 (P: 6.29 D: -22.6)		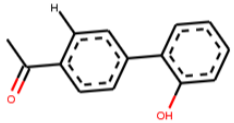	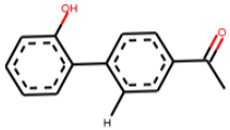
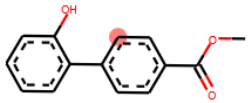	In base[64]	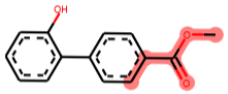 1 : FG_55 (P: 1.45 D: na)	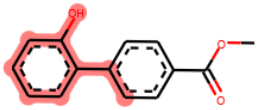 2 : FG_78 (P: 6.29 D: -22.6)		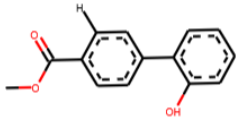	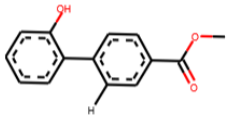
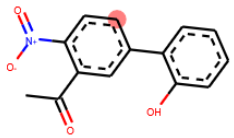	In base[65]	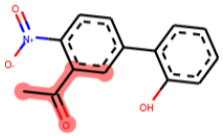 1 : FG_48 (P: -1.82 D: na)	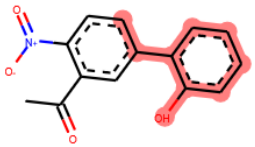 2 : FG_78 (P: 6.29 D: -22.6)		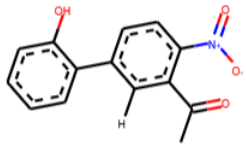	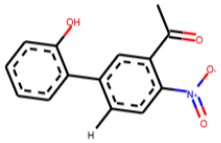

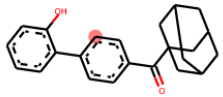	In base[65]	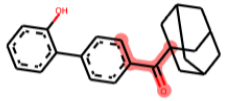 1 : FG_48 (P: -1.82 D: na)	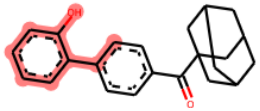 2 : FG_78 (P: 6.29 D: -22.6)		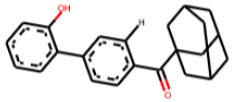	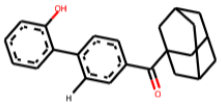
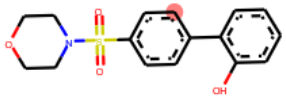	In base[65]	 1 : FG_31C (P: -2.65 D: na)	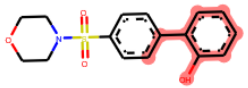 2 : FG_78 (P: 6.29 D: -22.6)		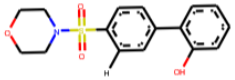	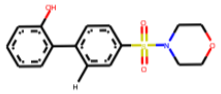
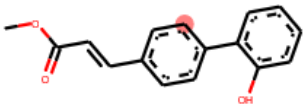	In base[65]	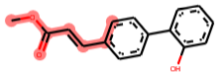 1 : FG_57 (P: 0.974 D: na)	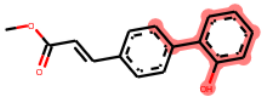 2 : FG_78 (P: 6.29 D: -22.6)		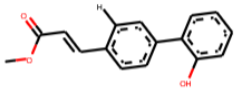	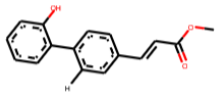
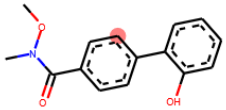	In base[65]	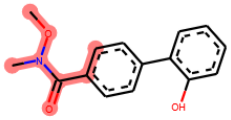 2 : FG_135 (P: -1.22 D: na)	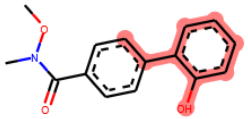 1 : FG_78 (P: 6.29 D: -22.6)		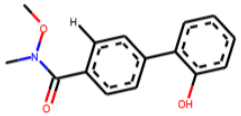	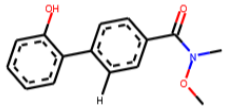
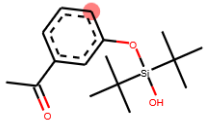	$Pd(TFA)_2$ [66]	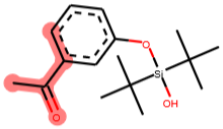 1 : FG_48 (P: -1.82 D: na)	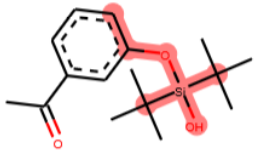 2 : FG_81 (P: 5.86 D: -19.6)		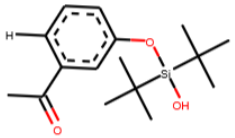	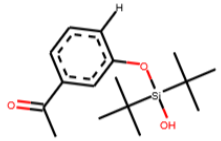

	$Pd(TFA)_2$ [66]	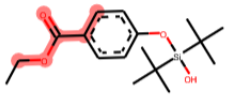 1 : FG_55 (P: 1.45 D: na)	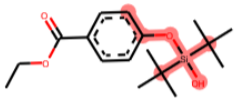 2 : FG_81 (P: 5.86 D: -19.6)		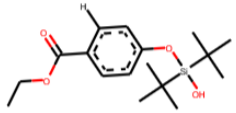	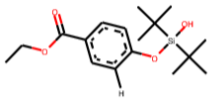
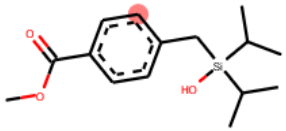	In base [67]	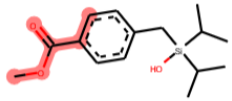 1 : FG_55 (P: 1.45 D: na)	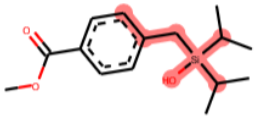 2 : FG_83 (P: 4.99 D: -18.4)		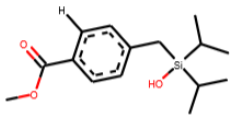	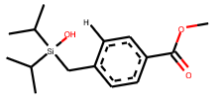
	With Ac-Gly-OH ligand[68]	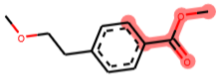 1 : FG_55 (P: 1.45 D: na)	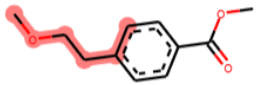 2 : FG_82 (P: 0.405 D: na)		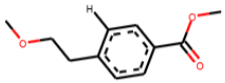	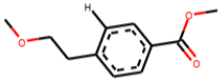
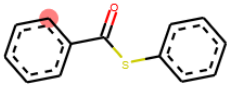	69	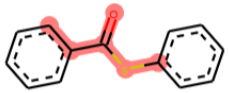 1 : FG_85B (P: -1.92 D: na)	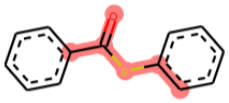 2 : FG_85C (P: 1.84 D: na)		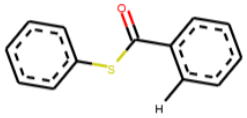	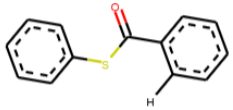
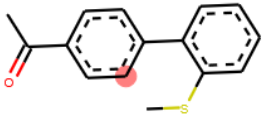	70	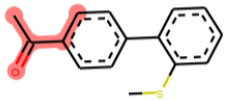 1 : FG_48 (P: -1.82 D: na)	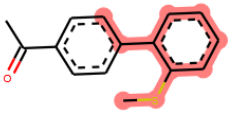 2 : FG_87 (P: -7.57 D: na)		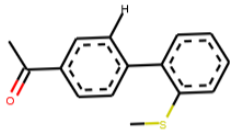	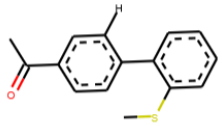

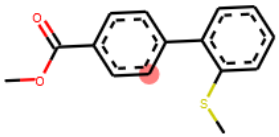	70	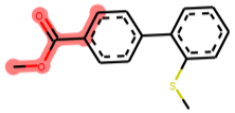 1 : FG_55 (P: 1.45 D: na)	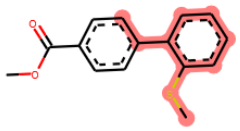 2 : FG_87 (P: -7.57 D: na)		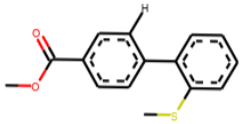	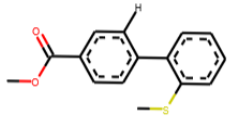
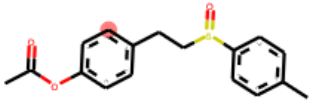	71	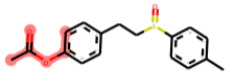 1 : FG_53 (P: -2.51 D: na)	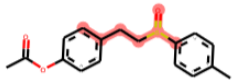 2 : FG_88 (P: -3.73 D: na)		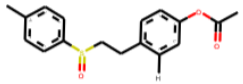	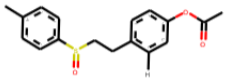
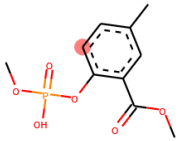	72	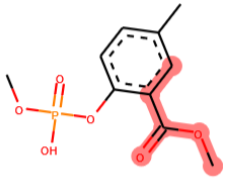 1 : FG_55 (P: 1.45 D: na)	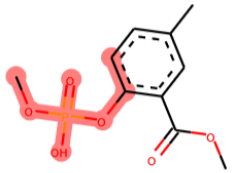 2 : FG_98 (P: 5.23 D: -9.22)		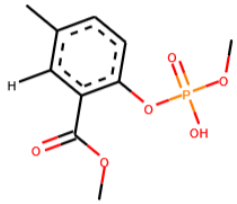	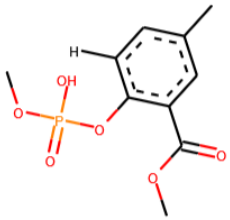
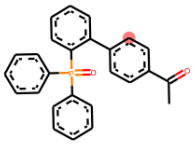	73	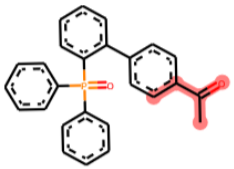 1 : FG_48 (P: -1.82 D: na)	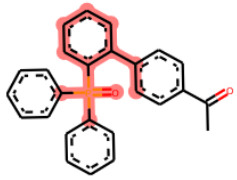 2 : FG_103 (P: -3.61 D: na)		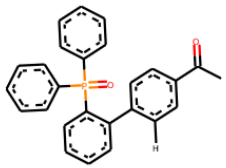	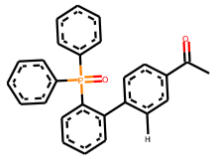
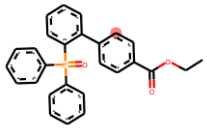	73	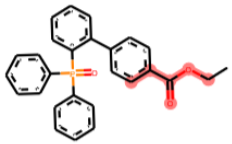 1 : FG_55 (P: 1.45 D: na)	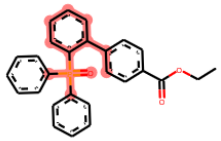 2 : FG_103 (P: -3.61 D: na)		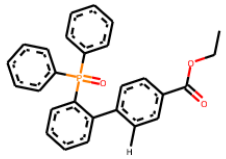	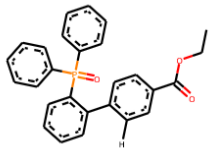

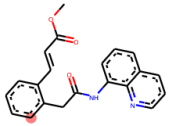	In base[74]	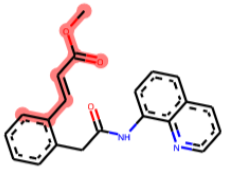 3 : FG_57 (P: 0.974 D: na)	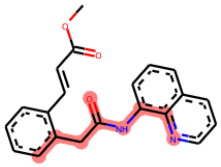 2 : FG_107A (P: 1.6 D: -27.6)	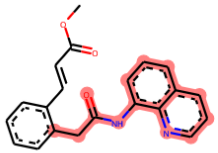 3 : FG_107B (P: -5.64 D: -20.9)	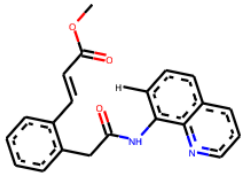	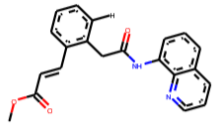
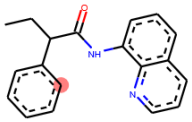	In base[74]	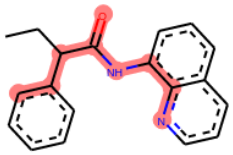 1 : FG_107A (P: 1.6 D: -27.6)	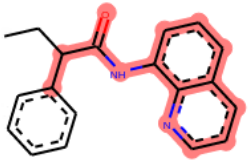 2 : FG_107B (P: -5.64 D: -20.9)			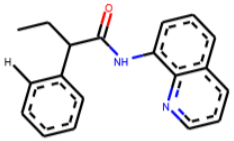
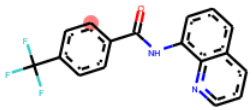	In base[75]	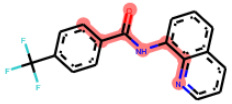 1 : FG_32A (P: 5.94 D: -44.2)	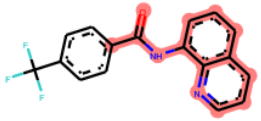 2 : FG_32B (P: -7.1 D: -20.5)		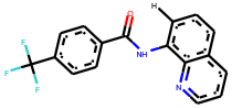	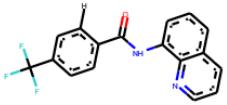
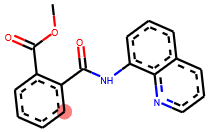	In base[75]	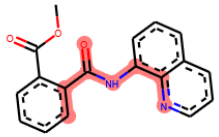 1 : FG_32A (P: 5.94 D: -44.2)	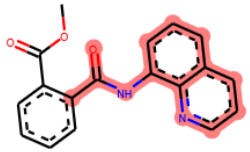 2 : FG_32B (P: -7.1 D: -20.5)	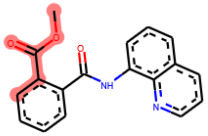 3 : FG_55 (P: 1.45 D: na)	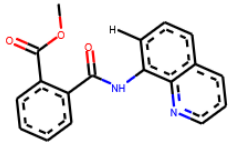	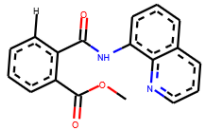
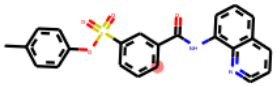	In base[75]	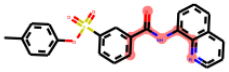 1 : FG_32A (P: 5.94 D: -44.2)		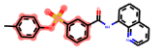 3 : FG_121A	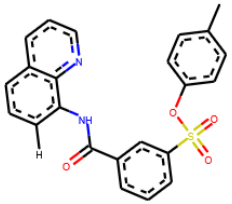	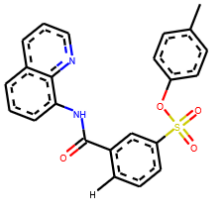

		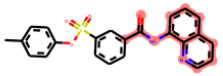 2 : FG_32B (P: -7.1 D: -20.5)	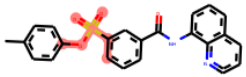 4 : FG_121B (P: 6.82 D: na) 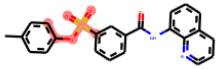 3 : FG_121A (P: 5.67 D: na)	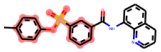 4 : FG_121B		
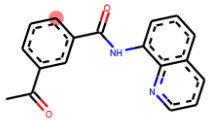	In base[75]	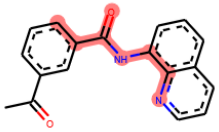 1 : FG_32A (P: 5.94 D: -44.2)	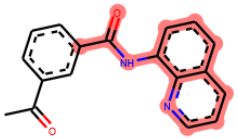 2 : FG_32B (P: -7.1 D: -20.5)	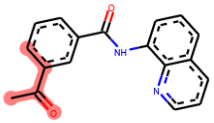 3 : FG_48 (P: -1.82 D: na)	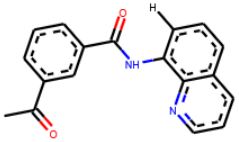	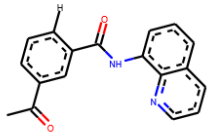
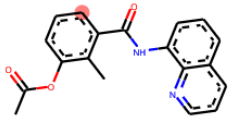	In base[75]	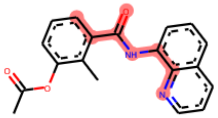 1 : FG_32A (P: 5.94 D: -44.2)	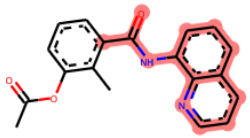 2 : FG_32B (P: -7.1 D: -20.5)	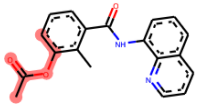 3 : FG_53 (P: -2.51 D: na)	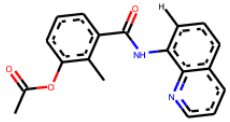	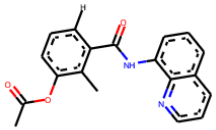
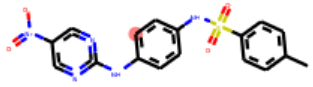	76	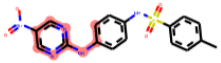 1 : FG_21 (P: -15.1 D: -26.2)	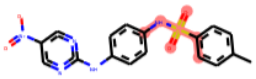 : FG_111A (P: -0.0184 D: -16.8)	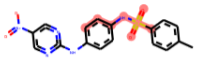 3 : FG_111C (P: 6.99 D: -5.39)		

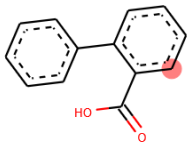	In base[51; 77]	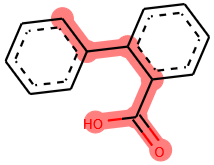 1 : FG_47A (P: 3.59 D: -14.9)	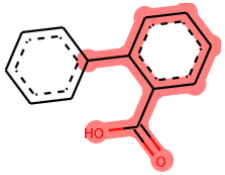 2 : FG_47B (P: 0.419 D: -18.6)		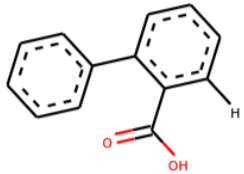	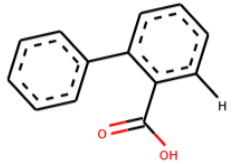
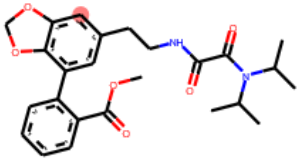	In base [78]	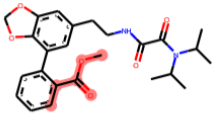 1 : FG_55 (P: 1.45 D: na)	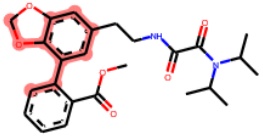 2 : FG_86 (P: 4.78 D: na)	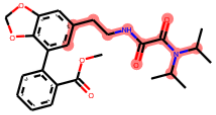 3 : FG_108 (P: 5.73 D: -28)	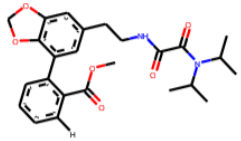	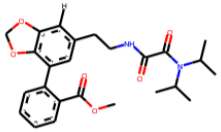
	79	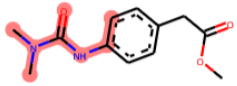 1 : FG_13 (P: -7.52 D: -21.1)	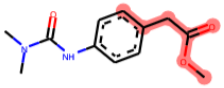 2 : FG_50 (P: 2.02 D: na)		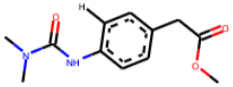	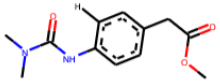
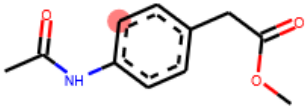	80	 1 : FG_01 (P: -7.41 D: -22.9)	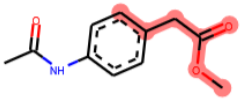 2 : FG_50 (P: 2.02 D: na)		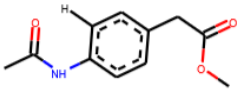	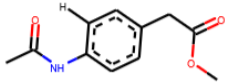
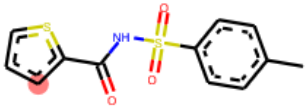	81	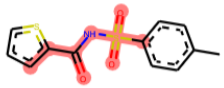 2 : FG_131A (P: 0.331 D: -19.6)	 3 : FG_131B (P: 5.99 D: -14)			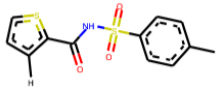

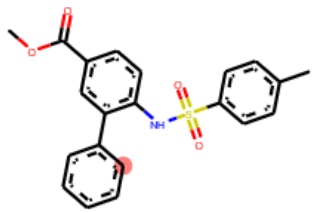	In base[82]	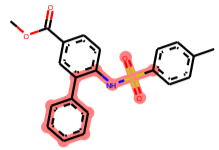 1 : FG_51A (P: -4.42 D: -20.6) 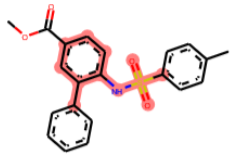 2 : FG_51B (P: 4.27 D: -6.8)	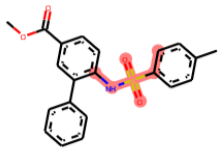 : FG_111A (P: -0.0184 D: -16.8)	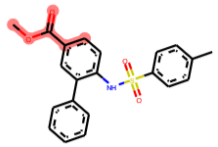 3 : FG_55 (P: 1.45 D: na)		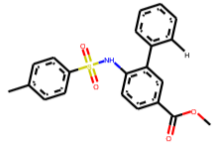
Examples of compounds where DGs are really close in energy (in either the netural or deprotonated forms), and other factors determine the regioselectivity (e.g. coupling partners, substituents on the rings, etc).						
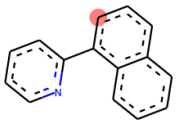	83; 84	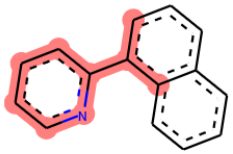 1 : FG_125A (P: -13 D: na)	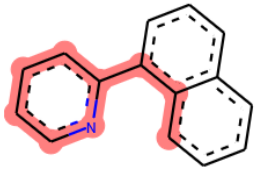 2 : FG_125B (P: -12.7 D: na)		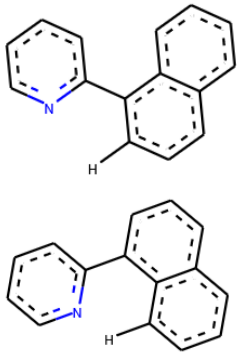	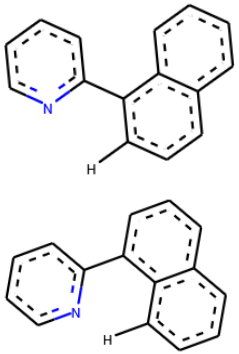

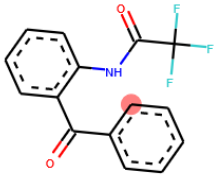	In acid[57]	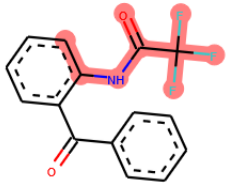 1 : FG_06 (P: -2.22 D: -17.7)	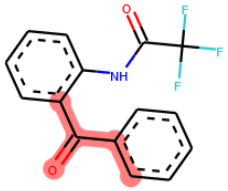 2 : FG_49 (P: -1.68 D: na)		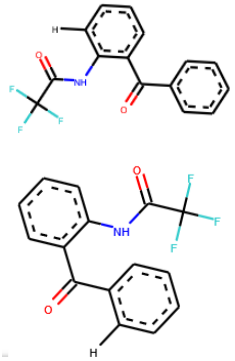	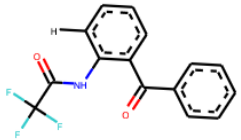
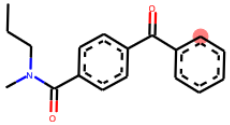	In acid[58]	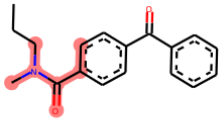 1 : FG_10 (P: -2.71 D: na)	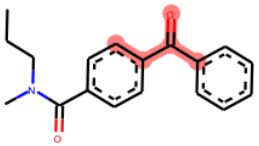 2 : FG_49 (P: -1.68 D: na)		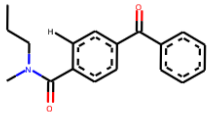 About 1 kcal/mol diff!	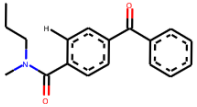
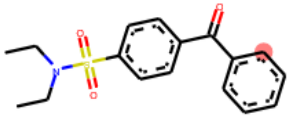	In acid[58]	 1 : FG_31C (P: -2.65 D: na)	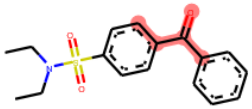 2 : FG_49 (P: -1.68 D: na)		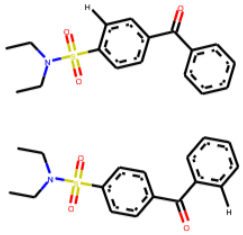	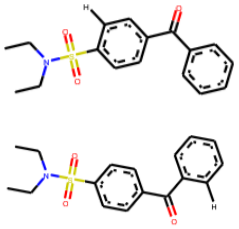
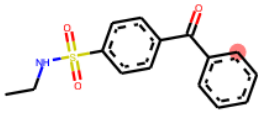	In acid[58]	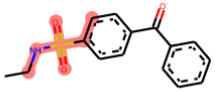 1 : FG_07C (P: -3.5 D: -20.1)	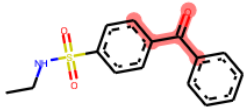 2 : FG_49 (P: -1.68 D: na)		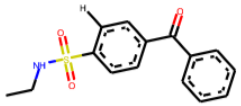 About 1 kcal/mol diff!	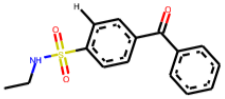

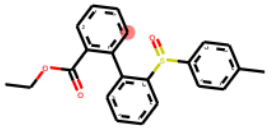	85	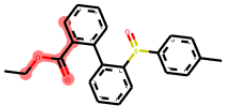 1 : FG_55 (P: 1.45 D: na)	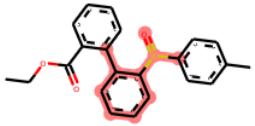 2 : FG_114B (P: -6.53 D: na)	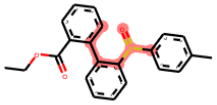 3 : FG_114C (P: -6.58 D: na)	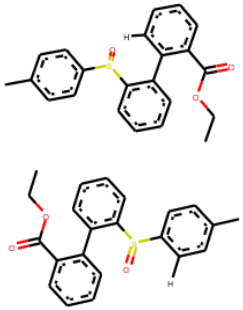	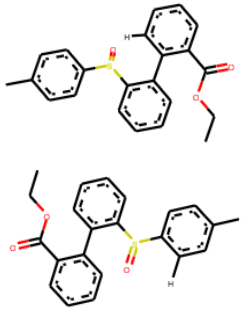

Data S6. Examples of compounds where cyclization happens because no coupling partner is present. (related to Figure 9)
In the first column, the experimental site is shown as a red circle. In columns “DG1” to “DG3”, the substructures that matched patterns of the corresponding fragments are highlighted in red.

Structure	Reaction Conditions/ References	DG1	DG2	DG3	Predicted if protonated	Predicted if deprotonated
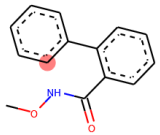	No coupling partner - cyclization[86]	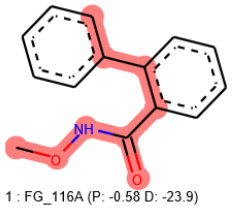 1 : FG_116A (P: -0.58 D: -23.9)	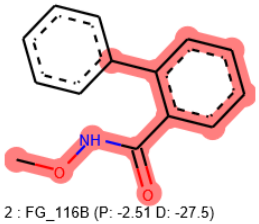 2 : FG_116B (P: -2.51 D: -27.5)		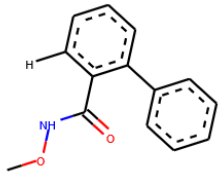	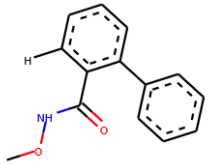
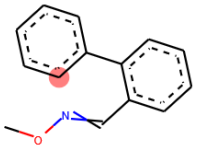	No coupling partner - cyclization[87]	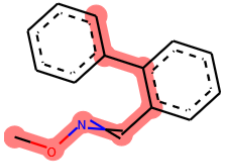 1 : FG_34A (P: -4.78 D: na)	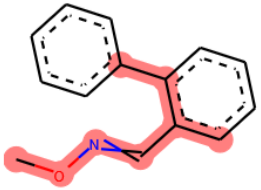 2 : FG_34B (P: -9.05 D: na)		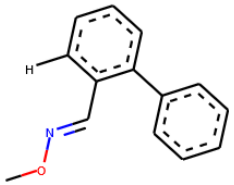	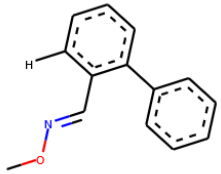

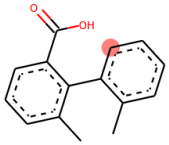	No coupling partner - cyclization [88]	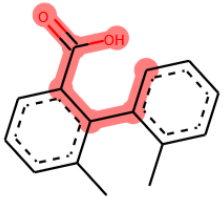 1 : FG_47A (P: 3.59 D: -14.9)	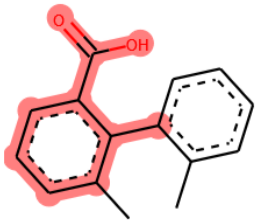 2 : FG_47B (P: 0.419 D: -18.6)		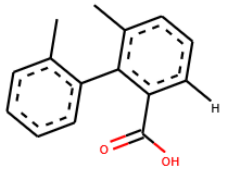	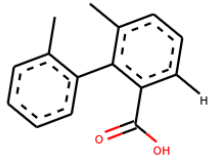
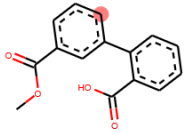	No coupling partner - cyclization [88]	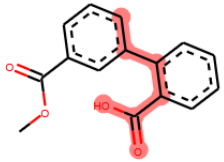 1 : FG_47A (P: 3.59 D: -14.9)	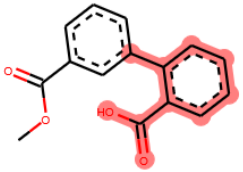 2 : FG_47B (P: 0.419 D: -18.6)	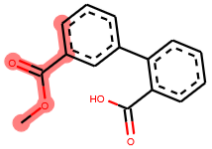 3 : FG_55 (P: 1.45 D: na)	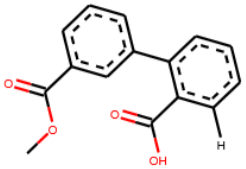	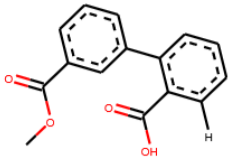
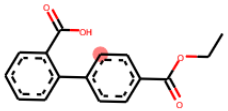	No coupling partner - cyclization [88]	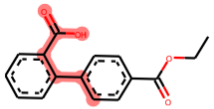 1 : FG_47A (P: 3.59 D: -14.9)	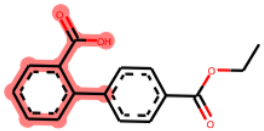 3 : FG_47B (P: 0.419 D: -18.6)	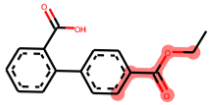 4 : FG_55 (P: 1.45 D: na)	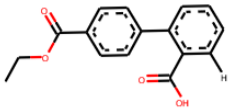	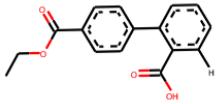
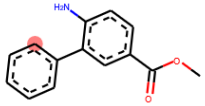	No coupling partner - cyclization [89]	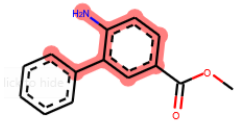 1 : FG_41 (P: -8.06 D: -37.8)	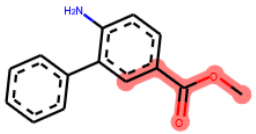 2 : FG_55 (P: 1.45 D: na)		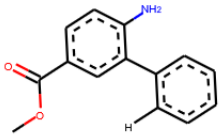	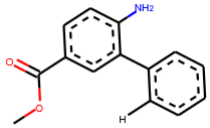
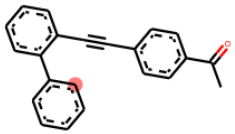	No coupling partner - cyclization[90]	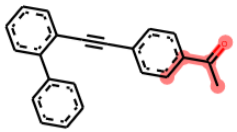 1 : FG_48 (P: -1.82 D: na)	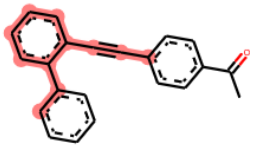 2 : FG_105 (P: 0.377 D: na)		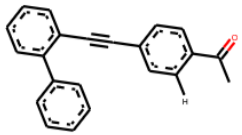	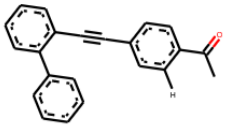

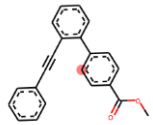	No coupling partner - cyclization[90]	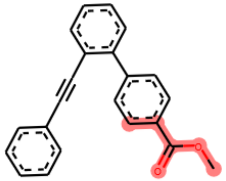 1 : FG_55 (P: 1.45 D: na)	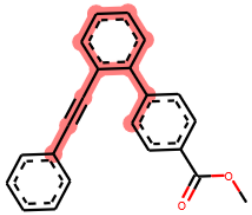 2 : FG_105 (P: 0.377 D: na)		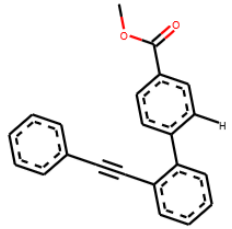	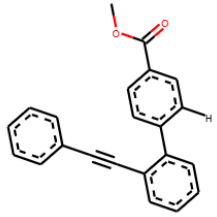
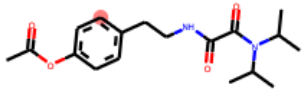	No coupling partner : N-cyclization[91]	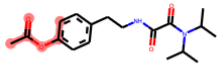 1 : FG_53 (P: -2.51 D: na)	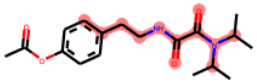 2 : FG_108 (P: 5.73 D: -28)		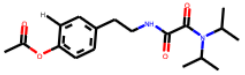	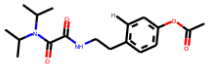

Data S7. Examples of compounds for which our predictions were incorrect. (related to Figure 13)
In the first column, the experimental site is shown as a red circle. In columns “DG1” to “DG3”, the substructures that matched patterns of the corresponding fragments are highlighted in red.

Structure	Reaction Conditions/ References	DG1	DG2	DG3	Predicted if protonated	Predicted if deprotonated
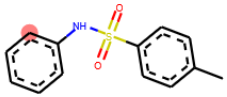	In acid[2]	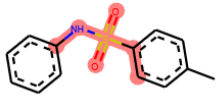 : FG_111A (P: -0.0184 D: -16.8)	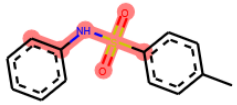 2 : FG_111C (P: 6.99 D: -5.39)		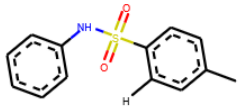	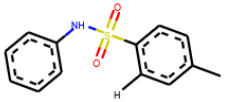

A: 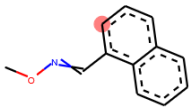 B : 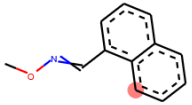	A: [92] B: [93]	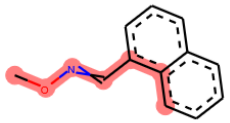 1 : FG_127A (P: -15.6 D: na)	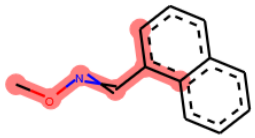 2 : FG_127B (P: -10.7 D: na)		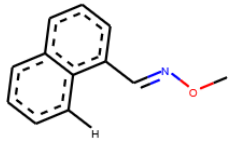	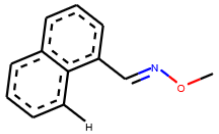
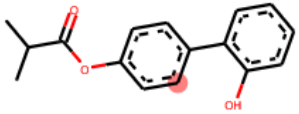	In mild acid[94]	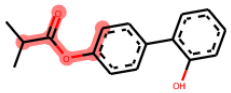 1 : FG_53 (P: -2.51 D: na)	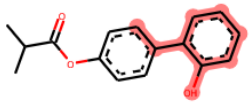 2 : FG_78 (P: 6.29 D: -22.6)		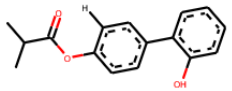	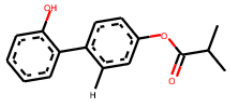

Transparent Methods

Computational section

All calculations were performed using Jaguar (Schrödinger Release 2019-1: Jaguar, Schrödinger, LLC, New York, NY, 2019).[75] The settings used were: B3LYP-D3/LACVP** (6-31G**, except on heavy atoms where ECP was used) with PBF solvation model in solvent 1,2-dichloroethane. The structures of substrates were converted from SMILES to 3D using RDkit (v. 2018.09.1)[76] with a non-exhaustive conformational analysis using MMFF. The structures of palladacycles were created manually. Where several conformations were possible, only the lowest energy one was retained. Formate was used as the model carboxylate. Energies were computed relative to the corresponding intermediate with benzene, using eq.1, where the different terms are illustrated in Scheme 2.2. The coordinates of optimized structures (all compounds and corresponding palladacycles) are collected in Data S17 in SDF format.

$$E_{rel} = E_{palladacycle\ with\ substrate} + E_{formic\ acid} + E_{benzene} - \left(E_{palladated\ benzene} + E_{substrate}\right) \qquad \text{(eq. 1)}$$

Experimental section (related to Data S8 to S16)

All reactions were performed under air atmosphere unless otherwise stated. 2-Phenylpyridine (S1) was purchased from Sigma-Aldrich and used as received; acetanilide (S2) was purchased from Merck KGaA and ground into thin powder before use, without any further purification. $Pd(OAc)_2$ was purchased from Sigma-Aldrich and crystallized from hot benzene.

Reactions were performed in microwave vials 5 – 20 ml (Biotage®). Reaction temperatures (>25 °C) were maintained using Thermowatch-controlled aluminium heating blocks.

All reactions were monitored by TLC (Merck 60F 254 nm silica gel coated glass or aluminium plates), visualized under UV (254 nm) and revealed in a $KMnO_4$ solution, as well as by LC-MS.

Purifications were performed by standard column chromatography (unless otherwise stated), using silica gel as stationary phase (Merck silica gel 60 Å pore size, particle size mesh 230-400) and the eluent as stated in each relevant experiment.

NMR spectroscopy was performed, unless stated otherwise, at 25˚C on Oxford AS500 (500/126 MHz $^1H/^{13}C$), Bruker 500 Ultrashield Plus (500/126 MHz $^1H/^{13}C$) and Bruker 600 Ultrashield (600/151 MHz $^1H/^{13}C$) instruments.
Chemical shifts (δ) are reported in ppm downfield of tetramethylsilane, using the residual solvent peak in $CDCl_3$ (δ_H = 7.26 and δ_C = 77.16 ppm) as internal reference. ^1H NMR signals are reported as follows: chemical shift δ_H (ppm), multiplicity (s = singlet, d = doublet, t = triplet; q = quartet; p = pentet, br = broad, */sh* = with shoulder; any combination of these abbreviations may be used e. g. br s = broad singlet, dt = doublet of triplets), number of protons (*n*H), assignment if relevant (e.g. H^A – as labeled on the structure drawn –). ^{13}C NMR signals are reported as follows: chemical shift δ_C (ppm), number of carbons (if $n \neq 1$), assignment if relevant.
Where crude ^1H NMRs where measured, 1,1,2,2-tetrachloroethane (TCE) was used as internal standard, unless otherwise stated.

Arylation of simplified fragments: 2-phenylpyridine (S1) and acetanilide (S2)

According to or by modification of the method reported by Sanford and co-workers. [29]

Arylation of 2-phenylpyridine (S1):

$Pd(OAc)_2$ (2.1 mg, 9.3 µmol, 0.05 equiv) and 2-phenylpyridine **S1** (29 mg, 0.19 mmol, 1 equiv) were placed in an 8-mL MW vial equipped with a magnetic stir bar. The solids were suspended/dissolved in the appropriate solvent (1.55 mL, ca. 0.12 M). Optionally an acidic additive was added (1.1–5 equiv) and the mixture stirred for 10 minutes at room temperature (ca. 25 °C) before addition of Ph_2IBF_4 (89 mg, 0.24 mmol, 1.3 equiv). The vial was sealed (under air) and the mixture was stirred vigorously and heated at 100 °C for 16–18h.

Arylation of acetanilide (S2):

$Pd(OAc)_2$ (2.1 mg, 9.3 µmol, 0.05 equiv) and acetanilide **S2** (25 mg, 0.185 mmol, 1 equiv) were placed in an 8-mL MW vial equipped with a magnetic stir bar. The solids were suspended/dissolved in the appropriate solvent (1.55 mL, ca. 0.12 M). Optionally an acidic additive was added (1.1–5 equiv) and the mixture stirred for 10 minutes at room temperature (ca. 25 °C) before addition of Ph_2IBF_4 (136 mg, 0.37 mmol, 2 equiv). The vial was sealed (under air) and the mixture was stirred vigorously and heated at 100 °C for 16–18h.
Note: to be able to quantify conversions/NMR yields reliably in crude mixtures, these reactions have to be filtered over a short silica plug eluting with heptane/EtOAc 1:1 to 2:3 and all fractions containing products or substrate combined, concentrated and an internal standard added. If filtration is not performed, the diagnostic peaks at 8.26 ppm and 8.57 ppm are presumably shifted and overlap with all other aromatic signals.

Synthesis and characterization of 2-([1,1'-biphenyl]-2-yl)pyridine S3

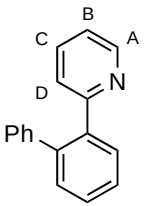

Prepared according to the procedure above, by treatment of 2-phenylpyridine **S1** with Ph_2IBF_4 (1.3 equiv) in the presence of $Pd(OAc)_2$ (5 mol%) in acetic acid (0.12 M), at 100 °C for 18h. Analysis of the crude ^1H NMR with internal standard (TCE) showed 15% unreacted 2-phenylpyridine, 41% of mono-arylation product **S3** and 35% di-arylation product **S4** (Table S4, entry 1). Isolated after column chromatography on silica gel eluting with heptane/EtOAc 4:1 to 2:1 followed by preparative TLC (heptane/EtOAc 4:1), to isolate the pure monoarylation product **S3** as a colorless crystalline solid (13 mg, 30%).

^{1}H NMR (500 MHz, $CDCl_3$) δ_H 8.64 (d, *J* 4.8 Hz, 1H, ***H^A***), 7.71 (dt, *J* 7.2, 3.6 Hz, 1H, ArC***H***), 7.50–7.42 (m, 3H, 3 × ArC***H***), 7.38 (td, *J* 7.7, 1.8 Hz, 1H, ***H^C***), 7.26–7.21 (m, 3H, 3 × PhC***H***), 7.19–7.14 (m, 2H, 2 × PhC***H***), 7.10 (ddd, *J* 7.5, 4.9, 1.0 Hz, 1H, ***H^B***), 6.89 (d, *J* 7.9 Hz, 1H, ***H^D***). *Note*: in blue font = diagnostic signal used to quantify in crude NMRs.

^{13}C NMR (126 MHz, $CDCl_3$) δ_C 159.3 (***ArCquat.=N***), 149.4 (***C^A***), 141.4 (***PhCquat.***), 140.7 (***ArCquat.***–Ph), 139.4 (***ArCquat.***–*pyridine*), 135.4 (***C^C***), 130.6 (Ar***C***H), 130.6 (Ar***C***H), 129.8 (2 × Ph***C***H), 128.7 (Ar***C***H), 128.2 (2 × Ph***C***H), 127.8 (Ar***C***H), 126.8 (***ArCquat.***), 125.6 (***C^D***), 121.5 (***C^B***).

LCMS (ESI+) *m/z* 232.04 ([M+H]$^+$, 100%) τ_R = 1.80 min; **HRMS** (ESI+) calculated mass for $[C_{17}H_{14}N]^+$ *m/z* 232.1121, measured mass *m/z* 232.1116.

Synthesis and characterization of 2-([1,1':3',1"-terphenyl]-2'-yl)pyridine S4

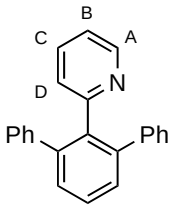

Prepared according to the procedure described for the synthesis of **S3** (Table S4, entry 1) and isolated from the same reaction crude mixture, by purification via column chromatography on silica gel eluting with heptane/EtOAc 4:1 to 2:1 followed by preparative TLC (heptane/EtOAc 4:1). The pure diarylation product **S4** was obtained as a colorless crystalline solid (14 mg, 24%).

^{1}H NMR (500 MHz, $CDCl_3$) δ_H 8.32 (d, *J* 4.2 Hz, 1H, ***H^A***), 7.53 (dd, *J* 8.4, 6.8 Hz, 1H, ***H^F***), 7.49–7.44 (m, 2H, 2 × ***H^E***), 7.32 (t, *J* 7.7 Hz, 1H, ***H^C***), 7.21–7.08 (m, 10H, 10 × PhC***H***), 6.94–6.92 (m, 1H, ***H^B***), 6.90 (d, *J* 7.8 Hz, 1H, ***H^D***). *Note*: in blue font = diagnostic signal used to quantify in crude NMRs.

^{13}C NMR (126 MHz, $CDCl_3$) δ_C 158.8 (***ArCquat.=N***), 148.4 (br, ***C^A***), 142.0 (***ArCquat.***), 141.6 (***ArCquat.***), 135.2 (br, ***C^C***), 129.8 (4 × Ph***C***H), 129.6 (2 × ***C^E***), 128.5 (br, ***C^F***), 127.8 (4 × Ph***C***H), 127.1 (br, ***C^D***), 126.5 (2 × Ph***C***H), 121.1 (***C^B***).

LCMS (ESI+) *m/z* 308.06 ([M+H]$^+$, 100%) τ_R = 2.42 min; **HRMS** (ESI+) calculated mass for $[C_{23}H_{18}N]^+$ *m/z* 308.1434, measured mass *m/z* 308.1442.

Synthesis and characterization of N-([1,1'-biphenyl]-2-yl)acetamide S5

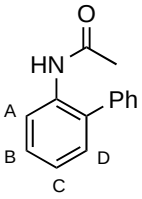

Prepared according to the procedure described for the arylation of acetanilide **S2**, in acetic acid as solvent (Table S4, entry 16) and isolated through purification by column chromatography on silica gel eluting with heptane/EtOAc 3:1 to 1:1. The product **S5** was obtained as a colorless solid (9 mg, 23%).

^{1}H NMR (500 MHz, $CDCl_3$) δ_H 8.26 (d, *J* 8.2 Hz, 1H, ***H^A***), 7.49 (t, *J* 7.4 Hz, 2H, 2 × PhC***H*** [*meta*]), 7.44–7.34 (m, 4H, 3 × PhC***H*** [*ortho/para*]+ ***H^B***), 7.26–7.22 (m, 1H, ***H^D***), 7.18 (t, *J* 7.4 Hz, 1H, ***H^C***), 7.14 (br s, 1H, N***H***), 2.02 (s, 3H, C***H$_3$***). *Note*: in blue font = diagnostic signal used to quantify in crude NMRs.

^{13}C NMR (126 MHz, $CDCl_3$) δ_C 169.3 (***C***=O), 138.2 (***PhCquat.***), 134.7 (***ArCquat.***—NHAc), 132.2 (***ArCquat.***—Ph), 130.1 (H***C^D***), 129.3 (2 × Ph***C***H), 129.1 (2 × Ph***C***H), 128.5 (H***C^B***), 128.0 (Ph***C***H *para*), 124.4 (H***C^C***), 121.7 (H***C^A***), 24.6 (***C***H$_3$).

LCMS (ESI+) *m/z* 212.0 ([M+H]$^+$, 100%) τ_R = 1.48 min; **HRMS** (ESI+) calculated mass for $[C_{14}H_{14}NO]^+$ *m/z* 212.1070, measured mass *m/z* 212.1070.

Synthesis and characterization of N-([1,1':3',1"-terphenyl]-2'-yl)acetamide S6

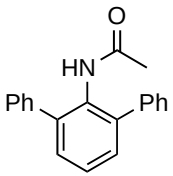

Prepared according to the procedure described for the arylation of acetanilide **S2**, in toluene as solvent (Table S4, entry 18) and isolated through purification by column chromatography on silica gel eluting with heptane/EtOAc 3:1 to 1:1. Obtained as a colorless solid (5 mg, 9%).
Note: this compound is rotameric and seemingly symmetrical protons and carbons are non-equivalent in ^{1}H and ^{13}C NMRs.

^{1}H NMR (500 MHz, $CDCl_3$) δ_H 8.57 (s /*sh*, 1H, ArC***H***), 7.68 (d, *J* 7.5 Hz, 2H, 2 × ArC***H***), 7.51 (t, *J* 7.4 Hz, 2H, 2 × ArC***H***), 7.48–7.39 (m, 6H, 6 × ArC***H***), 7.39–7.30 (m, 2H, 2 × ArC***H***), 7.19 (br s /*sh*, 1H, N***H***), 2.05 (s, 3H, C***H$_3$***). *Note*: in blue font = diagnostic signal used to quantify in crude NMRs.

^{13}C NMR (126 MHz, $CDCl_3$) δ_C 168.5 (***C***=O), 141.6 (Ar***C****quat.*), 140.6 (Ar***C****quat.*), 138.0 (Ar***C****quat.*), 135.2 (Ar***C****quat.*), 131.2 (Ar***C****quat.*), 130.6 (Ar***C***H), 129.4 (2 × Ar***C***H), 129.3 (2 × Ar***C***H), 128.9 (2 × Ar***C***H), 128.2 (2 × Ar***C***H), 127.7 (Ar***C***H), 127.4 (2 × Ar***C***H), 123.2 (Ar***C***H), 120.5 (Ar***C***H), 24.8 (***C***H_3).

LCMS (ESI+) *m/z* 288.09 ($[M+H]^+$, 100%) τ_R = 2.21 min; **HRMS** (ESI+) calculated mass for $[C_{20}H_{18}NO]^+$ *m/z* 288.1383, measured mass *m/z* 288.1382.

Stoichiometric deprotonation of S2 and subsequent arylation survey

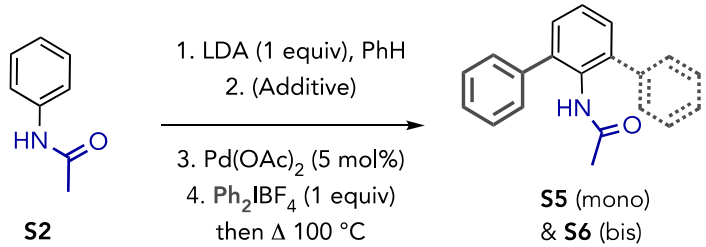

In the glovebox:

Preparation of lithium diisopropylamide (LDA): freshly distilled diisopropylamine (97 µL, 0.62 mmol, 3.3 equiv) was diluted with anhydrous benzene (0.4 mL) and to this solution was added *n*-BuLi (2.5 M in hexanes, 225 µL, 0.56 mmol, 3 equiv) slowly dropwise. The solution was diluted with anhydrous benzene to overall 1 mL of solution and left stirring at room temperature (ca. 25 °C) for 10 minutes prior to use.

Finely powdered acetanilide **S2** (25 mg, 0.19 mmol, 1 equiv) was suspended in anhydrous benzene (0.5 mL). To this suspension was added LDA (333 µL of abovementioned solution, 0.19 mmol, 1 equiv) dropwise. The resulting homogeneous gel-like mixture was stirred at room temperature for 10 minutes. It was then added to a suspension of $Pd(OAc)_2$ (42 mg, 0.19 mmol, 1 equiv) in anhydrous benzene (0.5 mL) washing the deprotonated acetamide-containing vial with anhydrous benzene (0.2 mL) and adding these washings to the $Pd(OAc)_2$-containign MW vial (overall concentration of ca. 0.12M). At this point all solids dissolved and a clear orange solution was obtained. It was stirred at room temperature for 10 minutes and solid Ph_2IBF_4 (69 mg, 0.19 mmol, 1 equiv) was added to the MW vial in one portion. The MW vial was sealed, removed from the glovebox and heated at 100 °C on a pre-heated aluminium heating block, for 18 hours.

The crude reaction mixture was then filtered over a cotton wool/sand plug and the MW vial washed with one portion of EtOAc (2 mL)/AcOH (0.5 mL), then one portion of EtOAc (2 mL)/DIPEA (0.5 mL) and finaly EtOAc (2 mL), these portions being filtered through the same cotton/sand plug. The filtrate was concentrated under vacuum and the resulting brown oil filtered on a short pad of silica gel eluting with heptane/EtOAc 9:1 to 1:1, combining all fractions containing possible products of the reaction. The combined fractions were concentrated, retaken in $CDCl_3$, 1,1,2,2-tetrachloroethane (39.4 µL, 2 equiv) was added as internal standard and a crude ^{1}H NMR measured. It indicated that only about 15% of monoarylation product **S5** has been formed, bis-arylation product **S6** could not be detected and >85% **S2** remained unreacted. This suggests that under these basic conditions, lower reactivity than under typical neutral conditions is observed.

Competition experiment:

The same experiment as above, adding 1 equivalent of 2-phenylpyridine (27 µL, 0.19 mmol, 1 equiv) to the acetanilide/LDA gel-like mixture in benzene, prior to adding this mixture to the $Pd(OAc)_2$ suspension was also performed.

It led to no observable arylation of acetanilide, however, significant arylation of 2-phenylpyridine was detected. This suggests that the conditions described herein do not allow to perform a regioselectivity switch/shift between acetanilide and pyridine DG; LDA is either not a suitable base or the conditions employed do not lead to the formation of a catalytically active acetanilide anion–Pd(II) metallacycle.

Arylations of substrate 19 featuring two directing groups

Synthesis and characterization of N-(4-(pyridin-2-yl)phenyl)acetamide 19

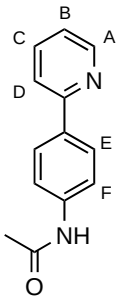

$Pd(OAc)_2$ (13 mg, 0.057 mmol, 0.015 equiv), XPhos (40 mg, 0.08 mmol, 0.022 equiv) and K_3PO_4 (2.42 g, 11.39 mmol, 3 equiv) and (4-acetamidophenyl)boronic acid (680 mg, 3.80 mmol, 1 equiv) were placed in a 20-mL MW vial equipped with a magnetic stir bar. The vial was sealed and placed under inert atmosphere (3 sequences vacuum/nitrogen). A 3:1 mixture of 1,4-dioxane / DI water (23 mL, degassed by sparging nitrogen for 20 minutes) was added, immediately followed by addition of 2-bromopyridine (0.72 mL, 7.60 mmol, 2 equiv). The resulting dark brown suspension was stirred vigorously and heated at 65 °C for 24h, whereupon an additional portion of $Pd(OAc)_2$ (13 mg, 0.057 mmol, 0.015 equiv), XPhos (40 mg, 0.08 mmol, 0.022 equiv) and 2-bromopyridine (0.36 mL, 3.80 mmol, 1 equiv) was added and heating was maintained for further 24h.
TLC (Hept/EtOAc 1:4) indicated full consumption of the starting boronic acid. The resulting mixture was concentrated *in vacuo* and the obtained oily residue partitioned between DI water (50 mL) and EtOAc (50 mL). The organic layer was collected and the aqueous layer re-extracted with EtOAc (2 x 30 mL). The combined organic layers were concentrated under vacuum and the resulting crude material purified by column chromatography on silica gel eluting with Hept/EtOAc 7:3 to 1:4 to afford the title compound **19** as a pale tan solid (750 mg, 62%).

Note: if traces of impurities (<5%) are observed after column chromatography, crystallization from hot EtOAc (ca. 2 mL per mmol) slowly layering with heptane (adding 1 mL portions every 30 minutes until a 1:3 ratio of EtOAc/Heptane is reached) usually afford analytically pure material.

^{1}H NMR (500 MHz, $CDCl_3$) δ_H 8.67 (d, *J* 4.7 Hz, 1H, H^A), 7.96 (d, *J* 8.6 Hz, 2H, 2 × H^E), 7.74 (td, *J* 7.6, 1.7 Hz, 1H, H^C), 7.70 (d, *J* 7.9 Hz, 1H, H^D), 7.63 (d, *J* 8.6 Hz, 2H, 2 × H^F), 7.50 (br s, 1H, N*H*), 7.24–7.19 (m, 1H, H^B), 2.20 (s, 3H, CH_3).

^{13}C NMR (126 MHz, $CDCl_3$) δ_C 168.5 (*C*=O), 156.8 (*pyridine* ***Cquat.***=N), 149.5 (*pyridine* C^A=N), 139.0 (***Cquat.***—NH), 137.1 (HC^C), 135.0 (***Cquat.***—*pyridine*), 127.7 (2 × HC^E), 122.1 (HC^B), 120.4 (HC^D), 119.9 (2 × HC^F), 24.9 (*C*H_3).

HRMS (ESI+) calculated mass for $[C_{13}H_{13}N_2O]^+$ *m/z* 213.1022, measured mass *m/z* 213.1016.

Pyridine vs. acetanilide directing strength comparison in compound 19

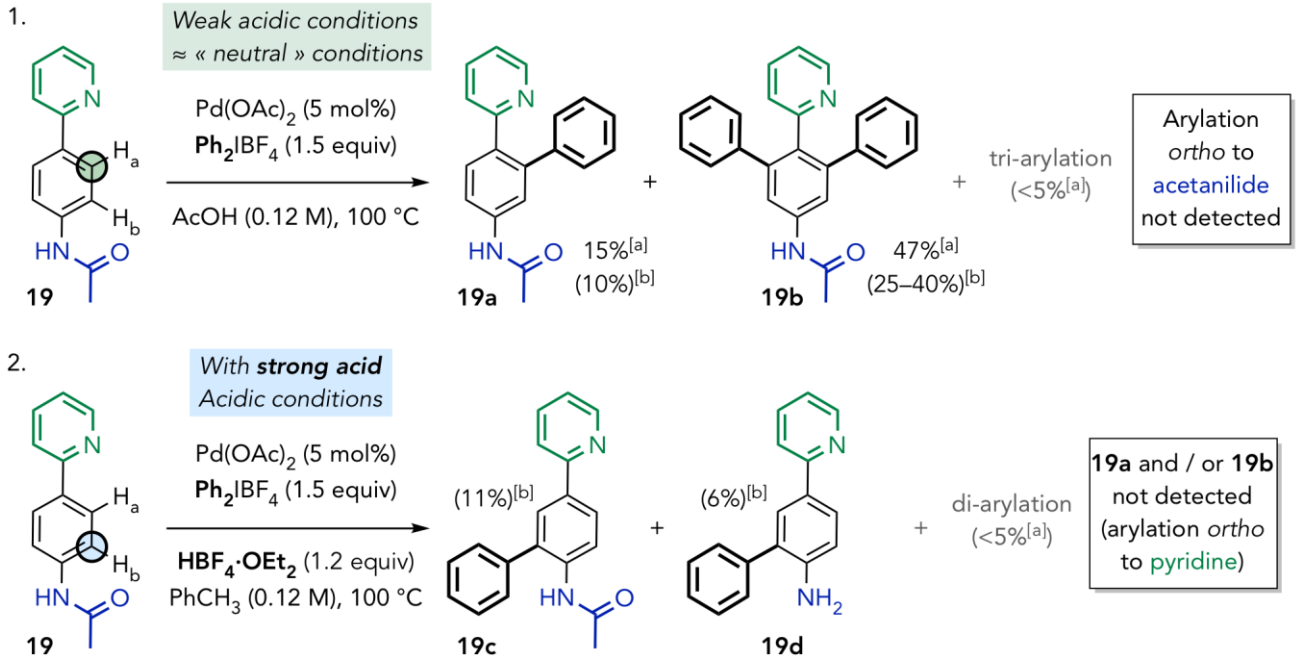

[a] ^{1}H NMR yield employing 1,1,2,2-tetrachloroethane as internal standard>; [b] Isolated yield (measured against 1,1,2,2-tetrachloroethane as internal standard).

A/ Under mildly acidic conditions (procedure A)

According to the procedure described by Sanford and co-workers. [29] $Pd(OAc)_2$ (2.01 mg, 8.9 µmol, 0.05 equiv), **19** (38 mg, 0.18 mmol, 1 equiv) and Ph_2IBF_4 (99 mg, 0.27 mmol, 1.5 equiv) were placed in an 8-mL MW vial equipped with a magnetic stir bar. The solid were suspended in acetic acid (1.55 mL, ca. 0.12 M). The vial was sealed (under air) and the suspension was stirred vigorously and heated at 100 °C for 20h.

TLC (Hept/EtOAc 1:3) indicated conversion to mainly 2 new products and small amount of a third component, which was also observed by LCMS. The resulting mixture was concentrated *in vacuo* and the obtained residue filtered on a short pad of silica gel eluting with Hept/EtOAc 7:3 to 1:4. All fractions with UV active compounds were combined, concentrated and dried under high vacuum. The obtained residue was dissolved in $CDCl_3$ and 1,1,2,2-tetrachloroethane (0.18 mmol, 1 equiv) was added as internal standard. Crude ^{1}H NMR showed 47% diarylation product **19b**, 15% monoarylation product **19a** and trace amount of tri-arylation product(s). The two main components **19a** and **19b** components were further separated either by column chromatography on silica gel (**19b** can be isolated) or by preparative HPLC.

Synthesis and characterization of N-(6-(pyridin-2-yl)-[1,1'-biphenyl]-3-yl)acetamide **19a**

Obtained according to procedure A.

May be obtained by preparative HPLC purification (acetonitrile/H_2O–NH_3 pH 10) (5 mg, 10%) as an off-white solid.

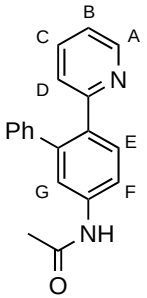

^{1}H NMR (500 MHz, $CDCl_3$) δ_H 8.60 (d, *J* 4.4 Hz, 1H, ***H^A***), 7.76 (br s, 1H, N***H***), 7.63 (d, *J* 8.3 Hz, 1H, ***H^E***), 7.60 (d, *J* 1.7 Hz, 1H, ***H^G***), 7.56 (dd, *J* 8.3, 1.8 Hz, 1H, ***H^F***), 7.40 (td, *J* 7.8, 1.7 Hz, 1H, ***H^C***), 7.25–7.17 (m, 3H, 3 × Ph-C***H*** *meta & para*), 7.17–7.08 (m, 3H, 2 × Ph-C***H*** *ortho &* ***H^B***), 6.86 (d, *J* 7.9 Hz, 1H, ***H^D***), 2.18 (s, 3H, C***H$_3$***).

^{13}C NMR (126 MHz, $CDCl_3$) δ_C 168.7 (***C***=O), 158.7 (*pyridine* ***Cquat.***=N), 149.1 (*pyridine* ***C^A***=N), 141.5 (Ph—***Cquat.***), 140.9 (Ph***Cquat.***), 138.5 (***Cquat.***—NH), 135.5 (H***C^C***), 135.0 (***Cquat.***—*pyridine*), 131.4 (H***C^E***), 129.8 (2 × Ph***C***H *ortho*), 128.3 (2 × Ph***C***H *meta*), 127.1 (Ph***C***H *para*), 125.7 (H***C^D***), 121.8 (H***C^G***), 121.5 (H***C^B***), 119.1 (H***C^F***), 24.8 (***C***H_3).

LCMS (ESI+) *m/z* 289.06 ([M+H]$^+$, 100%) τ_R = 1.20 min; **HRMS** (ESI+) calculated mass for $[C_{19}H_{17}N_2O]^+$ *m/z* 289.1335, measured mass *m/z* 289.1326.

Comment on assignment: **19a** was assigned this structure (arylation *ortho* to the pyridine DG) since the *pyridine* quaternary C(sp^2) carbon (***Cquat.***=N, δ_C 158.7 ppm) strongly correlates with ***H^E*** (as well as ***H^A***, ***H^C*** and ***H^D***). Furthermore, the quaternary C(sp^2) carbon bearing the *pyridine* moiety (***Cquat.***—*pyridine*, δ_C 135.0 ppm) strongly correlates with both ***H^G*** and ***H^F*** (as well as weakly with ***H^D***) in ***HMBS.*** In addition, the newly formed quaternary C(sp^2) carbon on the substrate core arene (Ph—***Cquat.***, δ_C 138.5 ppm) strongly correlates with ***H^E***. Finally, the quaternary C(sp^2) carbon bearing the *NHAc* moiety (***Cquat.***—NH, δ_C 138.5 ppm) strongly correlates with ***H^E*** and weakly with ***H^F*** and ***H^G***. All of this is consistent with the structure as drawn.

Synthesis and characterization of N-(2'-(pyridin-2-yl)-[1,1':3',1''-terphenyl]-5'-yl)acetamide **19b**

May be obtained after column chromatography on silica gel eluting with Hept/EtOAc 7:3 to 1:4 (28 mg, 43%) or by preparative HPLC purification (acetonitrile/H_2O–NH_3 pH 10) (30 mg, 46%) as a white solid.

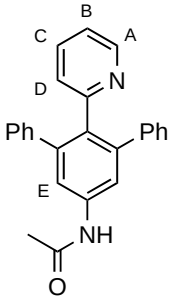

^{1}H NMR (500 MHz, $CDCl_3$) δ_H 8.84 (br s, 1H, N***H***), 8.30 (dq, *J* 5.0, 0.9 Hz, 1H, ***H^A***), 7.43 (s, 2H, 2 × ***H^E***), 7.32 (td, *J* 7.7, 1.8 Hz, 1H, ***H^C***), 7.10–7.00 (m, 6H, 6 × Ph-C***H*** *meta & para*), 7.00–6.93 (m, 5H, 4 × Ph-C***H*** *ortho &* ***H^B***), 6.84 (d, *J* 7.8 Hz, 1H, ***H^D***), 1.98 (s, 3H, C***H$_3$***).

^{13}C NMR (126 MHz, $CDCl_3$) δ_C 169.2 (***C***=O), 158.9 (*pyridine* ***Cquat.***=N), 148.3 (*pyridine* ***C^A***=N), 142.4 (Ph—***Cquat.***), 140.9 (2 × Ph***Cquat.***), 137.9 (***Cquat.***—NH), 135.5 (H***C^C***), 134.0 (***Cquat.***—*pyridine*), 129.5 (4 × Ph***C***H *ortho*), 127.7 (4 × Ph***C***H *meta*), 127.5 (H***C^D***), 126.5 (2 × Ph***C***H *para*), 122.2 (2 × H***C^E***), 121.3 (H***C^B***), 24.3 (***C***H_3).

LCMS (ESI+) *m/z* 365.10 ([M+H]$^+$, 100%) τ_R = 1.70 min; **HRMS** (ESI+) calculated mass for $[C_{25}H_{21}N_2O]^+$ *m/z* 365.1648, measured mass *m/z* 365.1658.

Comment on assignment: **19b** was assigned this structure (double arylation *ortho* to the pyridine DG) since the quaternary C(sp^2) carbon bearing the *pyridine* moiety (***Cquat.***—*pyridine*, δ_C 134.0 ppm) strongly correlates with ***H^E*** (and weakly with ***H^D***) in ***HMBS.*** In addition, the quaternary C(sp^2) carbon on the *phenyl substituents* (Ph***Cquat.***, δ_C 140.9 ppm) strongly correlates with both *meta* C***H*** on the phenyl ring as well as ***H^E***. This is consistent with the structure as drawn.

B/ In the presence of a strong acid (procedure B)

By modification of procedure A. **19** (38 mg, 0.18 mmol, 1 equiv) was placed in an 8-mL MW vial equipped with a magnetic stir bar. The solid was suspended in toluene (1.55 mL, ca. 0.12 M). $HBF_4.OEt_2$ (30 µL, 0.21 mmol, 1.2 equiv) was added and the suspension stirred for 10 minutes at room temperature (ca. 24 °C) [*Note*: a pink solid precipitated from the initial fine suspension]. $Pd(OAc)_2$ (2.01 mg, 8.9 µmol, 0.05 equiv) and Ph_2IBF_4 (99 mg, 0.27 mmol, 1.5 equiv) were then sequentially added. The vial was sealed (under air) and the suspension was stirred vigorously and heated at 100 °C for 20h.

TLC (Hept/EtOAc 1:3) indicated mostly starting material. LCMS indicated minor conversion to mainly 2 new products of masses *m/z* ($M+H^+$) = 247 (deacetylated monoarylated substrate), 289 (monoarylated substrate), and two trace amount peaks of *m/z* 323 (deacetylated bis-arylated substrate) and 365 (bis-arylated substrate). The resulting mixture was concentrated *in vacuo* and the obtained residue filtered on a short pad of silica gel eluting with Hept/EtOAc 7:3 to 1:4. All fractions with UV active compounds were combined, concentrated and dried under high vacuum. The two main components were further separated by preparative HPLC (acetonitrile/H_2O–HCO_2H pH 3).

Synthesis and characterization of N-(5-(pyridin-2-yl)-[1,1'-biphenyl]-2-yl)acetamide **19c**

Obtained according to procedure B. Isolated after purification by preparative HPLC (acetonitrile / H_2O-HCO_2H pH 3) as an off-white solid (ca. 6 mg, 11% isolated yield as measured with internal standard).

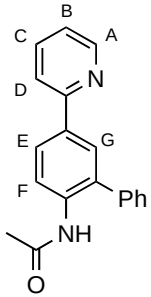

^{1}H NMR (500 MHz, $CDCl_3$) δ_H 8.67 (d, *J* 4.7 Hz, 1H, ***H^A***), 8.46 (d, *J* 8.3 Hz, ***H^F***), 7.99–7.94 (m, 2H, ***H^E*** + ***H^G***), 7.79–7.72 (m, 2H, ***H^C*** + ***H^D***), 7.54–7.48 (m, 2H, 2 × Ph-C***H*** *meta*), 7.47–7.41 (m, 3H, 3 × Ph-C***H*** *ortho* & *para*), 7.27–7.20 (m, 2H, ***H^B*** & N***H***), 2.05 (s, 3H, C***H$_3$***).

^{13}C NMR (126 MHz, $CDCl_3$) δ_C 168.4 (***C***=O), 156.7 (*pyridine* ***Cquat.***=N), 149.6 (*pyridine* ***C^A***=N), 138.0 (Ph***Cquat.***), 137.2 (H***C^C*** or H***C^D***), 135.8 (***Cquat.***—NH), 134.9 (***Cquat.***—*pyridine*), 132.3 (Ph—***Cquat.***), 129.5 (2 × Ph***C***H *ortho or meta*), 129.3 (2 × Ph***C***H *ortho or meta*), 128.9 (H***C^E*** or H***C^G***), 128.3 (Ph***C***H *para*), 127.0 (H***C^E*** or H***C^G***), 122.2 (H***C^B***), 121.4 (H***C^F***), 128.9 (H***C^C*** or H***C^D***), 24.9 (***C***H_3).

LCMS (ESI+) *m/z* 289.05 ($[M+H]^+$, 100%) τ_R = 1.43 min; **HRMS** (ESI+) calculated mass for $[C_{19}H_{17}N_2O]^+$ *m/z* 289.1335, measured mass *m/z* 289.1347.

Comment on assignment: **19c** was assigned this structure (double arylation *ortho* to the NHAc DG) since the *pyridine* quaternary C(sp^2) carbon (***Cquat.***=N, δ_C 156.7 ppm) strongly correlates with both ***H^E*** and ***H^G*** (as well as ***H^A*** and ***H^C***) while the quaternary C(sp^2) carbon bearing the *pyridine* moiety (***Cquat.***—*pyridine*, δ_C 134.0 ppm, rotameric and broad) correlates with ***H^F*** (and weakly with ***H^D***). Moreover, the phenyl substituent's quaternary C(sp^2) carbon (Ph***Cquat.***, δ_C 138.0 ppm) strongly correlates with ***H^G*** (and the *meta* PhC***H***s) in ***HMBS.*** In addition, the newly formed quaternary C(sp^2) carbon on the substrate core arene (Ph—***Cquat.***, δ_C 132.3 ppm) strongly correlates with ***H^F*** (and the *ortho* PhC***H***s). Finally, the quaternary C(sp^2) carbon bearing the *NHAc* moiety (***Cquat.***—NH, δ_C 135.8 ppm) strongly correlates with both ***H^E*** and ***H^G*** and only to these protons. This is consistent with the structure as drawn.

Synthesis and characterization of 5-(pyridin-2-yl)-[1,1'-biphenyl]-2-amine **19d**

Obtained according to procedure B. Isolated after purification by preparative HPLC (acetonitrile / H_2O-HCO_2H pH 3) as a yellow oil (ca. 3 mg, 6% isolated yield as measured with internal standard).

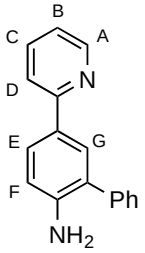

^{1}H NMR (500 MHz, $CDCl_3$) δ_H 8.63 (d, *J* 4.4 Hz, 1H, ***H^A***), 7.86 (d, *J* 8.3 Hz, ***H^E***), 7.80 (d, *J* 2.2 Hz, ***H^G***), 7.74–7.64 (m, 2H, ***H^C*** + ***H^D***), 7.54–7.49 (m, 2H, 2 × Ph-C***H*** *ortho*), 7.49–7.44 (m, 2H, 2 × Ph-C***H*** *ortho*), 7.40–7.34 (m, 1H, Ph-C***H*** *para*), 7.18 (br, 1H, ***H^B***), 6.86 (d, *J* 8.3 Hz, ***H^F***), 4.50–3.50 (br, 2H, N***H$_2$***).

^{13}C NMR (126 MHz, $CDCl_3$) δ_C 157.5 (*pyridine* ***Cquat.***=N), 149.6 (*pyridine* ***C^A***=N), 144.7 (***Cquat.***—NH_2), 139.4 (Ph***Cquat.***), 136.7 (H***C^D***), 129.4 (Ph—***Cquat.***), 129.3 (2 × Ph***C***H *ortho*), 129.3 (H***C^G***), 129.0 (2 × Ph***C***H *meta*), 127.8 (***Cquat.***—*pyridine*), 127.5 (Ph***C***H *para*), 127.3 (H***C^E***), 121.4 (H***C^B***), 119.6 (H***C^F***).

LCMS (ESI+) *m/z* 247.07 ([M+H]$^+$, 100%) τ_R = 1.17 min; **HRMS** (ESI+) calculated mass for $[C_{17}H_{15}N]^+$ *m/z* 247.1230, measured mass *m/z* 247.1234.

Comment on assignment: **19d** was assigned this structure (arylation *ortho* to the NHAc DG) since the *pyridine* quaternary C(sp^2) carbon (***Cquat.***=N, δ_C 157.5 ppm) strongly correlates with both ***H^E*** and ***H^G*** (as well as ***H^A*** and ***H^C***) in ***HMBS***. In addition, the quaternary C(sp^2) carbon on the *phenyl substituents* (Ph***Cquat.***, δ_C 139.4 ppm) strongly correlates with both *meta* C***H*** on the phenyl ring as well as ***H^G*** (and weakly to ***H^F***). Finally, the quaternary C(sp^2) carbon bearing the *NH_2 functionality* (***Cquat.***—NH_2, δ_C 144.7 ppm) strongly correlates with both *meta* ***H^E*** and ***H^G*** and no other proton. This is consistent with the structure as drawn.

C/ Attempt of regioselectivity switch by stoichiometric deprotonation

Similar to the approach described above for stoichiometric deprotonation of **S2**:

In the glovebox:

Preparation of lithium diisopropylamide (LDA): freshly distilled diisopropylamine (146 µL, 1.04 mmol, 11 equiv) was diluted with anhydrous benzene (1 mL) and to this solution was added *n*-BuLi (2.5 M in hexanes, 377 µL, 0.9 mmol, 10 equiv) slowly dropwise. The solution was diluted with anhydrous benzene to overall 2 mL of solution and left stirring at room temperature (ca. 25 °C) for 10 minutes prior to use.

Finely powdered acetanilide **19** (20 mg, 0.09 mmol, 1 equiv) was supended in anhydrous benzene (0.3 mL). To this suspension was added LDA (200 µL of abovementioned solution, 0.09 mmol, 1 equiv) dropwise. The resulting gel-like mixture was stirred at room temperature for 10 minutes. It was then added to a suspension of $Pd(OAc)_2$ (21.2 mg, 0.09 mmol, 1 equiv) in anhydrous benzene (0.2 mL) washing the deprotonated acetamide-containing vial with anhydrous benzene (0.1 mL) and adding these washings to the $Pd(OAc)_2$-containign MW vial (overall concentration of ca. 0.12M). At this point lighter orange suspension was obtained. It was stirred at room temperature for 10 minutes and solid Ph_2IBF_4 (35 mg, 0.09 mmol, 1 equiv) was added to the MW vial in one portion. The MW vial was sealed, removed from the glovebox and heated at 100 °C on a pre-heated aluminium heating block, for 18 hours.

The crude reaction mixture was then filtered over a cotton wool/sand plug and the MW vial washed with one portion of EtOAc (2 mL)/AcOH (0.2 mL), then one portion of EtOAc (2 mL)/DIPEA (0.2 mL) and finaly EtOAc (2 mL), these portions being filtered through the same cotton/sand plug. The filtrate was concentrated under vacuum and the resulting brown oil purified by silica gel column chromatography eluting with heptane/EtOAc 4:1 to 1:4. The main new component of the reaction (<5-10%) was isolated and its analytical data (^{1}H NMR and LCMS retention time and *m/z*) were consistent with it being **19b**. it is worth mentioning that a large part of the material decomposes into an insoluble black solid in the course of this procedure.

Data S8. Spectra for 2-([1,1'-Biphenyl]-2-yl)pyridine S3 (related to Scheme 6)

^{1}H NMR spectrum

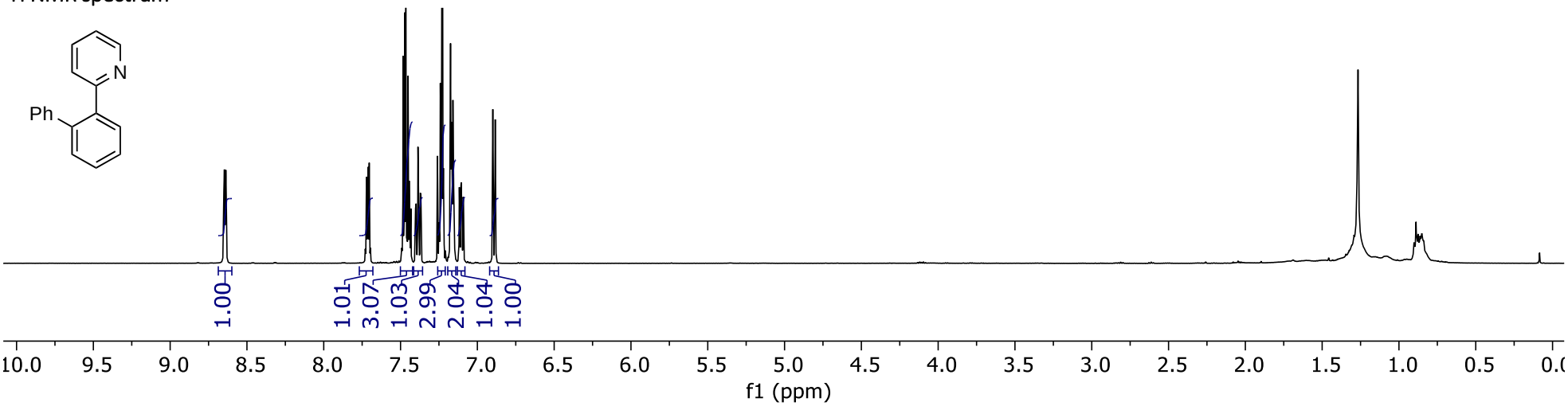

^{13}C NMR spectrum

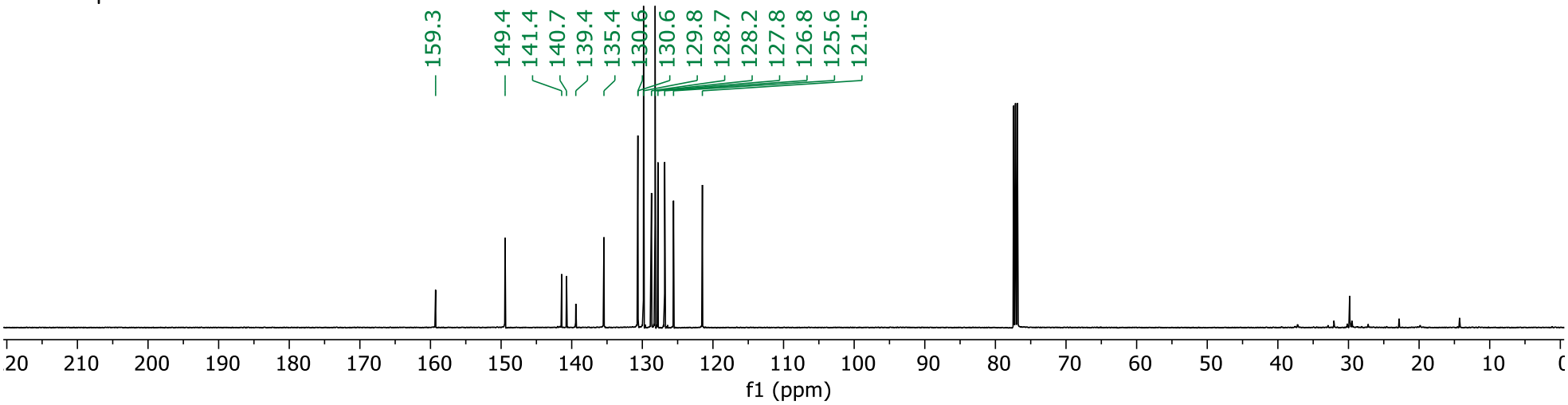

Data S9. Spectra for 2-([1,1':3',1''-Terphenyl]-2'-yl)pyridine S4 (related to Scheme 6)

^{1}H NMR spectrum

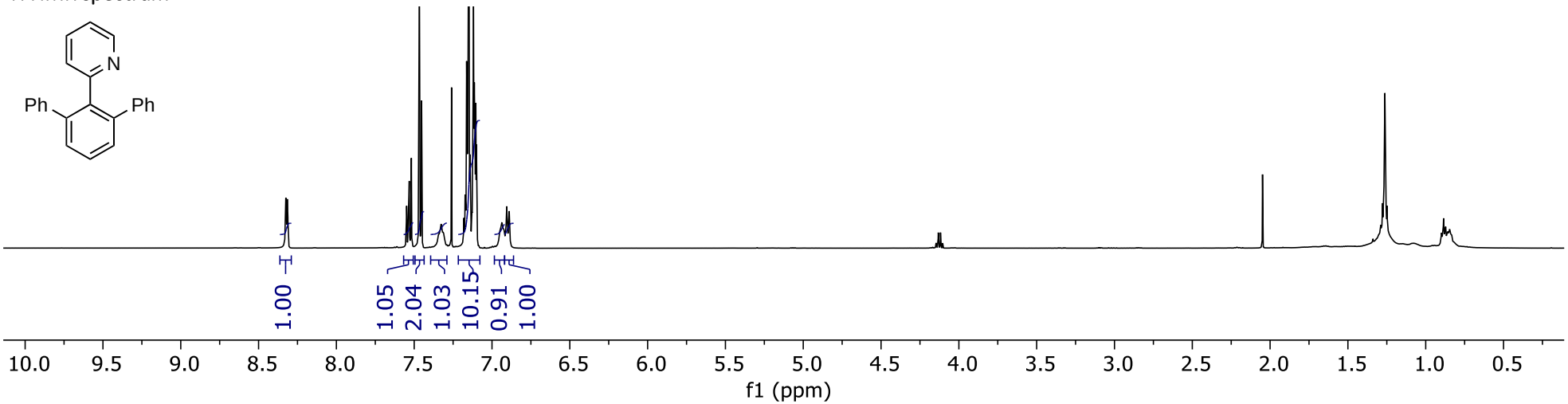

^{13}C NMR spectrum

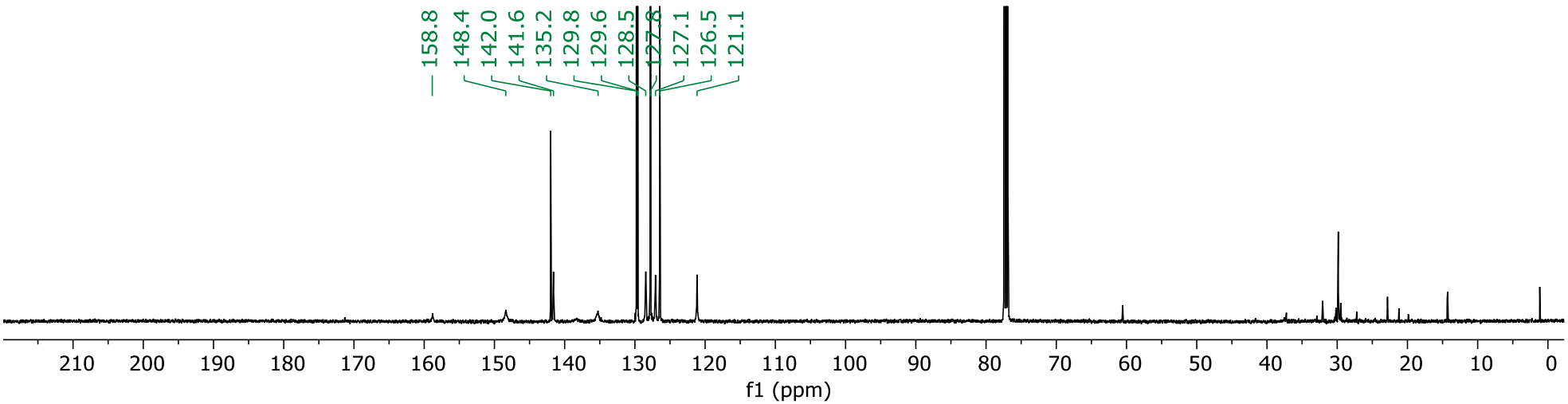

Data S10. Spectra for *N*-([1,1'-Biphenyl]-2-yl)acetamide S5 (related to Scheme 6)

^{1}H NMR spectrum

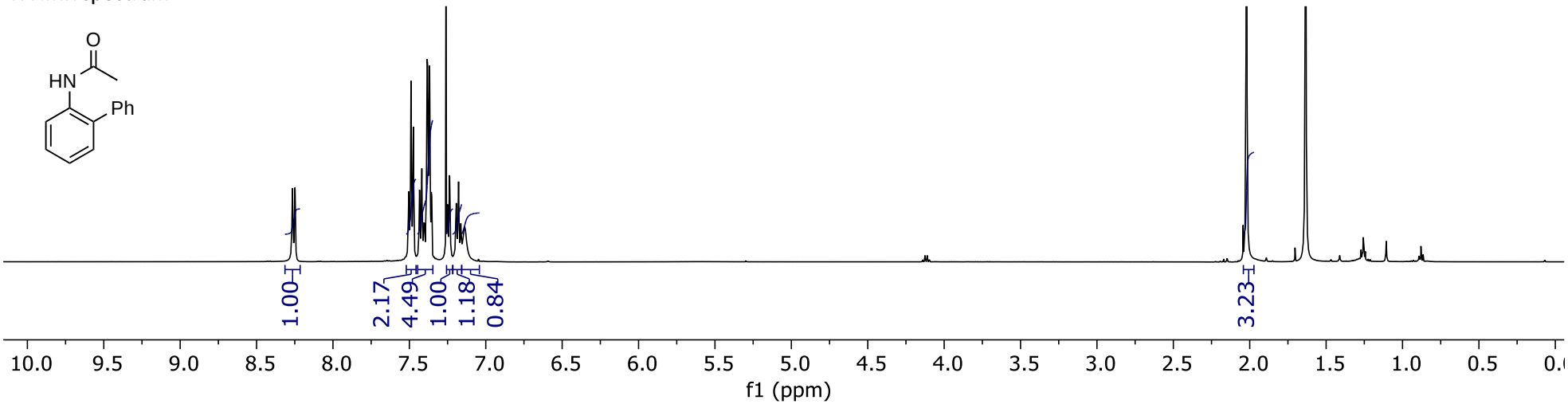

^{13}C NMR spectrum

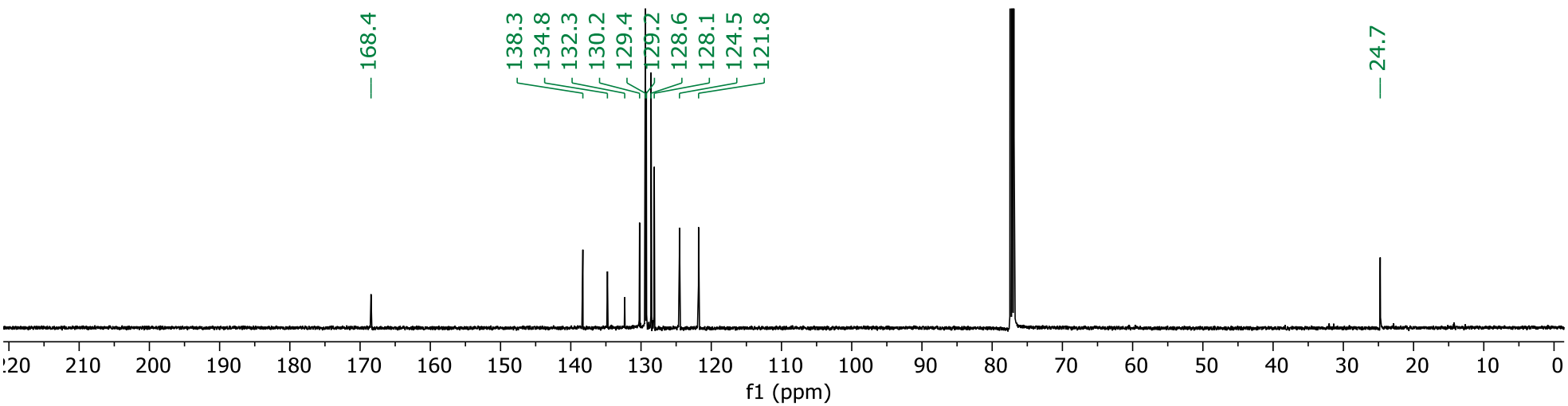

Data S11. Spectra for *N*-([1,1':3',1"-Terphenyl]-2'-yl)acetamide S6 (related to Scheme 6)

^{1}H NMR spectrum

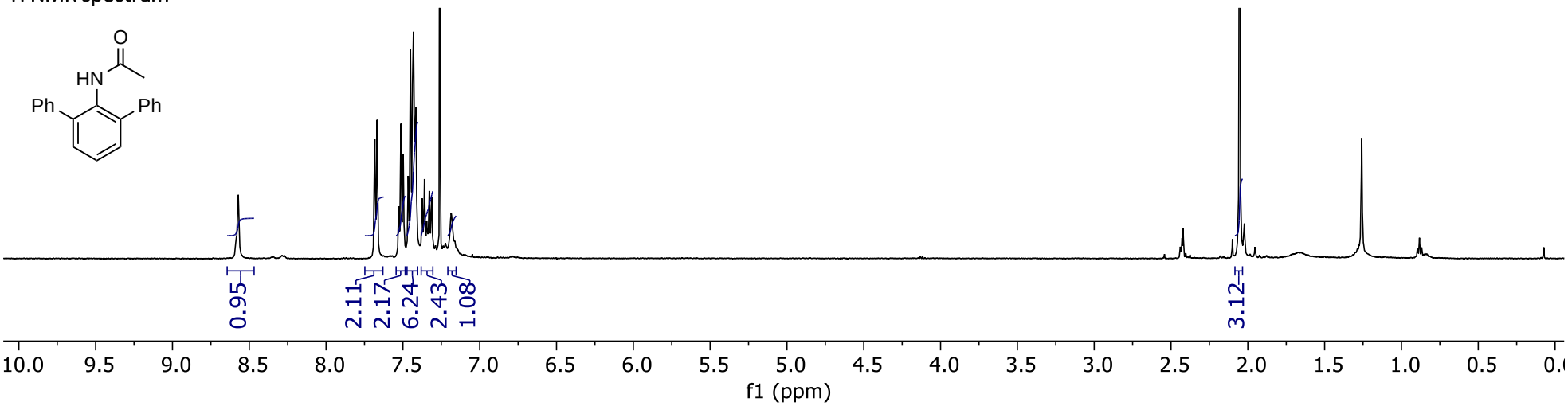

^{13}C NMR spectrum

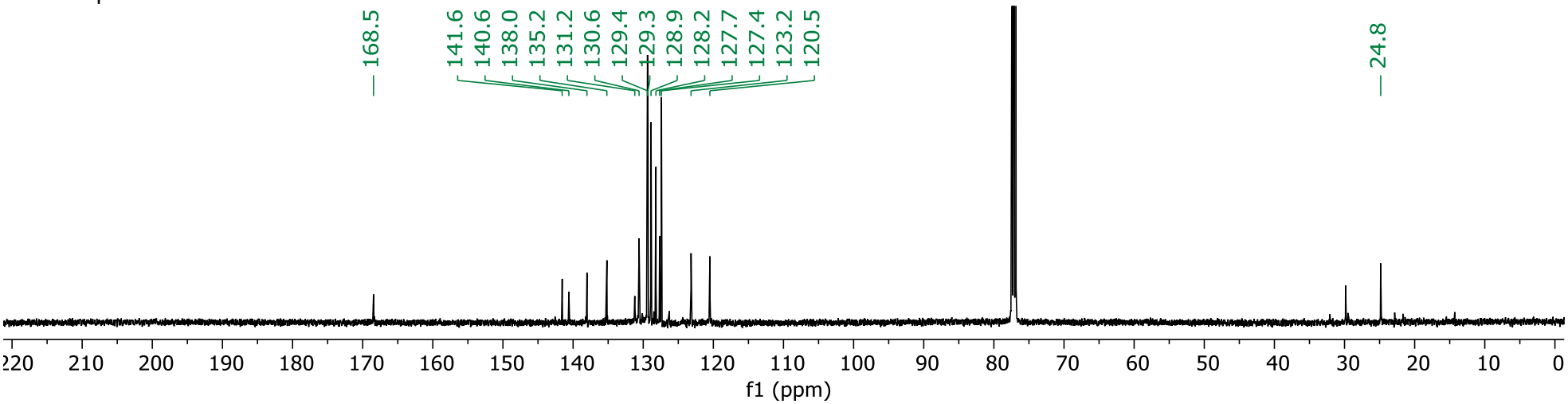

Data S12. Spectra for *N*-(4-(Pyridin-2-yl)phenyl)acetamide 19 (related to Scheme 6)

^{1}H NMR spectrum

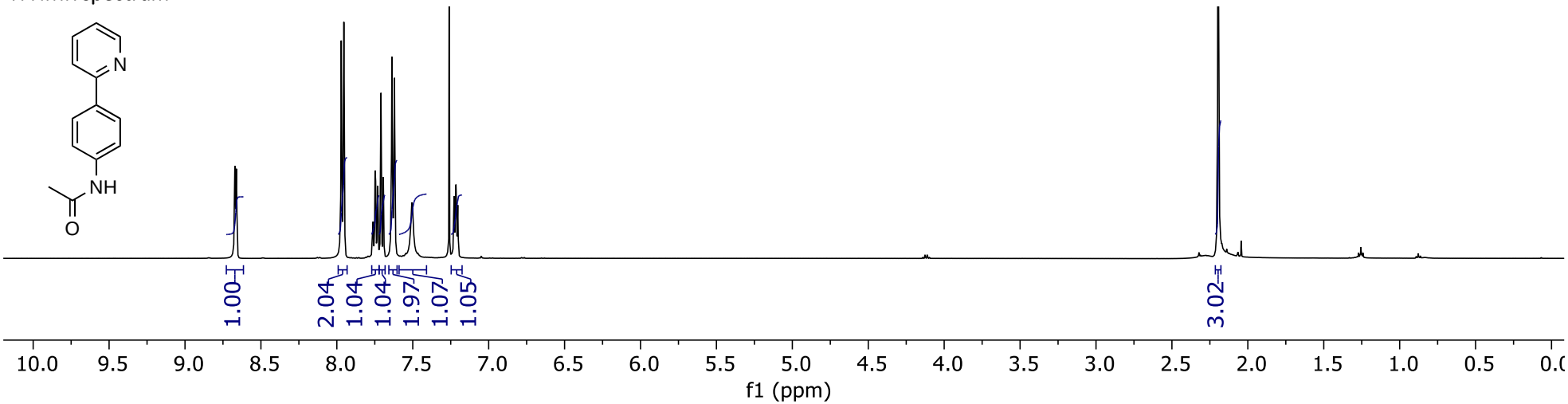

^{13}C NMR spectrum

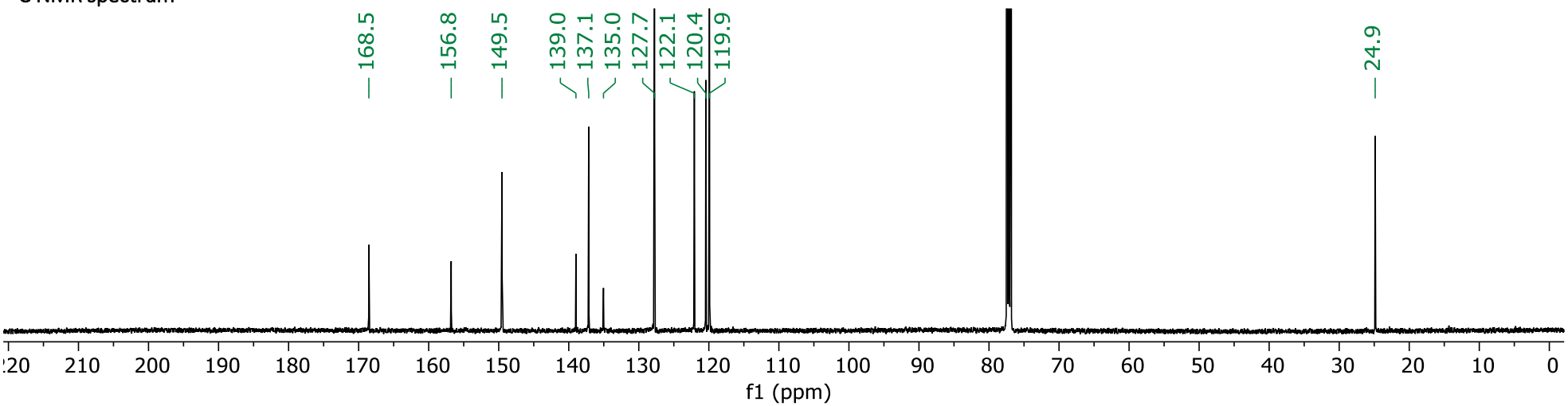

Data S13. Spectra for *N*-(6-(Pyridin-2-yl)-[1,1'-biphenyl]-3-yl)acetamide 19a (related to Scheme 6)

^{1}H NMR spectrum

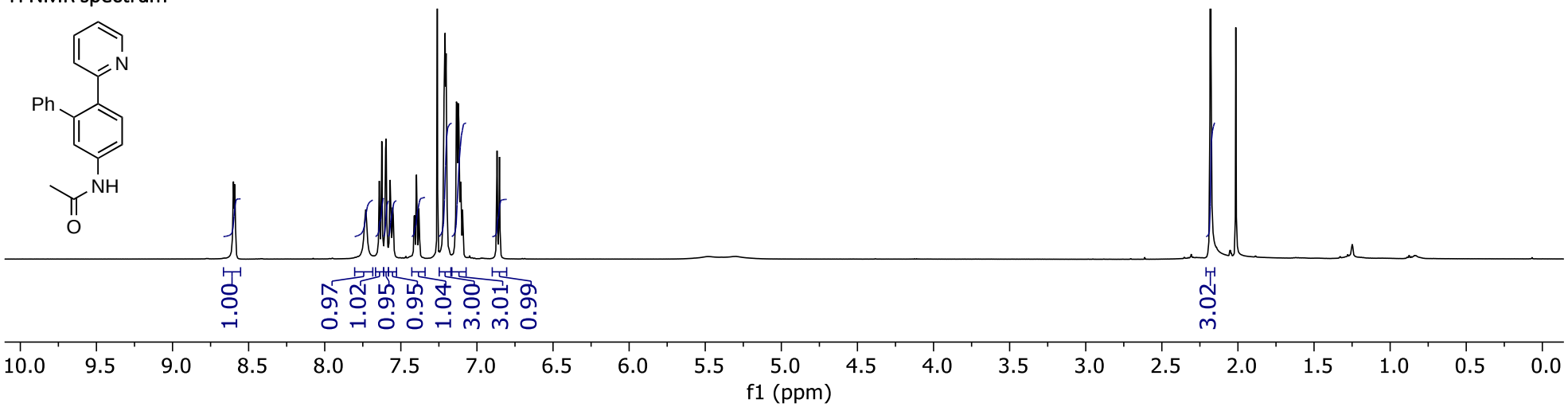

^{13}C NMR spectrum

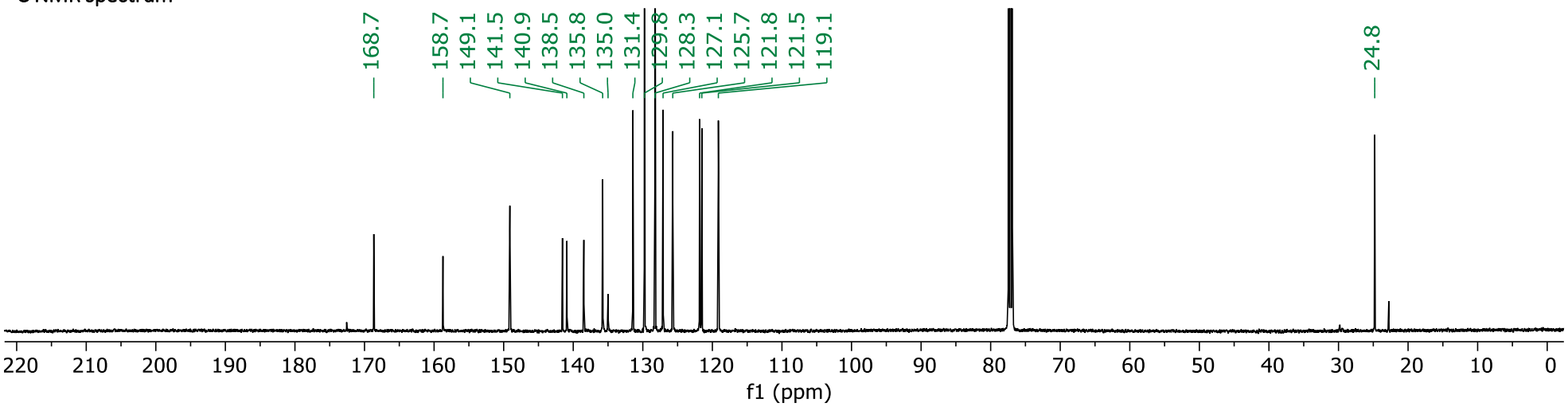

COSY correlation NMR

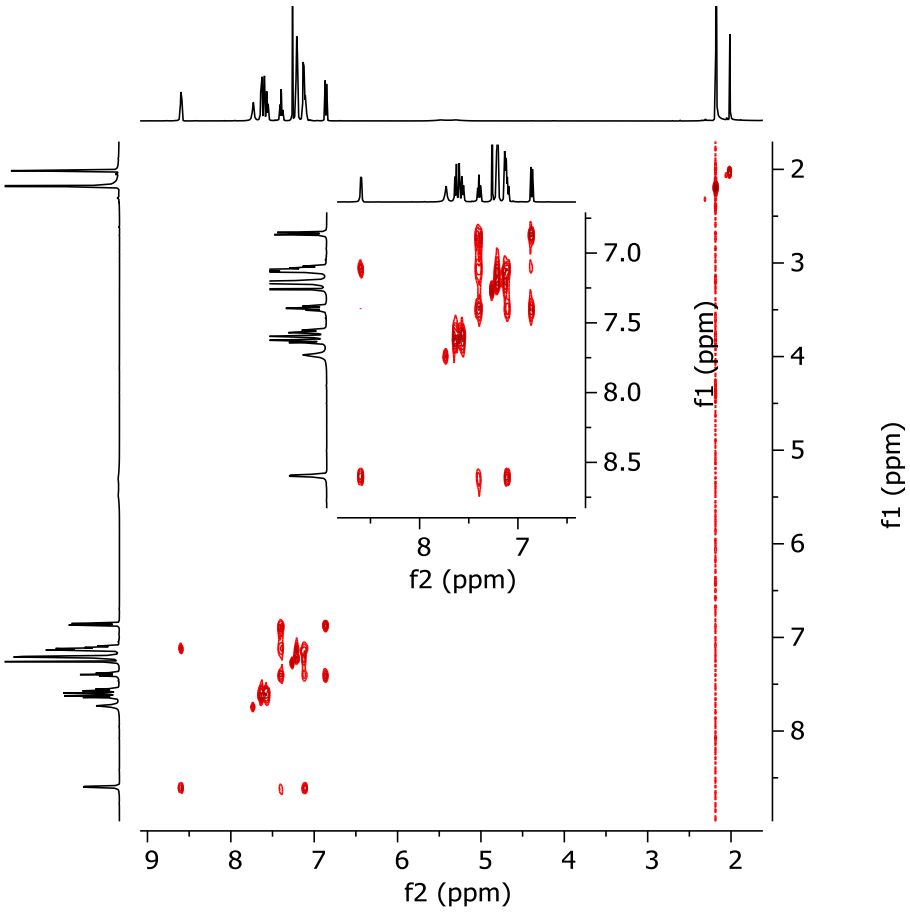

HSQC correlation NMR

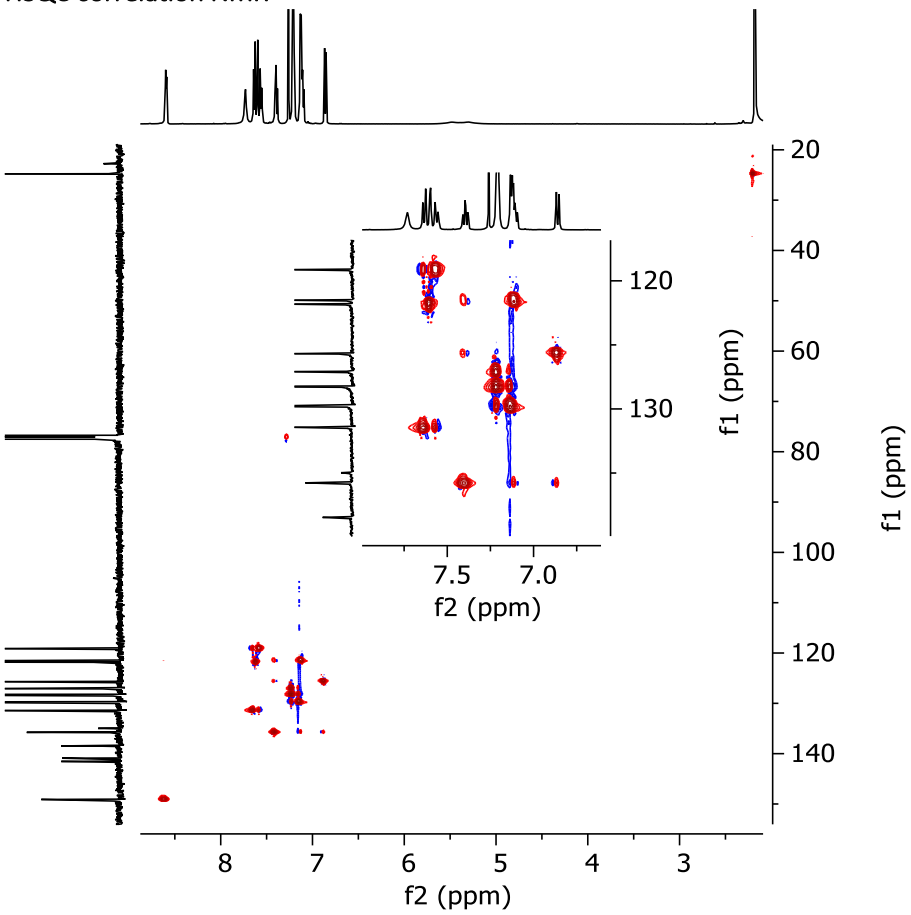

HMBC correlation NMR

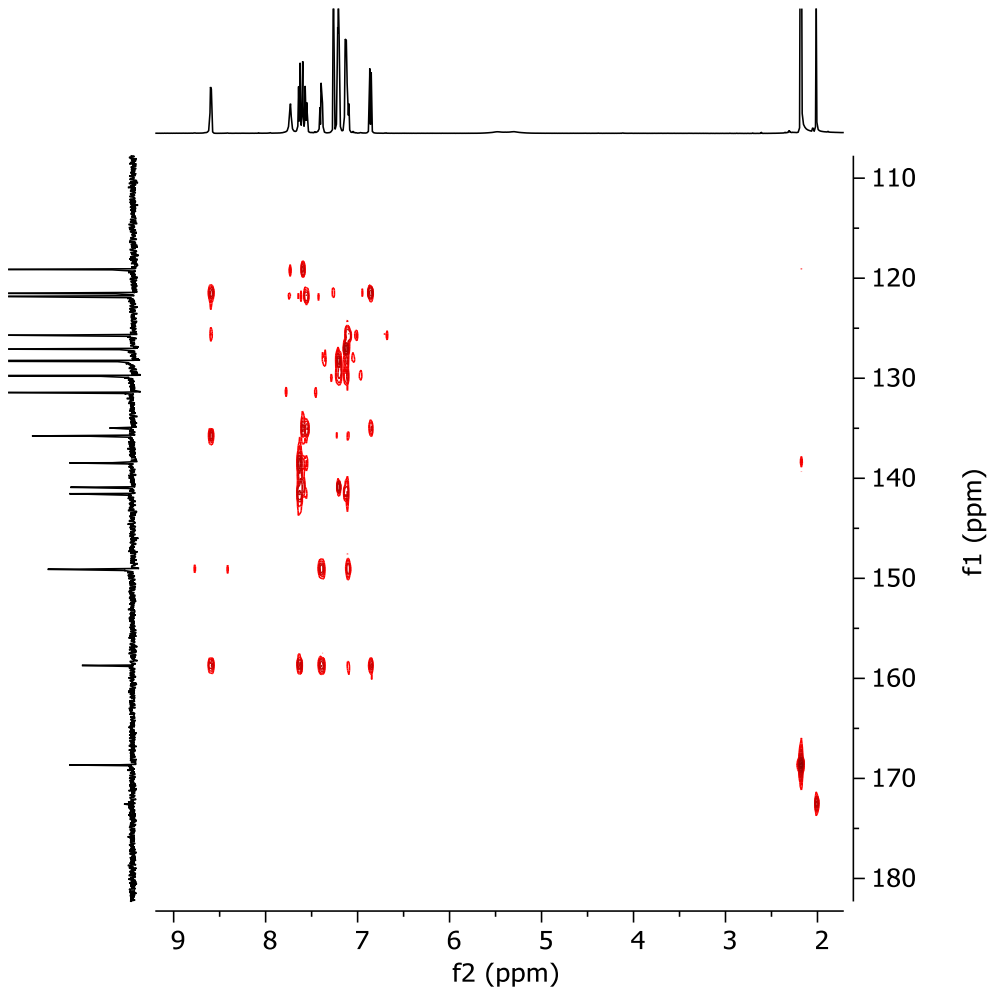

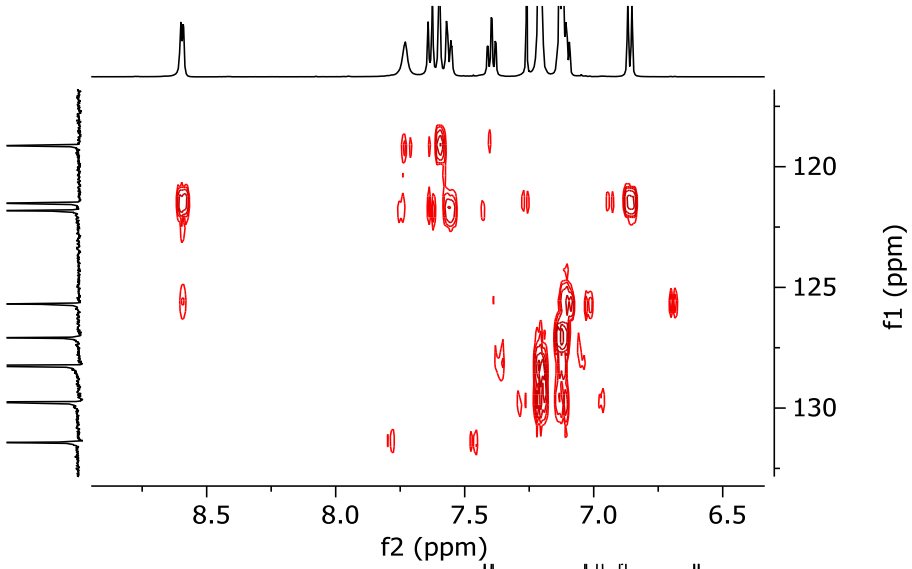

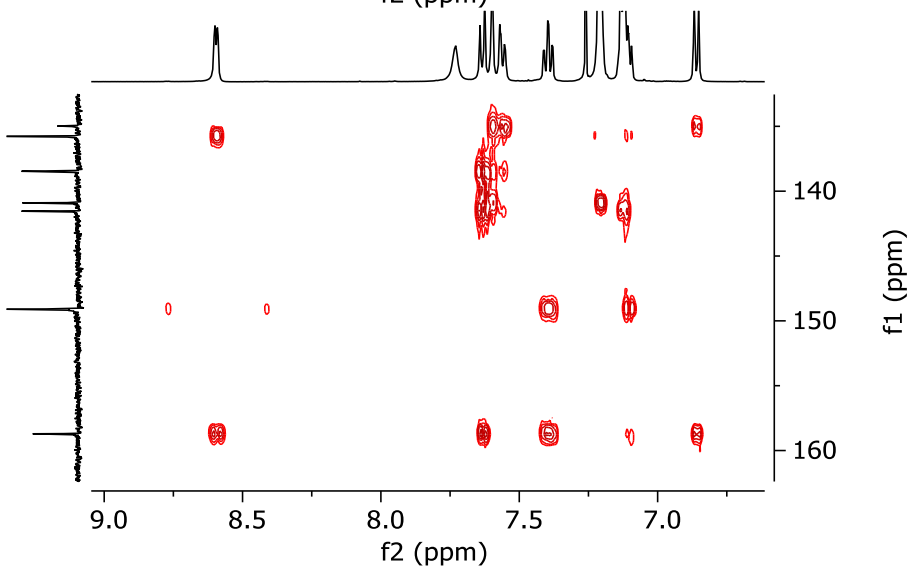

Data S14. Spectra for *N*-(2'-(Pyridin-2-yl)-[1,1':3',1''-terphenyl]-5'-yl)acetamide 19b (related to Scheme 6)

^{1}H NMR spectrum

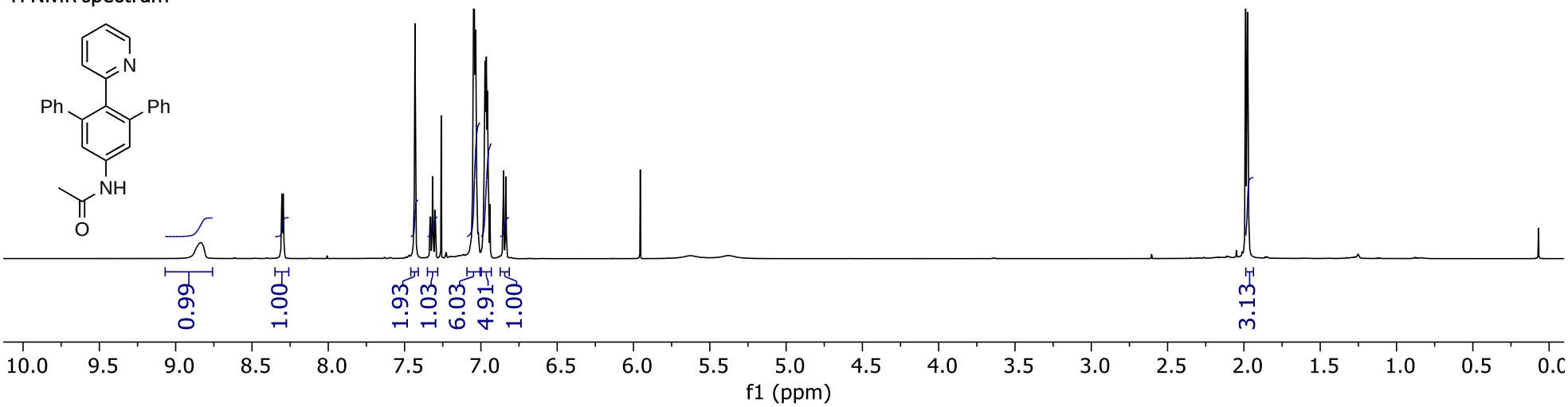

^{13}C NMR spectrum

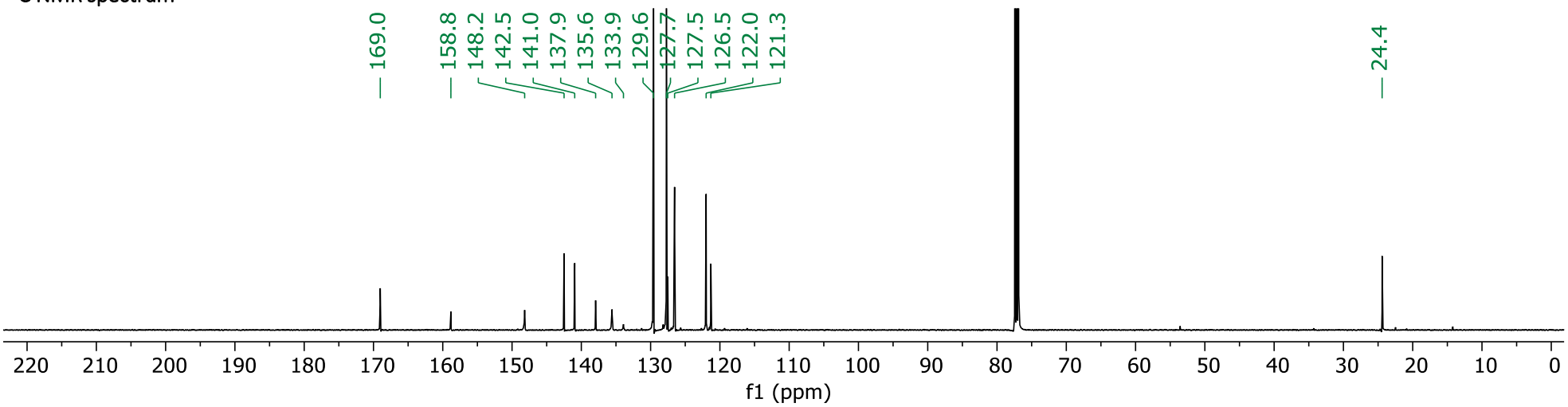

COSY correlation NMR

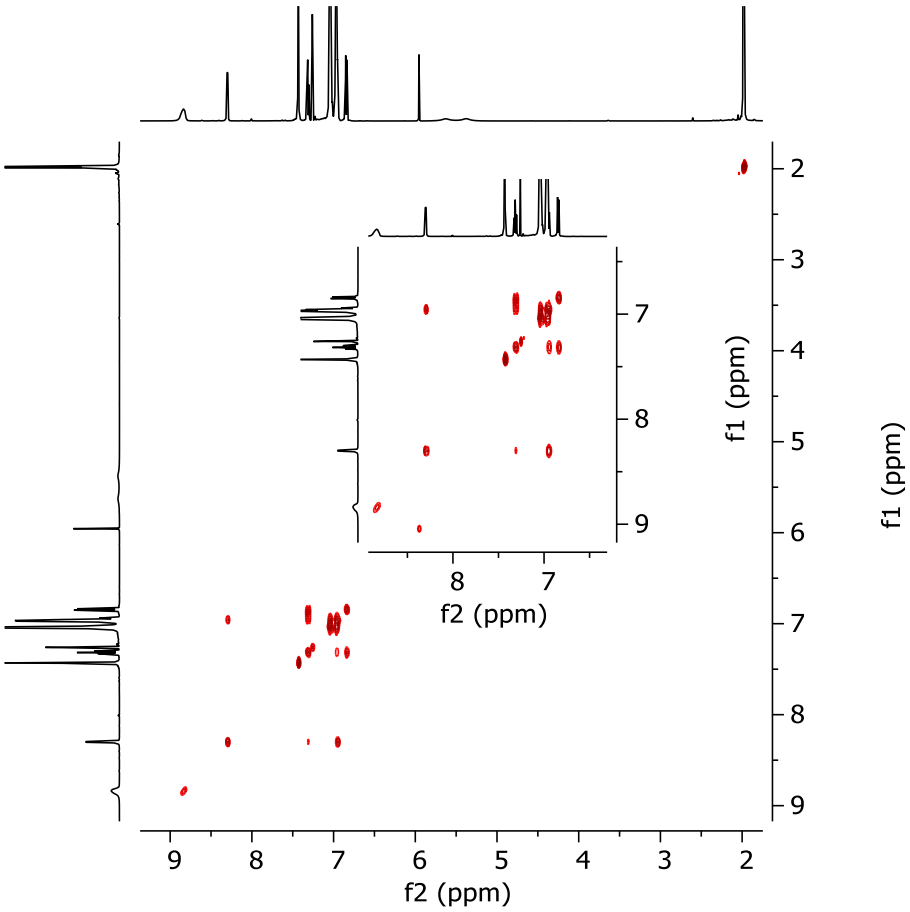

HSQC correlation NMR

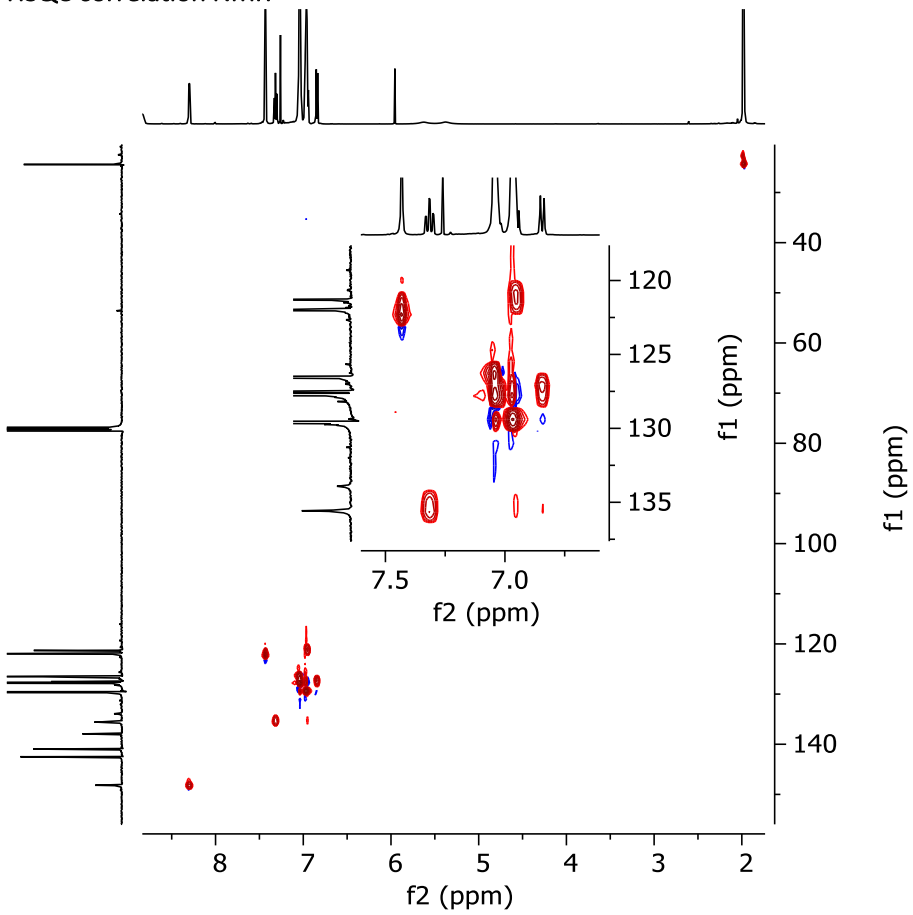

HMBC correlation NMR

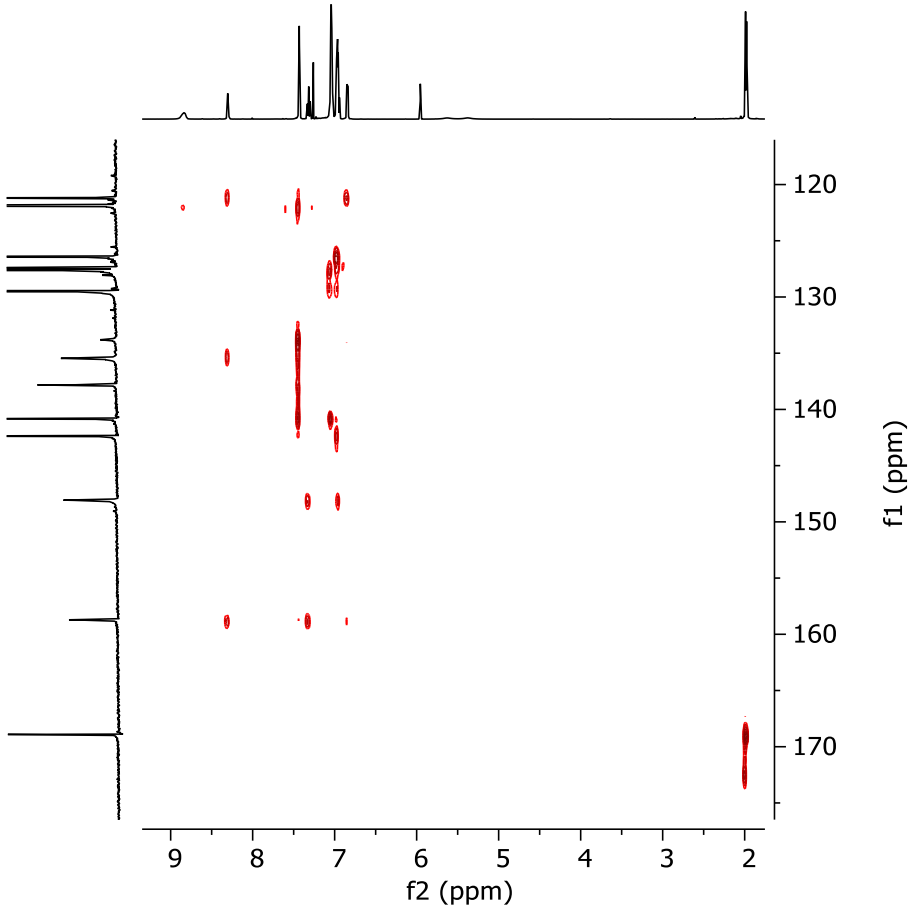

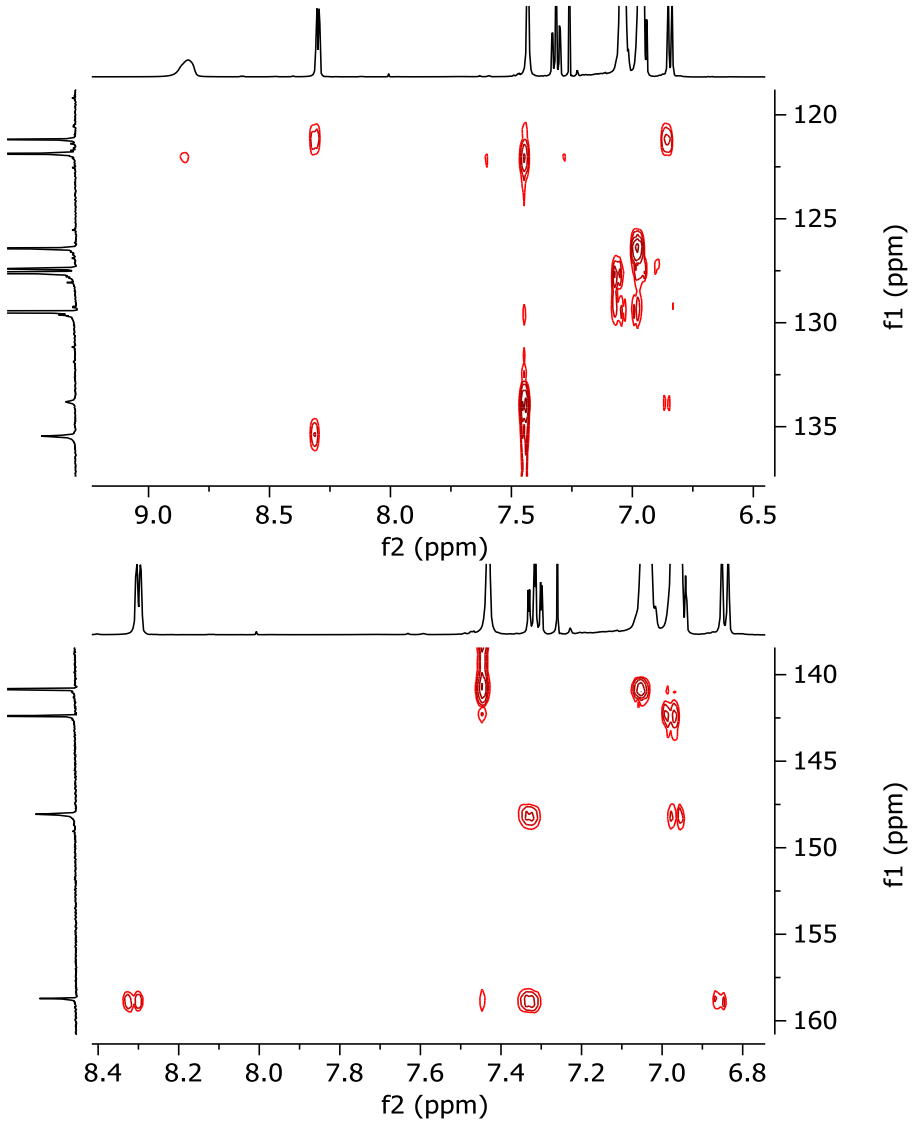

Data S15. Spectra for *N*-(5-(Pyridin-2-yl)-[1,1'-biphenyl]-2-yl)acetamide 19c (related to Scheme 6)

^{1}H NMR spectrum

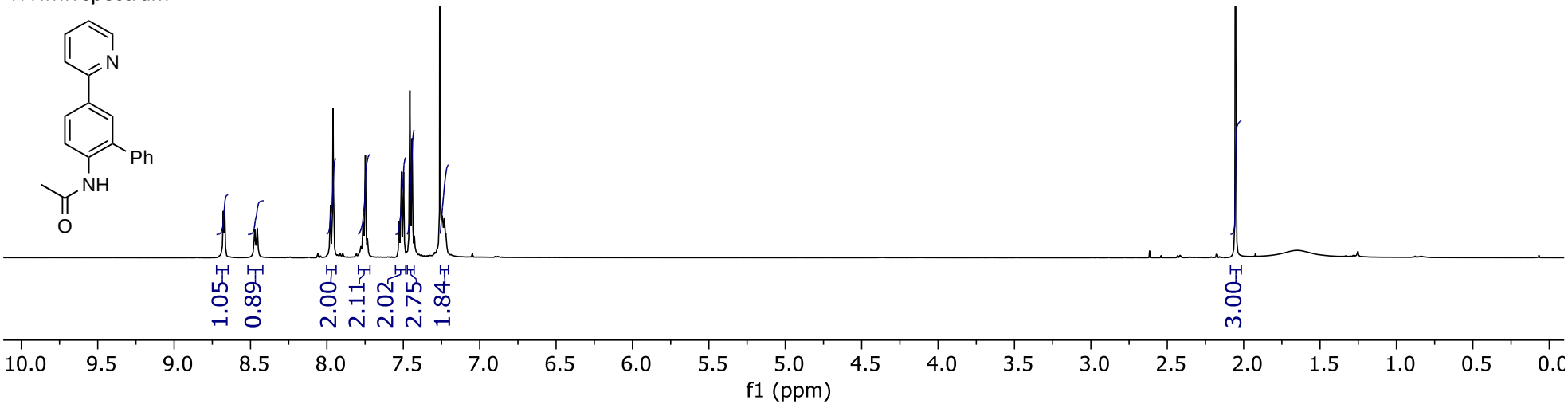

^{13}C NMR spectrum

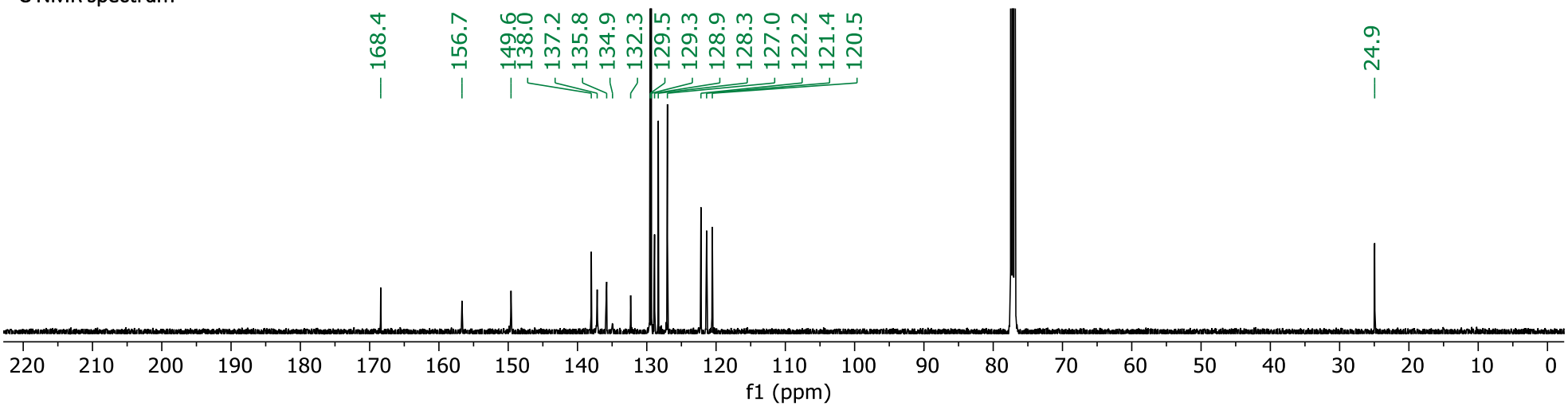

COSY correlation NMR

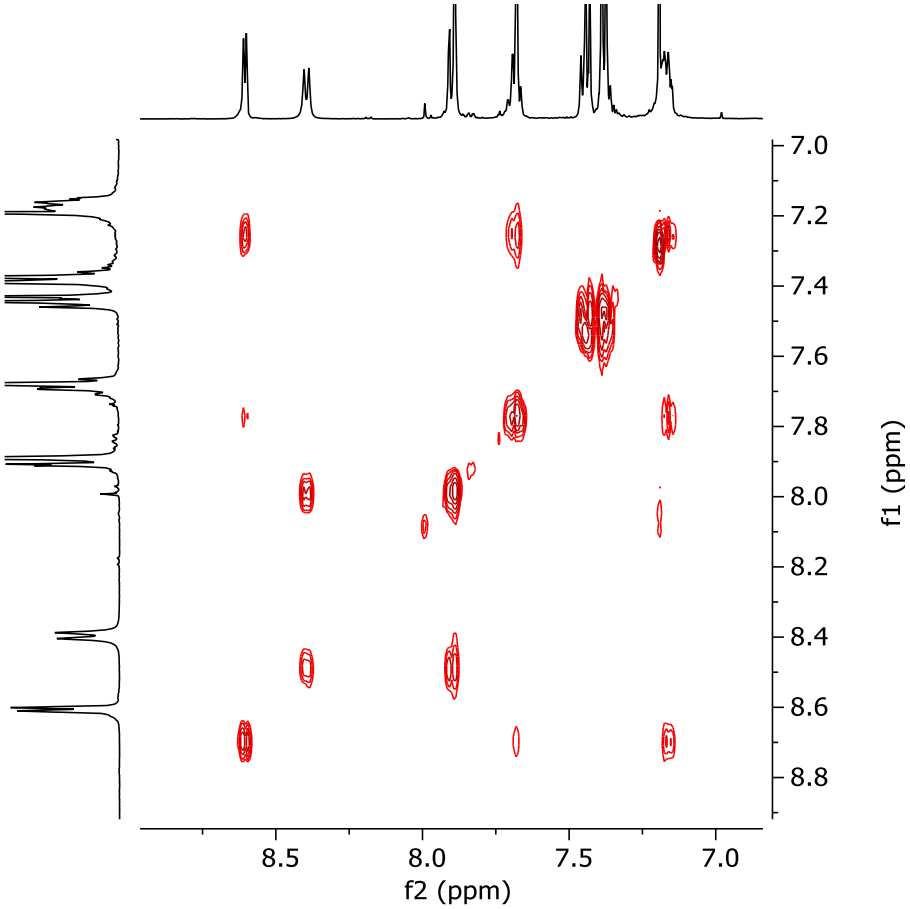

HSQC correlation NMR

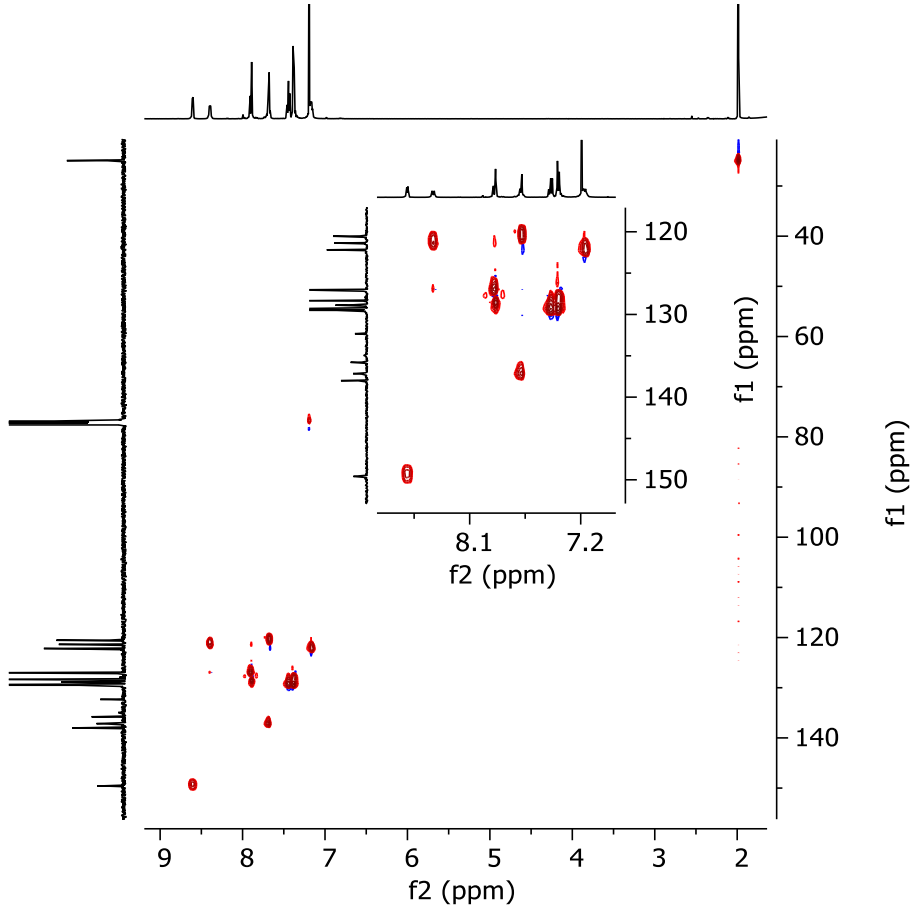

HMBC correlation NMR

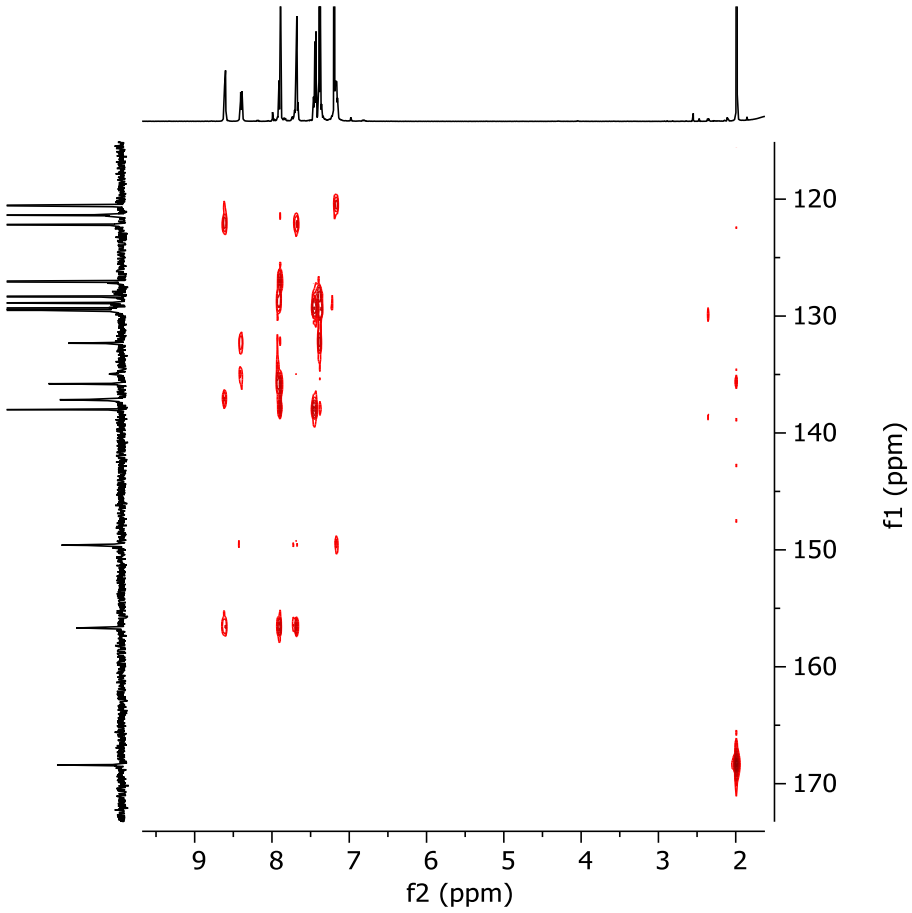

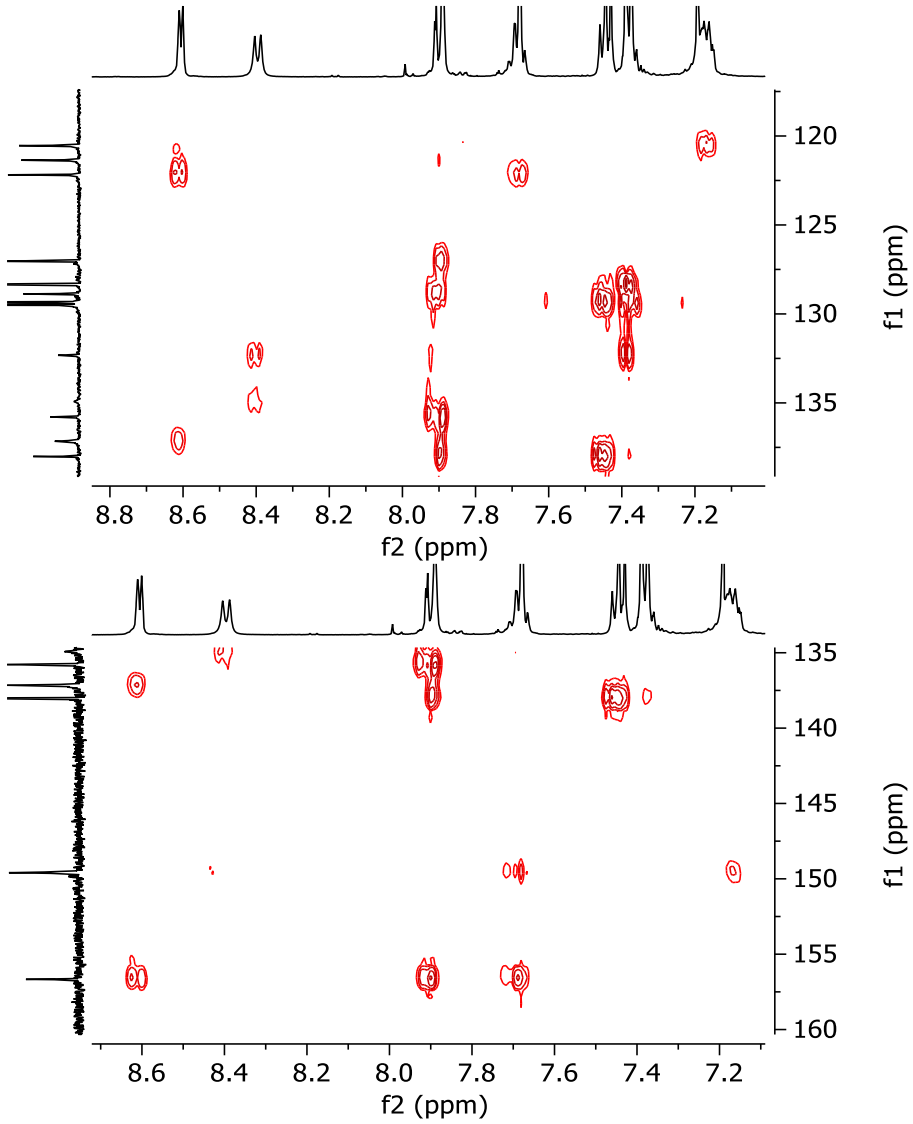

Data S16. Spectra for 5-(Pyridin-2-yl)-[1,1'-biphenyl]-2-amine 19d (related to Scheme 6)

^{1}H NMR spectrum

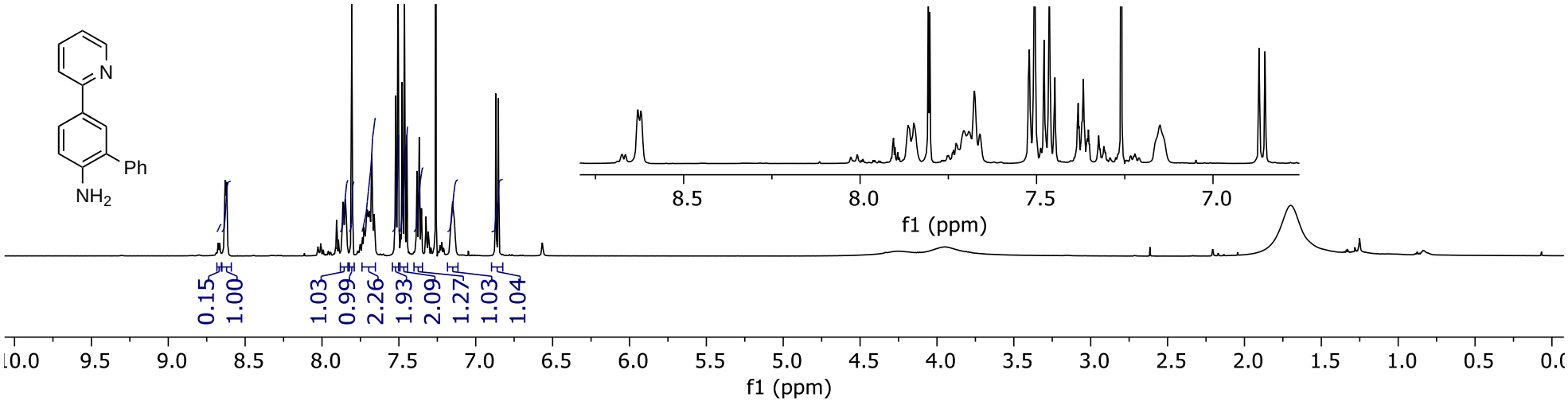

^{13}C NMR spectrum

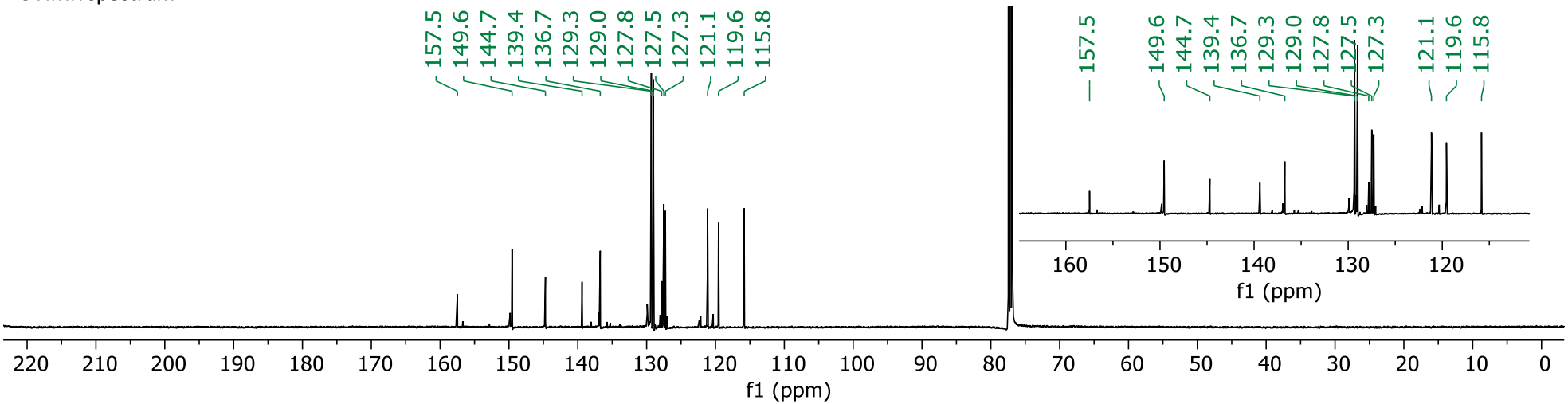

COSY correlation NMR

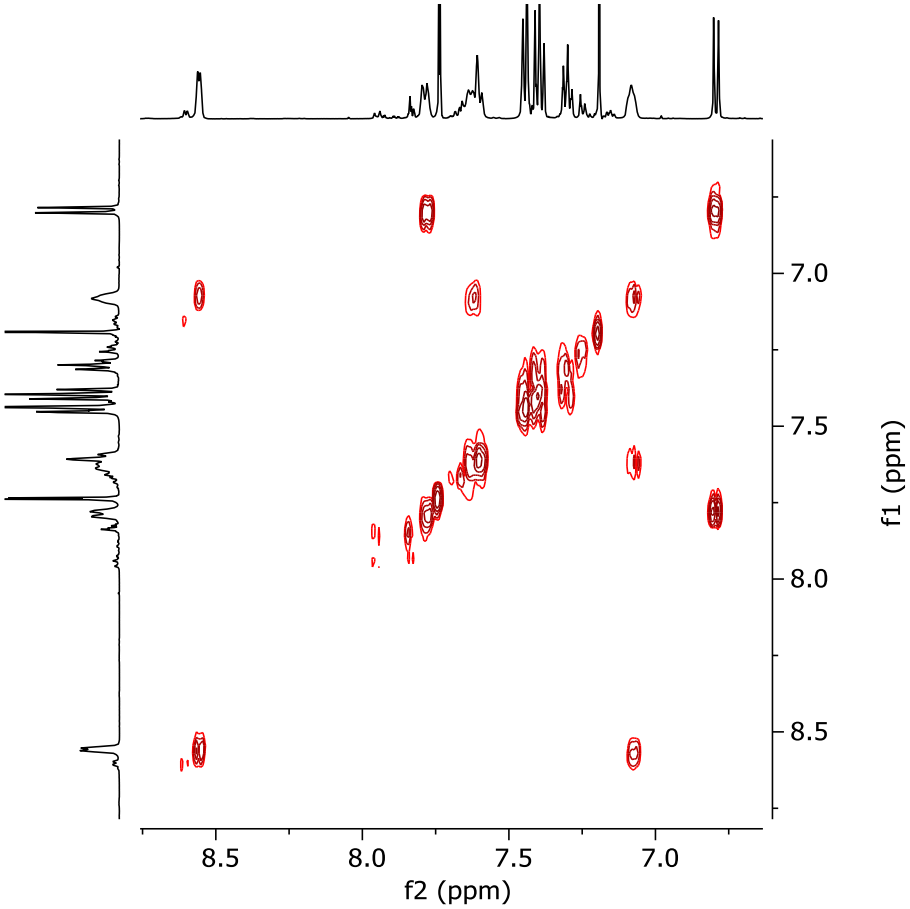

HSQC correlation NMR

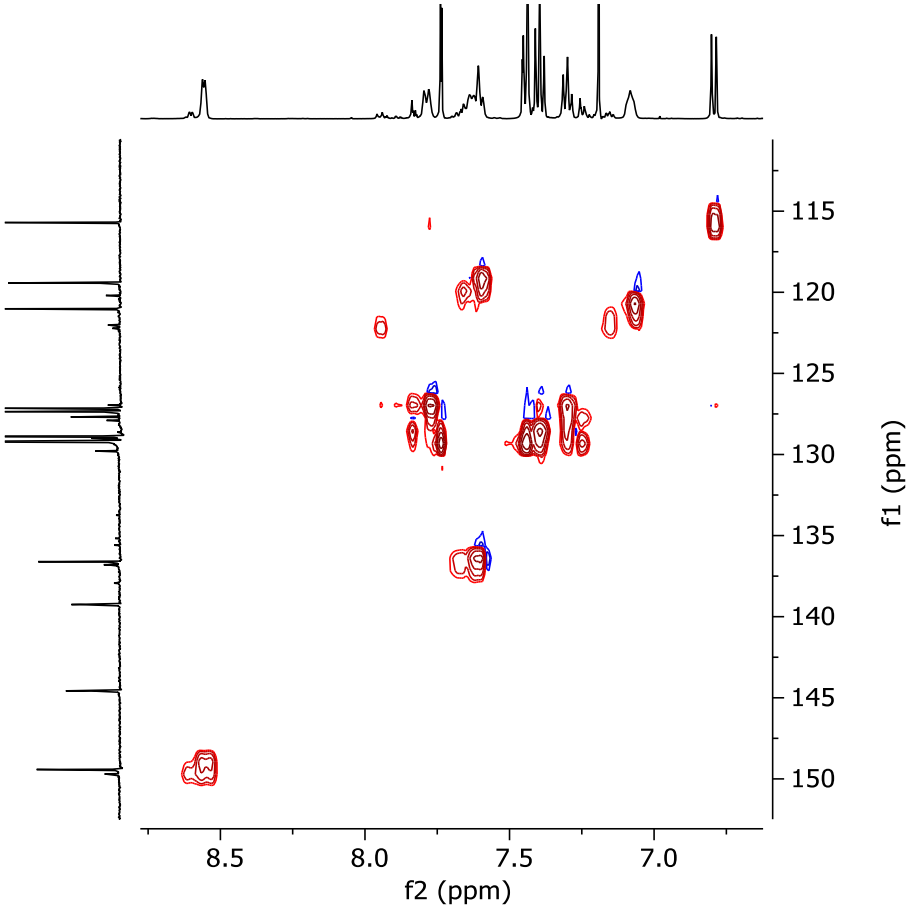

HMBC correlation NMR

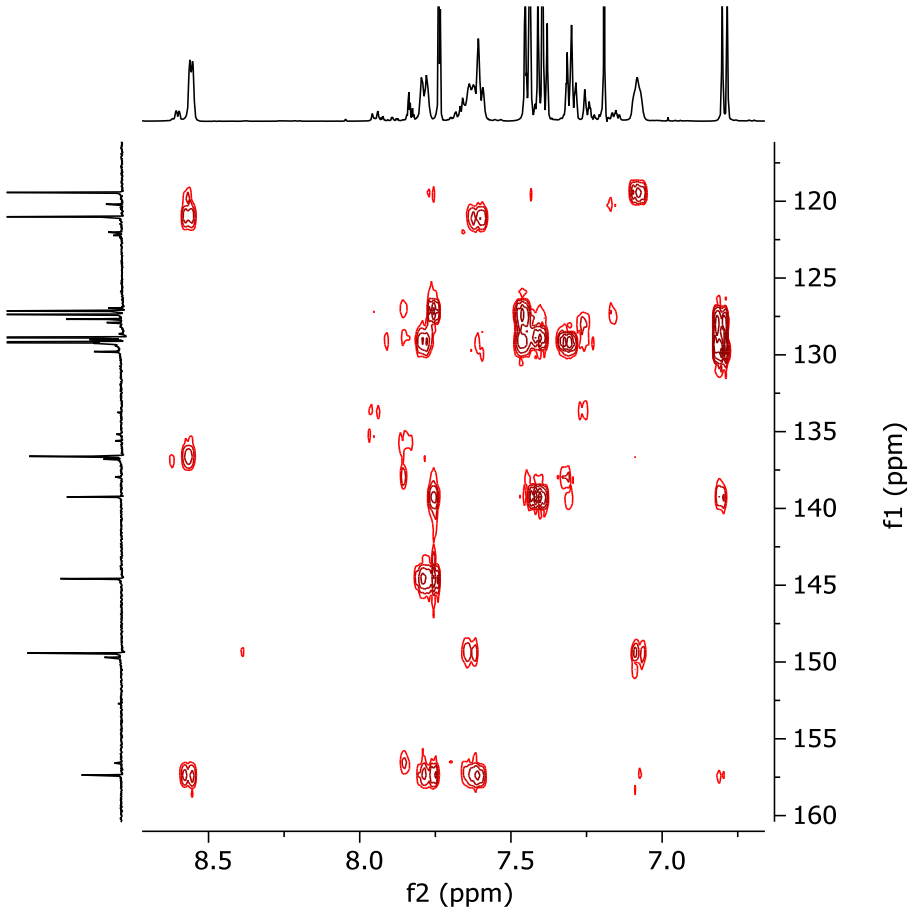

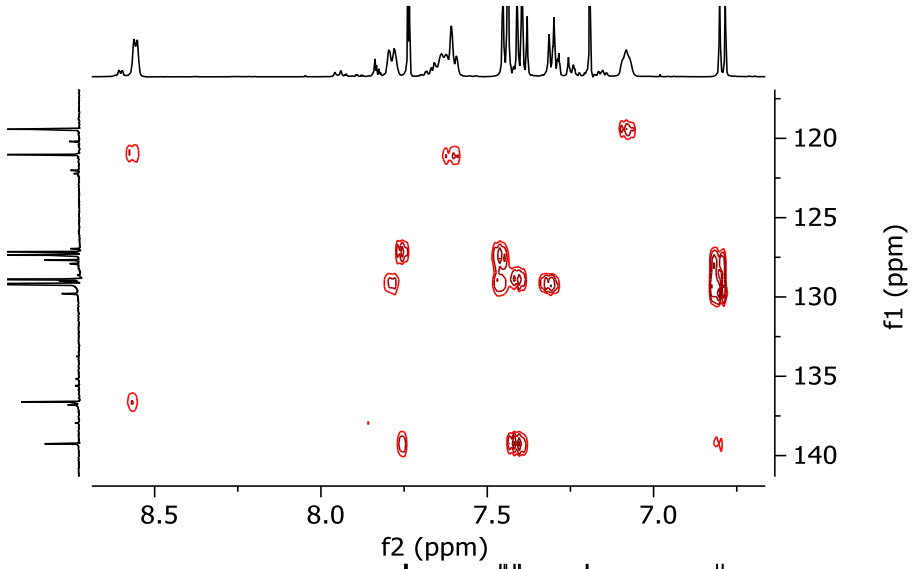

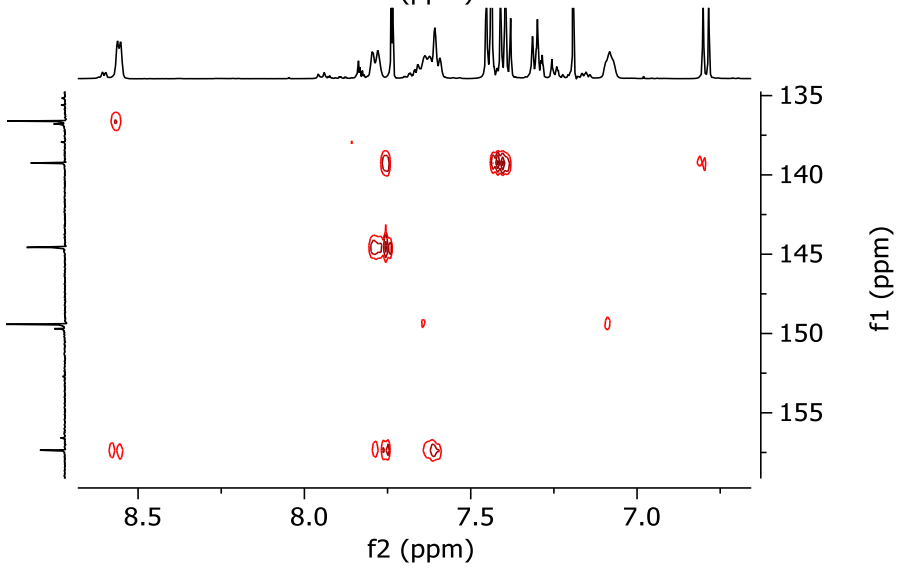

Data S17. This file, in the SDF format, contains all the xyz coordinates and the corresponding DFT energies of the molecules necessary to compute the directing strengths used to get the values in Data S1 to S4. (related to Data S1 to S4 and Scheme 2)

Supplemental References

1. Boele, M.D.K., van Strijdonck, G.P.F., de Vries, A.H.M., Kamer, P.C.J., de Vries, J.G., and van Leeuwen, P.W.N.M. (2002). Selective Pd-Catalyzed Oxidative Coupling of Anilides with Olefins through C–H Bond Activation at Room Temperature. J. Am. Chem. Soc. *124*, 1586-1587.
2. Zhu, R., Lu, S., Wang, Q., Bai, J., Wang, Y., Yu, Q., and Huang, J. (2018). Selectfluor-mediated mono-C–H activation: The syntheses of mono-ortho-substituted anilides. Tetrahedron *74*, 3879-3887.
3. Kametani, Y., Satoh, T., Miura, M., and Nomura, M. (2000). Regioselective arylation of benzanilides with aryl triflates or bromides under palladium catalysis. Tetrahedron Lett. *41*, 2655-2658.
4. Chou, H.-M., Jhou, J.-N., and Hong, F.-E. (2017). Incorporation of norbornene moiety onto the arene of diaryl substituted amides through C-H functionalization. J. Organomet. Chem. *853*, 178-183.
5. Cai, Z.-J., Yang, C., Wang, S.-Y., and Ji, S.-J. (2015). Palladium-Catalyzed Regioselective C–H Acylation of Biaryl-2-amines. J. Org. Chem. *80*, 7928-7936.
6. Kim, B.S., Lee, S.Y., and Youn, S.W. (2011). Pd-Catalyzed Sequential C−C and C−N Bond Formations for the Synthesis of N-Heterocycles: Exploiting Protecting Group-Directed C−H Activation under Modified Reaction Conditions. Chem. Asian J. *6*, 1952-1957.
7. Youn, S.W., Bihn, J.H., and Kim, B.S. (2011). Pd-Catalyzed Intramolecular Oxidative C–H Amination: Synthesis of Carbazoles. Org. Lett. *13*, 3738-3741.
8. Miura, M., Tsuda, T., Satoh, T., Pivsa-Art, S., and Nomura, M. (1998). Oxidative Cross-Coupling of N-(2′-Phenylphenyl)benzene- sulfonamides or Benzoic and Naphthoic Acids with Alkenes Using a Palladium−Copper Catalyst System under Air. J. Org. Chem. *63*, 5211-5215.
9. Rajeshkumar, V., Lee, T.-H., and Chuang, S.-C. (2013). Palladium-Catalyzed Oxidative Insertion of Carbon Monoxide to N-Sulfonyl-2-aminobiaryls through C–H Bond Activation: Access to Bioactive Phenanthridinone Derivatives in One Pot. Org. Lett. *15*, 1468-1471.
10. Choi, S., Chatterjee, T., Choi, W.J., You, Y., and Cho, E.J. (2015). Synthesis of Carbazoles by a Merged Visible Light Photoredox and Palladium-Catalyzed Process. ACS Catalysis *5*, 4796-4802.
11. Kim, B.S., Jang, C., Lee, D.J., and Youn, S.W. (2010). Highly Effective Pd-Catalyzed ortho Olefination of Acetanilides: Broad Substrate Scope and High Tolerability. Chem. Asian J. *5*, 2336-2340.
12. Kim, B.S., Lee, S.Y., and Youn, S.W. (2011). Pd-Catalyzed Sequential C−C and C−N Bond Formations for the Synthesis of N-Heterocycles: Exploiting Protecting Group-Directed C−H Activation under Modified Reaction Conditions. Chemistry – An Asian Journal *6*, 1952-1957.
13. Tsang, W.C.P., Munday, R.H., Brasche, G., Zheng, N., and Buchwald, S.L. (2008). Palladium-Catalyzed Method for the Synthesis of Carbazoles via Tandem C−H Functionalization and C−N Bond Formation. J. Org. Chem. *73*, 7603-7610.
14. Szabó, F., Daru, J., Simkó, D., Nagy, T.Z., Stirling, A., and Novák, Z. (2013). Mild Palladium-Catalyzed Oxidative Direct ortho-C−H Acylation of Anilides under Aqueous Conditions. Adv. Synth. Catal. *355*, 685-691.
15. Wu, Y., Li, B., Mao, F., Li, X., and Kwong, F.Y. (2011). Palladium-Catalyzed Oxidative C–H Bond Coupling of Steered Acetanilides and Aldehydes: A Facile Access to ortho-Acylacetanilides. Org. Lett. *13*, 3258-3261.

16. Das, R., and Kapur, M. (2017). Palladium-Catalyzed, ortho-Selective C–H Halogenation of Benzyl Nitriles, Aryl Weinreb Amides, and Anilides. J. Org. Chem. *82*, 1114-1126.
17. Yang, S., Li, B., Wan, X., and Shi, Z. (2007). Ortho Arylation of Acetanilides via Pd(II)-Catalyzed C−H Functionalization. J. Am. Chem. Soc. *129*, 6066-6067.
18. Yeung, C.S., Zhao, X., Borduas, N., and Dong, V.M. (2010). Pd-catalyzed ortho-arylation of phenylacetamides, benzamides, and anilides with simple arenes using sodium persulfate. Chem. Sci. *1*, 331-336.
19. Giri, R., Lam, J.K., and Yu, J.-Q. (2010). Synthetic Applications of Pd(II)-Catalyzed C−H Carboxylation and Mechanistic Insights: Expedient Routes to Anthranilic Acids, Oxazolinones, and Quinazolinones. J. Am. Chem. Soc. *132*, 686-693.
20. Kim, M., Kumar Mishra, N., Park, J., Han, S., Shin, Y., Sharma, S., Lee, Y., Lee, E.-K., Kwak, J.H., and Kim, I.S. (2014). Decarboxylative acylation of indolines with α-keto acids under palladium catalysis: a facile strategy for the synthesis of 7-substituted indoles. Chem. Commun. (Cambridge, U. K.) *50*, 14249-14252.
21. Chan, C.-W., Zhou, Z., and Yu, W.-Y. (2011). Palladium(II)-Catalyzed Direct ortho-C−H Acylation of Anilides by Oxidative Cross-Coupling with Aldehydes using tert-Butyl Hydroperoxide as Oxidant. Adv. Synth. Catal. *353*, 2999-3006.
22. Houlden, C.E., Hutchby, M., Bailey, C.D., Ford, J.G., Tyler, S.N.G., Gagné, M.R., Lloyd-Jones, G.C., and Booker-Milburn, K.I. (2009). Room-Temperature Palladium-Catalyzed C−H Activation: ortho-Carbonylation of Aniline Derivatives. Angew. Chem., Int. Ed. *48*, 1830-1833.
23. Ng, K.-H., Chan, A.S.C., and Yu, W.-Y. (2010). Pd-Catalyzed Intermolecular ortho-C−H Amidation of Anilides by N-Nosyloxycarbamate. J. Am. Chem. Soc. *132*, 12862-12864.
24. Zhu, D., Yang, G., He, J., Chu, L., Chen, G., Gong, W., Chen, K., Eastgate, M.D., and Yu, J.-Q. (2015). Ligand-Promoted ortho-C−H Amination with Pd Catalysts. Angew. Chem., Int. Ed. *54*, 2497-2500.
25. Wang, G.-W., Yuan, T.-T., and Li, D.-D. (2011). One-Pot Formation of C−C and C−N Bonds through Palladium-Catalyzed Dual C−H Activation: Synthesis of Phenanthridinones. Angew. Chem., Int. Ed. *50*, 1380-1383.
26. Rao, W.-H., Jiang, L.-L., Zhao, J.-X., Jiang, X., Zou, G.-D., Zhou, Y.-Q., and Tang, L. (2018). Selective O-Cyclization of N-Methoxy Aryl Amides with CH2Br2 or 1,2-DCE via Palladium-Catalyzed C–H Activation. Org. Lett. *20*, 6198-6201.
27. Zhu, C., and Falck, J.R. (2011). N-Acylsulfonamide Assisted Tandem C−H Olefination/Annulation: Synthesis of Isoindolinones. Org. Lett. *13*, 1214-1217.
28. Dai, H.-X., Stepan, A.F., Plummer, M.S., Zhang, Y.-H., and Yu, J.-Q. (2011). Divergent C–H Functionalizations Directed by Sulfonamide Pharmacophores: Late-Stage Diversification as a Tool for Drug Discovery. J. Am. Chem. Soc. *133*, 7222-7228.
29. Kalyani, D., Deprez, N.R., Desai, L.V., and Sanford, M.S. (2005). Oxidative C−H Activation/C−C Bond Forming Reactions: Synthetic Scope and Mechanistic Insights. J. Am. Chem. Soc. *127*, 7330-7331.
30. Hull, K.L., Anani, W.Q., and Sanford, M.S. (2006). Palladium-Catalyzed Fluorination of Carbon−Hydrogen Bonds. J. Am. Chem. Soc. *128*, 7134-7135.
31. Li, W., Yin, Z., Jiang, X., and Sun, P. (2011). Palladium-Catalyzed Direct Ortho C–H Arylation of 2-Arylpyridine Derivatives with Aryltrimethoxysilane. J. Org. Chem. *76*, 8543-8548.
32. Shi, B.-F., Maugel, N., Zhang, Y.-H., and Yu, J.-Q. (2008). PdII-Catalyzed Enantioselective Activation of C(sp2)−H and C(sp3)−H Bonds Using Monoprotected Amino Acids as Chiral Ligands. Angew. Chem., Int. Ed. *47*, 4882-4886.
33. Kalyani, D., and Sanford, M.S. (2005). Regioselectivity in Palladium-Catalyzed C−H Activation/Oxygenation Reactions. Org. Lett. *7*, 4149-4152.
34. Gulevich, A.V., Melkonyan, F.S., Sarkar, D., and Gevorgyan, V. (2012). Double-Fold C–H Oxygenation of Arenes Using PyrDipSi: a General and Efficient Traceless/Modifiable Silicon-Tethered Directing Group. J. Am. Chem. Soc. *134*, 5528-5531.

35. Shi, S., and Kuang, C. (2014). Palladium-Catalyzed Ortho-Alkoxylation of 2-Aryl-1,2,3-triazoles. J. Org. Chem. *79*, 6105-6112.
36. Feng, C.-G., Ye, M., Xiao, K.-J., Li, S., and Yu, J.-Q. (2013). Pd(II)-Catalyzed Phosphorylation of Aryl C–H Bonds. J. Am. Chem. Soc. *135*, 9322-9325.
37. Sun, C.-L., Liu, N., Li, B.-J., Yu, D.-G., Wang, Y., and Shi, Z.-J. (2010). Pd-Catalyzed C−H Functionalizations of O-Methyl Oximes with Arylboronic Acids. Org. Lett. *12*, 184-187.
38. Lou, S.-J., Xu, D.-Q., and Xu, Z.-Y. (2014). Mild and Versatile Nitrate-Promoted C−H Bond Fluorination. Angew. Chem., Int. Ed. *53*, 10330-10335.
39. Dong, J., Jin, B., and Sun, P. (2014). Palladium-Catalyzed Direct Ortho-Nitration of Azoarenes Using NO2 as Nitro Source. Org. Lett. *16*, 4540-4542.
40. Li, H., Li, P., Zhao, Q., and Wang, L. (2013). Unprecedented ortho-acylation of azoxybenzenes with α-oxocarboxylic acids by Pd-catalyzed C–H activation and decarboxylation. Chem. Commun. (Cambridge, U. K.) *49*, 9170-9172.
41. Miura, M., Feng, C.-G., Ma, S., and Yu, J.-Q. (2013). Pd(II)-Catalyzed Ortho-Trifluoromethylation of Benzylamines. Org. Lett. *15*, 5258-5261.
42. Kianmehr, E., Fardpour, M., and Kharat, A.N. (2017). Palladium-Catalyzed Chemo- and Regioselective Oxidative Cross-Dehydrogenative Coupling of Acetanilides with Benzothiazole. Eur. J. Org. Chem. *2017*, 3017-3021.
43. Li, D., Xu, N., Zhang, Y., and Wang, L. (2014). A highly efficient Pd-catalyzed decarboxylative ortho-arylation of amides with aryl acylperoxides. Chem. Commun. (Cambridge, U. K.) *50*, 14862-14865.
44. Liang, Z., Zhang, J., Liu, Z., Wang, K., and Zhang, Y. (2013). Pd(II)-catalyzed C(sp2)–H carbonylation of biaryl-2-amine: synthesis of phenanthridinones. Tetrahedron *69*, 6519-6526.
45. Cho, S.H., Hwang, S.J., and Chang, S. (2008). Palladium-Catalyzed C−H Functionalization of Pyridine N-Oxides: Highly Selective Alkenylation and Direct Arylation with Unactivated Arenes. J. Am. Chem. Soc. *130*, 9254-9256.
46. Crisenza, G.E.M., Dauncey, E.M., and Bower, J.F. (2016). C2-Alkenylation of N-heteroaromatic compounds via Brønsted acid catalysis. Org. Biomol. Chem. *14*, 5820-5825.
47. Stephens, D.E., Lakey-Beitia, J., Atesin, A.C., Ateşin, T.A., Chavez, G., Arman, H.D., and Larionov, O.V. (2015). Palladium-Catalyzed C8-Selective C–H Arylation of Quinoline N-Oxides: Insights into the Electronic, Steric, and Solvation Effects on the Site Selectivity by Mechanistic and DFT Computational Studies. ACS Catalysis *5*, 167-175.
48. Pan, S., Zhou, B., Zhang, Y., Shao, C., and Shi, G. (2016). A Versatile Approach for the Synthesis of para-Substituted Arenes via Palladium-Catalyzed C–H Functionalization and Protodecarboxylation of Benzoic Acids. Synlett *27*, 277-281.
49. Giri, R., Maugel, N., Li, J.-J., Wang, D.-H., Breazzano, S.P., Saunders, L.B., and Yu, J.-Q. (2007). Palladium-Catalyzed Methylation and Arylation of sp2 and sp3 C−H Bonds in Simple Carboxylic Acids. J. Am. Chem. Soc. *129*, 3510-3511.
50. Wang, D.-H., Mei, T.-S., and Yu, J.-Q. (2008). Versatile Pd(II)-Catalyzed C−H Activation/Aryl−Aryl Coupling of Benzoic and Phenyl Acetic Acids. J. Am. Chem. Soc. *130*, 17676-17677.
51. Chiong, H.A., Pham, Q.-N., and Daugulis, O. (2007). Two Methods for Direct ortho-Arylation of Benzoic Acids. J. Am. Chem. Soc. *129*, 9879-9884.
52. Zhang, Y.-H., Shi, B.-F., and Yu, J.-Q. (2009). Palladium(II)-Catalyzed ortho Alkylation of Benzoic Acids with Alkyl Halides. Angew. Chem., Int. Ed. *48*, 6097-6100.
53. Zhang, Y.-H., and Yu, J.-Q. (2009). Pd(II)-Catalyzed Hydroxylation of Arenes with 1 atm of O2 or Air. J. Am. Chem. Soc. *131*, 14654-14655.
54. Mei, T.-S., Wang, D.-H., and Yu, J.-Q. (2010). Expedient Drug Synthesis and Diversification via ortho-C−H Iodination using Recyclable PdI2 as the Precatalyst. Org. Lett. *12*, 3140-3143.

55. Shi, B.-F., Zhang, Y.-H., Lam, J.K., Wang, D.-H., and Yu, J.-Q. (2010). Pd(II)-Catalyzed Enantioselective C−H Olefination of Diphenylacetic Acids. J. Am. Chem. Soc. *132*, 460-461.
56. Yang, M., Jiang, X., Shi, W.-J., Zhu, Q.-L., and Shi, Z.-J. (2013). Direct Lactonization of 2-Arylacetic Acids through Pd(II)-Catalyzed C–H Activation/C–O Formation. Org. Lett. *15*, 690-693.
57. Shan, G., Yang, X., Ma, L., and Rao, Y. (2012). Pd-Catalyzed C−H Oxygenation with TFA/TFAA: Expedient Access to Oxygen-Containing Heterocycles and Late-Stage Drug Modification. Angew. Chem., Int. Ed. *51*, 13070-13074.
58. Sun, X., Shan, G., Sun, Y., and Rao, Y. (2013). Regio- and Chemoselective C−H Chlorination/Bromination of Electron-Deficient Arenes by Weak Coordination and Study of Relative Directing-Group Abilities. Angew. Chem., Int. Ed. *52*, 4440-4444.
59. Bedford, R.B., Webster, R.L., and Mitchell, C.J. (2009). Palladium-catalysed ortho-arylation of carbamate-protected phenols. Org. Biomol. Chem. *7*, 4853-4857.
60. Zhao, X., Yeung, C.S., and Dong, V.M. (2010). Palladium-Catalyzed Ortho-Arylation of O-Phenylcarbamates with Simple Arenes and Sodium Persulfate. J. Am. Chem. Soc. *132*, 5837-5844.
61. Xiao, B., Fu, Y., Xu, J., Gong, T.-J., Dai, J.-J., Yi, J., and Liu, L. (2010). Pd(II)-Catalyzed C−H Activation/Aryl−Aryl Coupling of Phenol Esters. J. Am. Chem. Soc. *132*, 468-469.
62. John, A., and Nicholas, K.M. (2012). Palladium Catalyzed C–H Functionalization of O-Arylcarbamates: Selective ortho-Bromination Using NBS. J. Org. Chem. *77*, 5600-5605.
63. Sun, X., Sun, Y., Zhang, C., and Rao, Y. (2014). Room-temperature Pd-catalyzed C–H chlorination by weak coordination: one-pot synthesis of 2-chlorophenols with excellent regioselectivity. Chem. Commun. (Cambridge, U. K.) *50*, 1262-1264.
64. Luo, S., Luo, F.-X., Zhang, X.-S., and Shi, Z.-J. (2013). Synthesis of Dibenzopyranones through Palladium-Catalyzed Directed C–H Activation/Carbonylation of 2-Arylphenols. Angew. Chem., Int. Ed. *52*, 10598-10601.
65. Xiao, B., Gong, T.-J., Liu, Z.-J., Liu, J.-H., Luo, D.-F., Xu, J., and Liu, L. (2011). Synthesis of Dibenzofurans via Palladium-Catalyzed Phenol-Directed C–H Activation/C–O Cyclization. J. Am. Chem. Soc. *133*, 9250-9253.
66. Huang, C., Ghavtadze, N., Chattopadhyay, B., and Gevorgyan, V. (2011). Synthesis of Catechols from Phenols via Pd-Catalyzed Silanol-Directed C–H Oxygenation. J. Am. Chem. Soc. *133*, 17630-17633.
67. Wang, C., and Ge, H. (2011). Silanol as a Removable Directing Group for the PdII-Catalyzed Direct Olefination of Arenes. Chem. Eur. J. *17*, 14371-14374.
68. Li, G., Leow, D., Wan, L., and Yu, J.-Q. (2013). Ether-Directed ortho-C–H Olefination with a Palladium(II)/Monoprotected Amino Acid Catalyst. Angew. Chem., Int. Ed. *52*, 1245-1247.
69. Yu, M., Xie, Y., Xie, C., and Zhang, Y. (2012). Palladium-Catalyzed C–H Alkenylation of Arenes Using Thioethers as Directing Groups. Org. Lett. *14*, 2164-2167.
70. Zhang, X.-S., Zhang, Y.-F., Chen, K., and Shi, Z.-J. (2014). Controllable mono-/di-alkenylation of aryl alkyl thioethers tuned by oxidants via Pd-catalysis. Org. Chem. Front. *1*, 1096-1100.
71. Wang, B., Shen, C., Yao, J., Yin, H., and Zhang, Y. (2014). Palladium(II)-Catalyzed ortho-Olefination of Arenes Applying Sulfoxides as Remote Directing Groups. Org. Lett. *16*, 46-49.
72. Chan, L.Y., Meng, X., and Kim, S. (2013). ortho-Acetoxylation of Phosphonic and Phosphoric Monoacids via Pd(II) Catalysis. J. Org. Chem. *78*, 8826-8832.
73. Zhang, H., Hu, R.-B., Zhang, X.-Y., Li, S.-X., and Yang, S.-D. (2014). Palladium-catalyzed R2(O)P directed C(sp2)–H acetoxylation. Chem. Commun. (Cambridge, U. K.) *50*, 4686-4689.

74. Deb, A., Bag, S., Kancherla, R., and Maiti, D. (2014). Palladium-Catalyzed Aryl C–H Olefination with Unactivated, Aliphatic Alkenes. J. Am. Chem. Soc. *136*, 13602-13605.
75. Kanyiva, K.S., Kuninobu, Y., and Kanai, M. (2014). Palladium-Catalyzed Direct C–H Silylation and Germanylation of Benzamides and Carboxamides. Org. Lett. *16*, 1968-1971.
76. Feng, P., Chen, T., Chen, J., and Huang, Y. (2018). Process for preparation of ortho-aminophenol derivatives using carbon-hydrogen bond activation (Jinan University, Peop. Rep. China .), pp. 25pp.
77. Daugulis, O., and Chiong, H. (2009). Use of aryl chlorides in palladium-catalyzed arylation of heterocycles, benzoates, and phenols (The University of Houston System, USA .), pp. 101pp.
78. Han, J., Wang, N., Huang, Z.-B., Zhao, Y., and Shi, D.-Q. (2017). Pd-Catalyzed regioselective sequential meta-, ortho-C–H functionalization of arenes: a predictable approach to the synthesis of polysubstituted β-arylethylamines. Org. Biomol. Chem. *15*, 5112-5116.
79. Kovács, S., Tóth, B.L., Borsik, G., Bihari, T., May, N.V., Stirling, A., and Novák, Z. (2017). Direct ortho-Trifluoroethylation of Aromatic Ureas by Palladium Catalyzed C-H activation: A Missing Piece of Aromatic Substitutions. Adv. Synth. Catal. *359*, 527-532.
80. Tóth, B.L., Kovács, S., Sályi, G., and Novák, Z. (2016). Mild and Efficient Palladium-Catalyzed Direct Trifluoroethylation of Aromatic Systems by C−H Activation. Angew. Chem., Int. Ed. *55*, 1988-1992.
81. Xia, X.-F., Wang, Y.-Q., Zhang, L.-L., Song, X.-R., Liu, X.-Y., and Liang, Y.-M. (2014). Palladium-Catalyzed C−H Activation and Intermolecular Annulation with Allenes. Chem. Eur. J. *20*, 5087-5091.
82. Jiang, H., Gao, H., Liu, B., and Wu, W. (2014). Synthesis of 6-aminophenanthridines via palladium-catalyzed insertion of isocyanides into N-sulfonyl-2-aminobiaryls. RSC Advances *4*, 17222-17225.
83. Wang, X., Truesdale, L., and Yu, J.-Q. (2010). Pd(II)-Catalyzed ortho-Trifluoromethylation of Arenes Using TFA as a Promoter. J. Am. Chem. Soc. *132*, 3648-3649.
84. Chaitanya, M., and Anbarasan, P. (2018). Lewis Acid/Brønsted Acid Controlled Pd(II)-Catalyzed Chemodivergent Functionalization of C(sp2)–H Bonds with N-(Arylthio)i(a)mides. Org. Lett. *20*, 3362-3366.
85. Hazra, C.K., Dherbassy, Q., Wencel-Delord, J., and Colobert, F. (2014). Synthesis of Axially Chiral Biaryls through Sulfoxide-Directed Asymmetric Mild C−H Activation and Dynamic Kinetic Resolution. Angew. Chem., Int. Ed. *53*, 13871-13875.
86. Karthikeyan, J., and Cheng, C.-H. (2011). Synthesis of Phenanthridinones from N-Methoxybenzamides and Arenes by Multiple Palladium-Catalyzed C−H Activation Steps at Room Temperature. Angew. Chem., Int. Ed. *50*, 9880-9883.
87. Thirunavukkarasu, V.S., Parthasarathy, K., and Cheng, C.-H. (2008). Synthesis of Fluorenones from Aromatic Aldoxime Ethers and Aryl Halides by Palladium-Catalyzed Dual C−H Activation and Heck Cyclization. Angew. Chem., Int. Ed. *47*, 9462-9465.
88. Li, Y., Ding, Y.-J., Wang, J.-Y., Su, Y.-M., and Wang, X.-S. (2013). Pd-Catalyzed C–H Lactonization for Expedient Synthesis of Biaryl Lactones and Total Synthesis of Cannabinol. Org. Lett. *15*, 2574-2577.
89. Liang, D., Hu, Z., Peng, J., Huang, J., and Zhu, Q. (2013). Synthesis of phenanthridinones via palladium-catalyzed C(sp2)–H aminocarbonylation of unprotected o-arylanilines. Chem. Commun. (Cambridge, U. K.) *49*, 173-175.
90. Chernyak, N., and Gevorgyan, V. (2009). Synthesis of Fluorenes via the Palladium-Catalyzed 5-exo-dig Annulation of o-Alkynylbiaryls. Adv. Synth. Catal. *351*, 1101-1114.

91. Wang, C., Chen, C., Zhang, J., Han, J., Wang, Q., Guo, K., Liu, P., Guan, M., Yao, Y., and Zhao, Y. (2014). Easily Accessible Auxiliary for Palladium-Catalyzed Intramolecular Amination of C(sp2)−H and C(sp3)−H Bonds at δ- and ε-Positions. Angew. Chem., Int. Ed. *53*, 9884-9888.
92. Yu, W.-Y., Sit, W.N., Lai, K.-M., Zhou, Z., and Chan, A.S.C. (2008). Palladium-Catalyzed Oxidative Ethoxycarbonylation of Aromatic C−H Bond with Diethyl Azodicarboxylate. J. Am. Chem. Soc. *130*, 3304-3306.
93. Thirunavukkarasu, V.S., and Cheng, C.-H. (2011). Pd-Catalyzed Multiple C−H Functionalization to Construct Biologically Active Compounds from Aryl Aldoxime Ethers with Arenes. Chem. Eur. J. *17*, 14723-14726.
94. Zhang, C., Ji, J., and Sun, P. (2014). Palladium-Catalyzed Alkenylation via sp2 C–H Bond Activation Using Phenolic Hydroxyl as the Directing Group. J. Org. Chem. *79*, 3200-3205.